pmod wrc

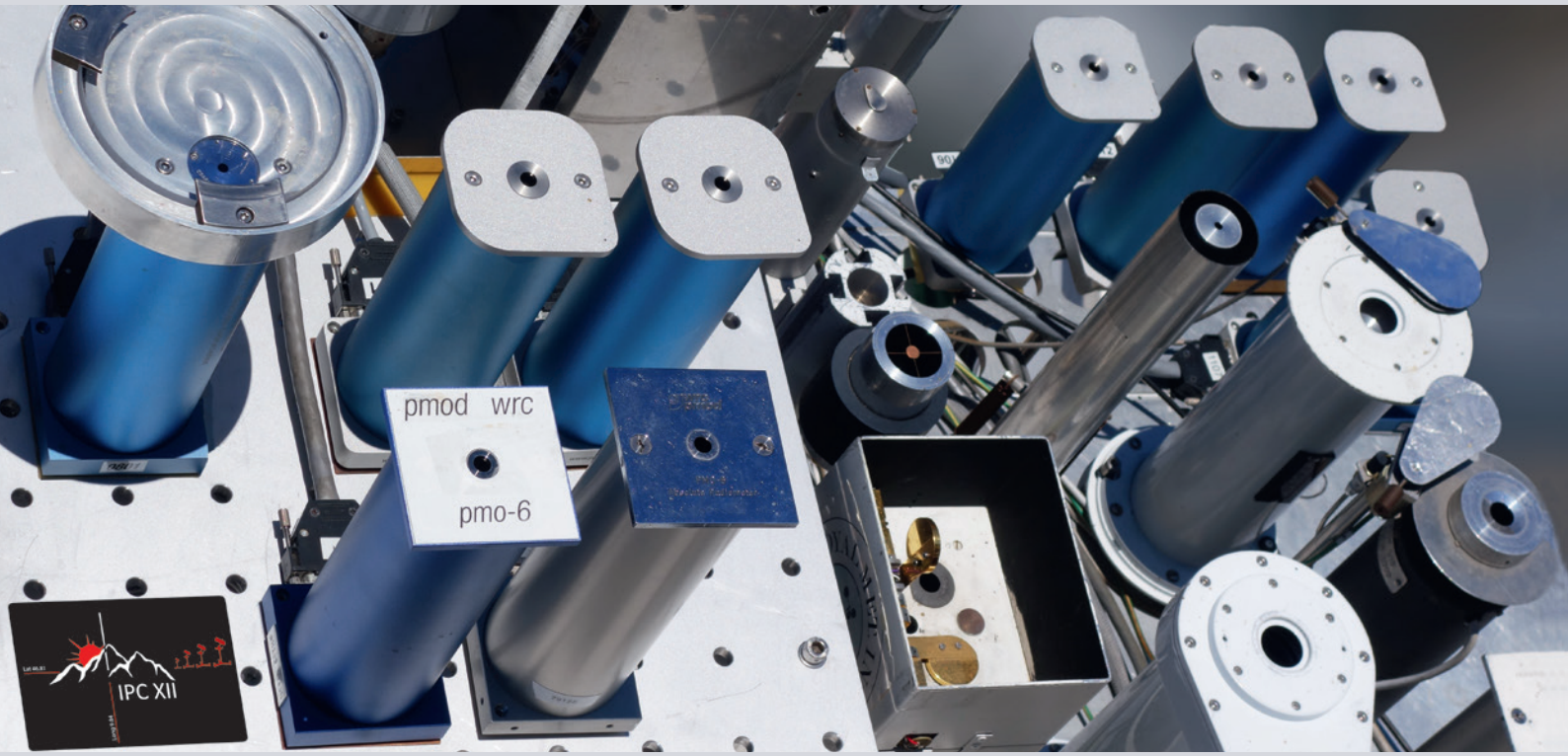

Annual Report
Jahresbericht 2015

Physikalisch-Meteorologisches Observatorium Davos und Weltstrahlungszentrum

Mission

Das PMOD/WRC

- dient als internationales Kalibrierzentrum für meteorologische Strahlungsmessinstrumente
- entwickelt Strahlungsmessinstrumente für den Einsatz am Boden und im Weltraum
- erforscht den Einfluss der Sonnenstrahlung auf das Erdklima.

Auftragerteilung

Das Physikalisch-Meteorologische Observatorium Davos (PMOD) beschäftigt sich seit seiner Gründung im Jahr 1907 mit Fragen des Einflusses der Sonnenstrahlung auf das Erdklima. Das Observatorium schloss sich 1926 dem Schweizerischen Forschungsinstitut für Hochgebirgsklima und Medizin Davos an und ist seither eine Abteilung dieser Stiftung. Auf Ersuchen der Weltmeteorologischen Organisation (WMO) beschloss der Bundesrat im Jahr 1970 die Finanzierung eines Kalibrierzentrums für Strahlungsmessung als Beitrag der Schweiz zum Weltwetterwacht-Programm der WMO. Nach diesem Beschluss wurde das PMOD beauftragt, das Weltstrahlungszentrum (World Radiation Center, WRC) zu errichten und zu betreiben.

Kerntätigkeiten

Das Weltstrahlungszentrum unterhält das Primärnormal für solare Bestrahlungsstärke bestehend aus einer Gruppe von hochpräzisen Absolut-Radiometern. Auf weitere Anfragen der WMO wurden 2004 das Kalibrierzentrum für Messinstrumente der atmosphärischen Langwellenstrahlung eingerichtet und 2008 das Kalibrierzentrum für spektrale Strahlungsmessungen zur Bestimmung der atmosphärischen Trübung. Seit 2013 wird auch das Europäische UV Kalibrierzentrum durch das Weltstrahlungszentrum betrieben. Das Weltstrahlungszentrum besteht heute aus vier Sektionen:

- Solare Radiometrie (WRC-SRS)
- Infrarot Radiometrie (WRC-IRS)
- Atmosphärische Trübungsmessungen (WRC-WORCC)
- UV Kalibrierzentrum (WRC-WCC-UV)

Die Kalibriertätigkeit ist in ein international anerkanntes Qualitätssystem eingebettet (ISO 17025) um eine zuverlässige und nachvollziehbare Einhaltung des Qualitätsstandards zu gewährleisten.

Das PMOD/WRC entwickelt und baut Radiometer, die zu den weltweit genauesten ihrer Art gehören und sowohl am Boden als auch im Weltraum eingesetzt werden. Diese Instrumente werden auch zum Kauf angeboten und kommen seit langem bei Meteorologischen Diensten weltweit zum Einsatz. Ein globales Netzwerk von Stationen zur Überwachung der atmosphärischen Trübung ist mit vom Institut entwickelten Präzisionsfilterradiometern ausgerüstet.

Im Weltraum und mittels Bodenmessungen gewonnene Daten werden in Forschungsprojekten zum Klimawandel und der Sonnenphysik analysiert. Diese Forschungstätigkeit ist in nationale, insbesondere mit der ETH Zürich, und internationale Zusammenarbeit eingebunden.

Das PMOD/WRC ist eine Abteilung der Stiftung
Schweizerisches Forschungsinstitut für
Hochgebirksklima und Medizin in Davos.

Physikalisch-Meteorologisches Observatorium Davos
und World Radiation Center (PMOD/WRC)
Dorfstrasse 33
7260 Davos Dorf
Schweiz

pmod wrc

Annual Report
Jahresbericht 2015

Table of Contents

Jahresbericht 2015

Werner Schmutz

International Pyrheliometer Comparisons IPC-XII

Die Resolution 13 des Executive Council der WMO regelt die Qualitätssicherung der weltweiten Strahlungsmessungen mit Pyrheliometer, d.h. mit Instrumenten, welche die einfallende totale Sonnenstrahlung messen. Diese sieht vor, dass das Weltstrahlungszentrum alle fünf Jahre Internationale Pyrheliometer-Vergleiche durchführt, damit die weltweit verteilten operationellen Standardinstrumente direkt mit der am PMOD/WRC stationierten Referenz-Instrumentengruppe verglichen werden können. Die elften IPC waren im Herbst 2010 und daher organisierte das Observatorium im letzten Jahr die zwölften Vergleiche vom 28. September bis 16. Oktober 2015. Analog zu den früheren Veranstaltungen wurden auch bei diesen IPCs parallel Filterradiometer- und Pyrgeometer-Vergleiche angesetzt. Schon Monate vor dem Anlass war die Mehrheit der Belegschaft mit den Vorbereitungen beschäftigt und während den Monaten September und Oktober waren praktisch alle Mitarbeiter für die Betreuung des Anlasses im Einsatz. Der Aufwand hat sich ausbezahlt und wir können auf reibungslose und erfolgreiche Vergleiche zurückblicken. Ich danke den Mitarbeitern für ihren Einsatz und kann ihnen mit Stolz auch die vielen Komplimente weitergeben, die mir von etlichen Teilnehmern zur guten Durchführung der Vergleiche gemacht worden sind. Auch der Generalsekretär der Meteorologischen Weltorganisation hat dem Observatorium in einem Anerkennungsschreiben seinen Dank ausgedrückt. Die Messresultate waren ausgezeichnet und diese lassen sich schlussendlich in genauen Kalibrierfaktoren für die teilnehmenden Instrumente ausdrücken.

Von zentraler Bedeutung für die zukünftige Rückführbarkeit der Strahlungsreferenz auf das Internationale Einheitensystem ist die Messgenauigkeit des Instruments CSAR, ein kryogenes Absolutradiometer, das in einer Kollaboration mit dem Londoner National Physical Laboratory und dem Berner Eidgenössischen Institut für Metrologie entwickelt wurde. Während den vorletzten Vergleichen wurde CSAR zum ersten Mal eingesetzt und nun konnten wir mit dem letztjährigen Vergleich nachweisen, dass das Instrument innerhalb der Vergleichsunsicherheit von 0.05% über die fünf Jahre stabil geblieben ist. Allerdings ist die absolute Genauigkeit von CSAR nur 0.4% und das Ziel ist es, diese wesentlich zu verbessern. Limitierender Faktor der absoluten Messgenauigkeit des CSAR Instruments ist die Bestimmung der Transmissionsverluste des Vakuumfensters zum kryogenen Radiometer. Diese Verluste sind abhängig vom Spektrum der einfallenden Strahlung, und das Sonnenspektrum am Boden ist wiederum abhängig von den meteorologischen Bedingungen sowie der Zenitdistanz der Sonne. Somit ist die Strahlungs-Transmission des Vakuumfensters während der Messdauer über einen Tag variabel. Das Instrument MITRA ist ein Teilsystem von CSAR, mit dem die Fenstertransmission laufend erfasst wird. Die zweite Generation des MITRA, die während den IPC-XII zum Einsatz kam, hat eine wesentliche Verbesserung dieser Messung gebracht. Trotzdem ist das eigentliche Ziel des CSAR Projektes, eine absolute Messunsicherheit von 0.01%, noch nicht erreicht. Ideen für Verbesserungen sind vorhanden und eine dritte Generation des MITRA Instruments wird in den nächsten Jahren gebaut. Es wird aber noch einige Jahre dauern, bis CSAR zur SI Realisierung der Messungen der solaren Bestrahlungsstärke wird, und daher wird voraussichtlich auch an den nächsten IPC die Davoser Weltstandardgruppe immer noch als massgebende Weltreferenz dienen.

Externes Audit

Die Vergleichskampagne im Herbst war nicht das einzige herausragende Ereignis am Observatorium Davos im vergangenen Jahr. Ebenso bedeutend für das Institut war ein Audit durch ein externes Audit-Team. Prof. Hubert van den Bergh von der ETH Lausanne leitete ein fünf-köpfiges Gremium von renommierten internationalen Wissenschaftlern, die das Observatorium Davos vom 17. bis 19. Juni unter die Lupe nahmen. Ihr Auftrag war es, sowohl die Dienstleistung als auch die Forschung am PMOD/WRC umfassend zu beurteilen. Sie überprüften alle Aktivitäten des Observatoriums, befragten die Gruppenleiter und sprachen auch mit der weiteren Belegschaft. Das Resultat war ausserordentlich erfreulich und der wesentliche Auszug aus dem Report lautet:

> *The Committee recognised that PMOD/WRC is one of the two leading institutions world-wide in the field of total solar irradiance metrology and provides very high-quality services to international and national organisations such as the World Meteorological Organisation (WMO), space agencies (in particular, ESA), and the Federal Institute of Metrology (METAS); and makes important scientific and engineering contributions to such organisations as well as to academia. The audit committee was of the opinion this success had been achieved through the close interaction between science and engineering and the personal engagement of the collaborators at the institute, and its director, who all contributed to creating a good "team spirit".*

Die Exzellenz der Institutstätigkeiten wurde durch diesen Auditbericht ausgewiesen und gelobt und ich schätze diese Anerkennung ausserordentlich hoch ein. Allerdings bemerkte das Komitee auch die Schwäche des Instituts:

> *The staff of PMOD/WRC had grown by a factor of two since about 2000, mainly due to external funding, but that this funding did not always cover the internal overhead costs which increasingly presented challenges.*

Diese Beobachtung ist durchaus zutreffend, da Einkommen aus Drittmitteln inhärent instabil sind und keine verlässliche Einnahmequelle darstellen. Dies ist insbesondere für den Bau von Weltraumexperimenten zutreffend. Das schweizweit spezielle Knowhow des Observatoriums im Bau von Weltraum Hardware sollte eine solide Grundfinanzierung haben, die zumindest die indirekten Kosten dieser Tätigkeit deckt. Diese Schwachstelle wurde nicht nur vom Audit-Komitee bemerkt, sondern wurde auch von der Aufsichtskommission des Weltstrahlungs-zentrums und dem Ausschuss der Stiftung aufgegriffen. Diese zwei Gremien haben es sich zur Aufgabe gestellt, Möglichkeiten zu evaluieren, die hier Abhilfe schaffen könnten. Man darf keinen sofortigen Erfolg erwarten, aber immerhin besteht langfristig und aufgrund des guten Audit-Resultates eine Chance auf eine positive Entwicklung für die Weltraum-Aktivität des Instituts.

Die Verlängerung des Vertrags für die Finanzierung des Weltstrahlungszentrums in der Periode 2016 bis 2019 musste letztes Jahr unterzeichnet werden. Eine Fortsetzung der Dienstleistungstätigkeit am PMOD/WRC erscheint selbstverständlich, wenn man die stetig steigende Zahl der Institute und Firmen betrachtet, die an den Internationalen Pyrheliometer-Vergleichen teilnahmen. Zudem wurde im vergangenen Jahr eine neue Rekordzahl von Instrumenten am PMOD/WRC kalibriert. In der Tat haben alle involvierten Parteien, Bund, Kanton und die Gemeinde Davos, den neuen Vertrag mit einer leicht erhöhten Finanzierung unterzeichnet. Die erneuerte Grundfinanzierung behebt ein strukturelles Defizit, das in den letzten Jahren zugenommen und eine Weiterführung aller Kalibrieraktivitäten gefährdet hatte. Ich bin den Finanzierungpartnern für ihre positive Entscheidung zugunsten unserer Dienstleistungen sehr dankbar, so dass wir diese in Qualität und Quantität uneingeschränkt weiter anbieten können.

Personelles

Ende 2014 war die Administration wegen Krankheit und Kündigung von zwei Mitarbeitern unterbesetzt und die anfallende Arbeit musste von einem kleinen Team erledigt werden. Es freut mich sehr, in diesem Report berichten zu können, dass durch die Neubesetzungen der Leitung der Administration mit Frau Barbara Bücheler und der Sekretariatsstelle mit Frau Angela Lehner wieder Stabilität und Zuverlässigkeit zurückgekehrt sind. Zusammen mit dem weiteren Team gewähren sie einen erfolgreichen Betrieb des Observatoriums.

Auszeichnung

Passend zum guten Urteil des Audits kann ich in eigener Sache berichten, dass mir die Internationale Kristian Birkeland Medaille für Weltraumwetter und Weltraumklima verliehen worden ist. Diese Medaille wird jährlich anlässlich der Europäischen Konferenz für Weltraumwetter vergeben, die letztes Jahr im November im belgischen Ostende stattgefunden hat. Die Kristian Birkeland Medaille ist eine Auszeichnung für eine Kombination von Grundlagen- und angewandter Forschung zum Bau eines Instruments zur Messung einer Grösse mit Relevanz bezüglich Weltraumwetter oder Weltraumklima. In der Laudatio wird vor allem der Beitrag des PMOD/WRC Instruments PREMOS auf dem Französischen Satelliten PICARD hervorgehoben, das als erstes SI-kalibriertes Instrument den Absolutwert der solaren Bestrahlungsstärke aus dem Weltraum bestimmt hat. PREMOS war ein Instrument, zu dessen Bau sehr viele Institutsmitarbeiter beigetragen haben. Ich verstehe daher diese Medaille vor allem als eine Auszeichnung für die hervorragenden Leistung des ganzen Instituts.

Dank

Für die Erneuerung der Grundfinanzierung des Weltstrahlungszentrums braucht es Einsatz und Beiträge von vielen Personen und Institutionen. Danken möchte ich vor allem dem Präsidenten der Stiftung SFI, Dr. Walter Ammann, und dem ständigen Delegierten der Schweiz an der Meteorologischen Weltorganisation und Direktor der MeteoSchweiz, Peter Binder, sowie dem Präsidenten der Aufsichtskommission und Stellvertretenden Direktor der MeteoSchweiz, Prof. Dr. Bertrand Calpini. Weiter waren die ehemalige Präsidentin der Aufsichtskommission des WRC, Dr. Gabriela Seiz, sowie Peter Morscher, Leiter der Finanzen und Logistik an der MeteoSchweiz, essenziell am Gelingen der neuen Finanzierung beteiligt. Die Verhandlungspartner auf Seiten Bund, Kanton Graubünden und der Gemeinde Davos waren mit ihrem Vertrauen ins Institut die Entscheidungsträger, die der Erhöhung der Finanzierung zugestimmt hatten. Ihnen allen gilt mein herzliches Dankeschön im Namen des Instituts. Die Finanzierung des Weltstrahlungszentrums ist die Basis für die gute Leistung, die von den Mitarbeitern des PMOD/WRC erbracht wird. Diesen gebührt der grösste Dank, da sie es sind, die den grundlegenden Beitrag zum Erfolg des Observatoriums Davos erbringen. Letztes Jahr war dieser grosse Einsatz auch durch den hervorragenden Audit Bericht und die Internationale Kristian Birkeland Medaille gewürdigt worden.

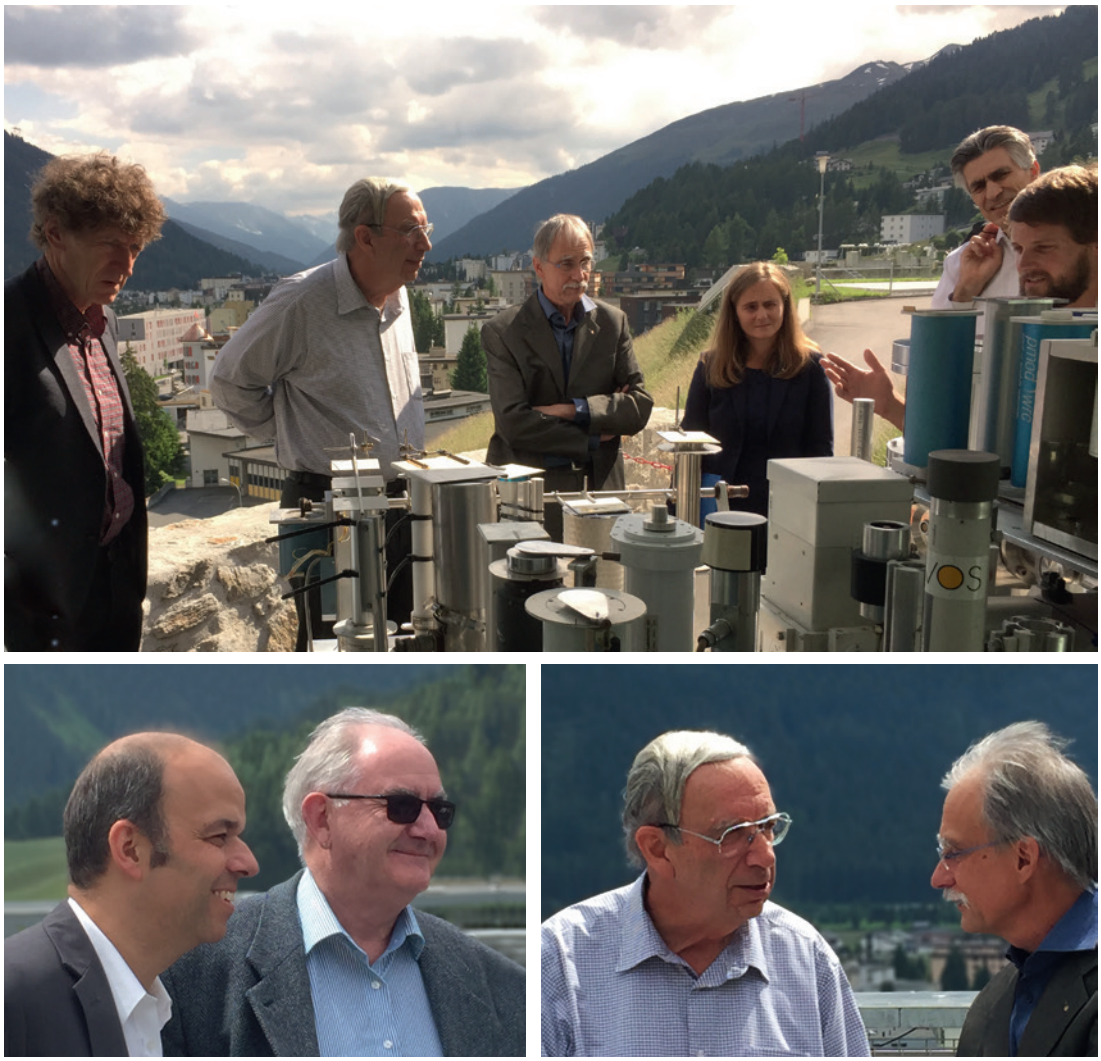

Figure 1. Top: The international panel of experts inspecting the World Standard Group at the PMOD/WRC. From left to right: Dr. Bo Andersen (Director Norwegian Space Centre), panel Chairman Prof. Hubert van den Bergh, Prof. Werner Schmutz (Director PMOD/WRC), Prof. Irena Hajnsek (ETH Zurich), Prof. Bertrand Calpini (MeteoSwiss), and Dr. Benjamin Walter (WSG Scientist). Bottom left: Dr. Peter Blattner (METAS) and Dr. Bruce Forgan (Bureau of Meteorology, Australia). Bottom right: Chairman Prof. Hubert and Prof. Werner Schmutz. Photos courtesy of Dr. Jörg Klausen (MeteoSwiss).

Introduction

Werner Schmutz

According to Resolution 13 of the WMO's Executive Council, the World Radiation Center is mandated to hold International Pyrheliometer Comparisons (IPCs) every five years. The 12th comparisons (IPC-XII) took place from 28 September to 16 October 2015 under very favourable weather conditions. Similar to previous IPCs, a simultaneous comparison of filter radiometers to determine aerosol optical depth, and a comparison of pyrgeometers, to measure infrared radiation, took place. It was the 4th Davos comparison of filter radiometers and the 2nd for pyrgeometers. Months before IPC-XII began, a large fraction of the observatory's staff was involved in preparations, while almost everyone was fully occupied with organisational duties in September and October. I am proud to state that their efforts resulted in very smooth and successful comparisons. I express my fullest appreciation of the staff's efforts and forward numerous compliments received from IPC-XII participants. The General Secretary of the WMO also expressed his appreciation of the organisation of the International Pyrheliometer Comparisons. I am glad that the hard work and dedication of the observatory staff has paid off.

Of central importance to the future of the World Radiation Center is the performance of a Cryogenic Solar Absolute Radiometer (CSAR). This project was a collaboration with two metrology institutes, the National Physical Laboratory, UK, and METAS, Bern. During IPC-XI, CSAR was operated for the first time and we now have confirmation that within the uncertainty limits of the assessment, it was stable over the last five years. The limiting factor of CSAR's absolute uncertainty is the measurement of the window transmission, which depends on the spectrum of the incoming irradiance and thus, varies throughout the day. The Monitor to measure the Integral TRAnsmittance of Windows (MITRA), a subsystem of CSAR, is the tool to measure the window transmission, and the second generation of MITRA has led to significant progress. Nevertheless, we have not yet reached the goal of an absolute measurement uncertainty of 0.01%, and ideas for a third generation of MITRA have been formulated and will be implemented in the next years. Thus, it will still take several years until CSAR becomes the primary link of the World Radiometric Reference to the SI system, and at the next IPC in 2020, the World Standard Group will still serve as the world reference.

The past year was not only dominated by IPC-XII. An audit by an external expert team took place from 17 – 19 June 2015 and was composed of five internationally renowned experts under the under the chairmanship of Prof. Hubert van den Bergh (EPFL). Their mandate was to conduct an independent comprehensive science and technology audit of the PMOD/WRC, including all aspects of the organisation and operations. They scrutinised all facets, interviewed the group leaders, and talked to the staff. I am happy to report that they came to a very favourable conclusion. Citing from the report, the summarising sentence reads:

> *The Committee recognised that PMOD/WRC is one of the two leading institutions world-wide in the field of total solar irradiance metrology and provides very high-quality services to international and national organisations such as the World Meteorological Organisation (WMO), space agencies (in particular, ESA), and the Federal Institute of Metrology (METAS); and makes important scientific and engineering contributions to such organisations as well as to academia. The audit committee was of the opinion this success had been achieved through the close interaction between science and engineering and the personal engagement of the collaborators at the institute, and its director, who all contributed to creating a good "team spirit".*

Thus, the success of the PMOD/WRC was praised, and I highly value this acclamation. However, they also recognised that the PMOD/WRC staff had grown two-fold since about 2000, mainly due to external funding, but that this did not always cover the internal overhead costs which increasingly presented challenges. It is an aspect that I also recognise. Third-party funding is inherently unstable over the long-term, and it is indeed not an optimal situation that important institute activities fully depend on the income of such projects. This is especially true when designing and constructing space hardware. The expertise at the institute should also be based on a stable foundation. This has been recognised not only by the audit committee but also by the Supervising Board of the World Radiation Center and the Board of Trustees. They have started to explore ways of obtaining core funding for PMOD/WRC activities related to Space. The outcome is difficult to anticipate, given the present challenging times when cuts in public funding are high on the political agenda. Nevertheless, given the very good outcome of the audit, the chances that various opportunities arise in the future look positive.

A renewal of the contract to fund the World Radiation Center in the next period from 2016 to 2019 was negotiated in the past year with our funding partners. A continuation would appear evident given the interest of an ever-increasing number of institutions and companies who participate in the IPCs. In addition, a new record number of instruments were calibrated in 2015. The outcome of negotiations was that all partners formally agreed to a small increase in funding to eliminate a structural deficit in our Sections offering calibration services.

Thus, the financial future of the World Radiation Center appears to have a solid foundation again. I am very thankful to our funding partners for this positive outcome and display of confidence in our motivation and expertise.

International Comparisons

The 12th International Pyrheliometer Comparison (IPC-XII)

Wolfgang Finsterle

The 12th WMO International Pyrheliometer Comparisons (IPC-XII) were organised and hosted by PMOD/WRC from 28 Sep. to 16 Oct. 2015 with 111 participants from 33 countries. New WRR factors were determined for 134 participating radiometers (Finsterle, 2016).

An increasing number of participants from the solar energy sector took part in IPC-XII (Figure 1) due to the growing demand for traceable solar irradiance data in this emerging field. IPC-XII was also held for the first time as a Euramet supplementary comparison (EURAMET, PR-S6) which allows calibration laboratories holding a current "Calibration and Measurement Capabilities" (CMC) for solar radiation to compare and validate their standards.

Weather conditions during IPC-XII allowed measurements on 11 days, although all data from 2–5 October were later rejected due to unstable atmospheric conditions. On the remaining 9 days, 578 valid WRR data points were acquired which were used to determine the new WRR factors for the six World Standard Group (WSG) and all participating radiometers. Throughout IPC-XII, an increasing nuisance was the growing fraction of high cirrus clouds induced by contrails. Although the air traffic controllers (Skyguide) were helpful by routing air traffic away from Davos whenever possible, some measurements were still adversely affected by contrails.

Unfortunately, two of six WSG instruments have not passed the stability test since IPC-XI in 2010, which therefore prevents them from being considered in the new WRR calculation. Accumulated dust in the cavities may have affected the sensitivity of the WSG instruments, HF18748 and MK67814, over the years. With help from the manufacturer and other experts, these instruments were thoroughly cleaned and put back in to service. It remains to be seen if the cleaning fixed the stability problems. On the other hand, CSAR/MITRA performed well, and work continues towards the eventual replacement of the conventional WSG standard with this new technology-based standard. The CSAR/MITRA data confirmed the previously detected WRR-to-SI scale difference of a few tenths of a percent. The CIMO Task Team on Radiation References is addressing this issue and will publish recommendations to further improve traceability of solar irradiance by harmonising both scales. Meanwhile the IPC-XII has confirmed the stability of the WRR over the past inter-IPC period, as shown in Figure 2. During bad weather the IPC-XII symposium was held, which consisted of over 40 talks and several posters. PMOD/WRC staff also helped to repair instruments which had suffered shipping damage or had otherwise failed during IPC-XII.

Figure 1. An aerial view of the IPC-XII measurement field.

References: Finsterle W.: 2016, The International Pyrheliometer Comparison IPC-XII, WMO IOM Report No. 124.

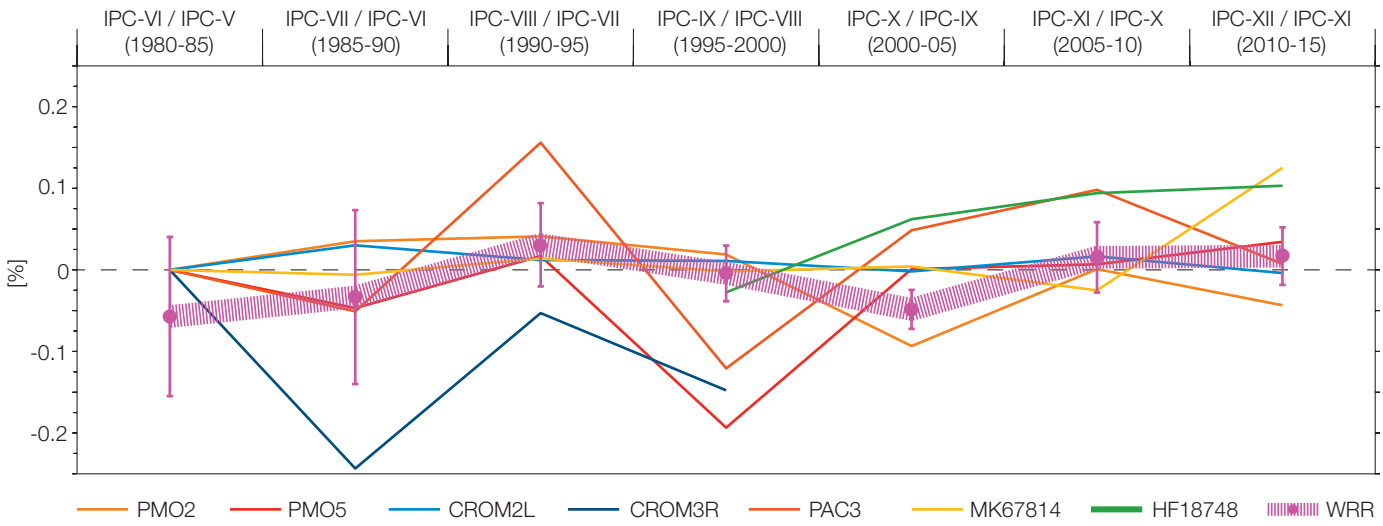

Figure 2. Changes in the WRR factors of the WSG instruments since 1980 (IPC-V) in percent compared to the preceding IPC. Note that in this analysis all WRR factors are normalised to the calibration constant C1 which was used at the time. The thick magenta line is the average of all participating cavities. This line is interpreted as the inter-IPC stability of the WSG. In this metric, any potential drift of the WSG between IPC-XI (2010) and IPC-XII (2015) was below the detection limit indicated by the 2-σ uncertainty bars. (The measured drift is 0.017 ± 0.035%.)

The 4th Filter Radiometer Comparison (FRC-IV)

Stelios Kazadzis and Natalia Kouremeti

Concurrent with the IPC-XII, the Fourth Filter Radiometer Comparison FRC-IV was held at Davos, Switzerland. Instruments belonging to different aerosol optical depth global networks were invited to participate. The comparison took place at the PMOD/WRC from 28 September to 16 October, 2015. Thirty filter radiometers and spectroradiometers from 12 countries participated in this intercomparison campaign.

The objective of this campaign was to compare different instruments belonging to different global or national networks in order to quantify the main factors that are responsible for possible deviations. The activity aims to homogenise AOD measurements on a global scale, and the comparison protocol was formulated according to the WMO (2005) recommendations. The participating instruments represented state-of-the-art filter radiometers and spectroradiometers that belong to AERONET, GAW-PFR, Skynet, SURFRAD, the Australian AOD network and others. In brief: 1) nine PFR (used in GAW-PFR network, 2) two Carter-Scott SP02, 3) three Cimel CE318 (used in AERONET), 4) four MFRSR, 5) three Precision Solar Radiometers (PSR), 6) four POM-2 sky-radiometers (SKYNET), 7) four Solar Spectral irradiance meters (Cofovo Energy Inc), and 8) a Microtops hand-held instrument.

Measurements covered the wavelength range 340–2200 nm, where the channels 368±3, 412±3, 500±3, and 865±5 nm were defined as the AOD intercomparison wavelengths. Instruments measured 1-minute AOD values when possible, and the results were evaluated for five cloudless days during the campaign. Each operator processed data using their own algorithms. A common evaluation algorithm was used, comparing all synchronous 1-minute values to the average AOD as retrieved from the WORCC PFR reference triad. The WMO recommendations for instrument comparisons concerning the number of days and measurements were fulfilled during FRC-IV. Using the U95 WMO criterion (95% of data should be within $\pm 0.005 + 0.01/m$, where m is the air mass), 26 and 24 out of 29 instruments at 500 and 862 nm, respectively, were within the limits. At 368 and 412 nm, 14 out of 20 and 16 out of 24, respectively, were within the U95 limits. It is estimated that improvements in pointing, homogenisation of inputs used in the AOD retrieval algorithm (common set of ozone cross-sections, NO_2 optical depth determination, air mass calculation and Rayleigh scattering formulas), the characterisation of instruments, and calibration of the radiometers could improve the agreement in AOD.

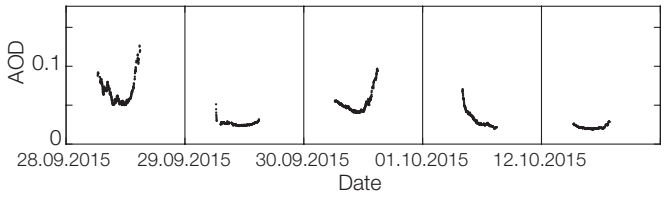

Figure 1. Overview of the diurnal variation in AOD at 500±5 nm measured by the WORCC triad during FRC-IV at Davos. The graphs show 1-minute measurements.

Concerning the determination of the Ångström exponent: Comparisons at low AOD (AOD<0.1 at 500 nm) lead to differences of about 0.5 to 1 even when AOD agreement is within the WMO limits. The results of the FRC-IV that included a large variety of AOD instruments with the participation of reference instruments from global networks, could be considered as a starting point for global AOD homogeneity initiatives. The final goal would be a unified AOD product to be used for long-term aerosol and radiative forcing studies and satellite validation related activities.

References: WMO, 2005: GAWPFR: A network of Aerosol Optical Depth observations with Precision Filter Radiometers. GAW No. 162, WMO TD No. 1287 WMO Geneva.

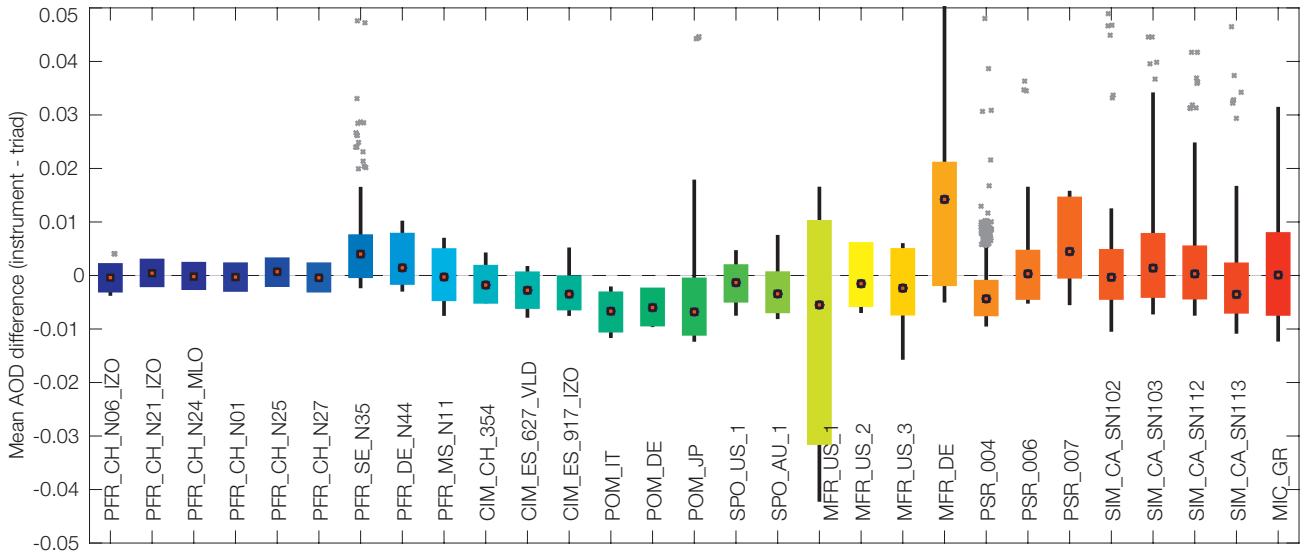

Figure 2. Mean difference of each participating instrument from the WORCC triad mean at 500 nm over five FRC-IV days. The coloured boxes represent the 10th and 90th percentiles and the black lines the minimum and maximum values of the distribution excluding the outliers.

The 2nd International Pyrgeometer Intercomparison (IPgC-II)

Julian Gröbner and Christian Thomann

The second International Pyrgeometer Intercomparison (IPgC-II) was organised in conjunction with the IPC-XII and FRC-IV at PMOD/WRC from 26 September to 16 October, 2015. Thirty-three pyrgeometers from 23 institutions and 18 countries were calibrated relative to the World Infrared Standard Group of Pyrgeometers (WISG). In addition, four IRIS radiometers and two ACPs were also operated alongside the WISG.

The participating pyrgeometers were from three manufacturers, including: 19 K&Z CG4/CGR4, 5 Eppley PIR, and 9 Hukseflux IR20. Even though most pyrgeometers were operated using the PMOD/WRC data acquisition system, several groups brought their own systems and collected the pyrgeometer signals themselves. Due to the large number of instruments, only a small sub-set could be installed at shaded positions, while the large majority was installed at unshaded positions on the roof platform. Nevertheless, all instruments were operated in ventilated units, most of them of PMOD/WRC type, while a few participants brought their own ventilation units. Figure 1 shows the roof platform on which the comparison took place.

The calibration against the WISG was obtained from atmospheric night-time measurements. Furthermore, all pyrgeometers were also placed in the PMOD/WRC blackbody cavity in order to determine their instrument parameters according to the standard PMOD/WRC equation and to derive a black-body based calibration as well.

Of the 33 pyrgeometers, 19 had been previously calibrated relative to the WISG, where their last calibration dates ranged from 2006 to 2013. The sensitivities of 15 of these pyrgeometers were within 1% or better compared to their previous calibration, as shown in Figure 2.

In view of establishing the WISG traceability to the international system of units, four IRIS radiometers and two ACP were operated during IPgC-II on the roof platform during clear nights. Measurements during the night on 29 and 30 September are shown in Figure 3. IRIS and ACP agree to within ±2 Wm^{-2}, while the WISG measured between 4–5 Wm^{-2} less. The close agreement between the IRIS, ACP and WISG during the first hours of the first night occurred during cloudy conditions when the net radiation was near zero, and the emission from the radiometer was the largest component of the downwelling long-wave irradiance. However, this is not the case during clear conditions. These measurements confirm previously published results (Gröbner et al., 2014).

The results of IPgC-II will be published in a separate WMO report.

References: Gröbner J., Reda I., Wacker S., Nyeki S., Behrens K., Gorman J.: 2014, A new absolute reference for atmospheric long-wave irradiance measurements with traceability to SI units, J. Geophys. Res. Atmos., 119, doi:10.1002/2014JD021630.

Figure 1. Roof platform of PMOD/WRC at sunrise during the pyrgeometer comparison. The WISG pyrgeometers are mounted on the far left-hand solar tracker, while the IRIS radiometers are on the unshaded roof platform, on the right-hand side.

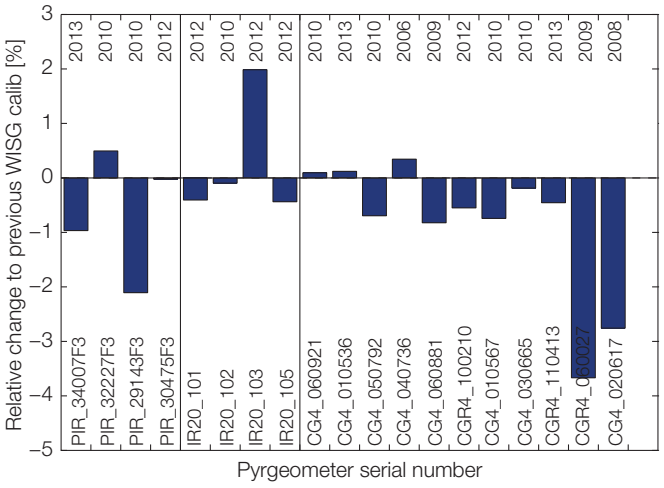

Figure 2. Sensitivity changes relative to the WISG between the current calibration during IPgC-II and a previous calibration at PMOD/WRC. The year of the previous calibration is displayed at the top of the figure.

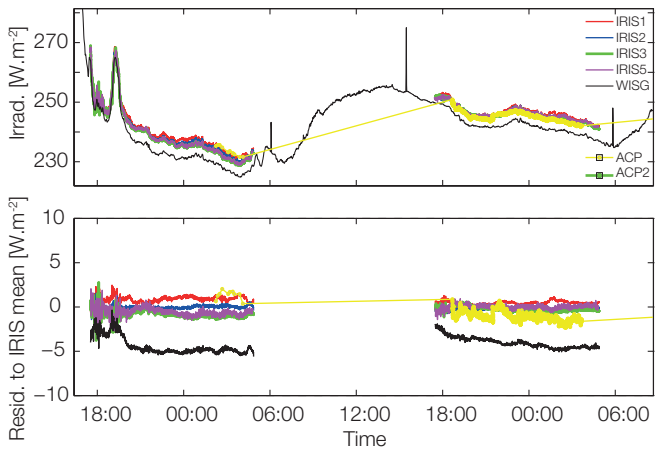

Figure 3. Measurements of downwelling long-wave irradiance from four IRIS, an ACP, and the WISG on the nights of 29 and 30 September 2015.

International Comparisons: Impressions



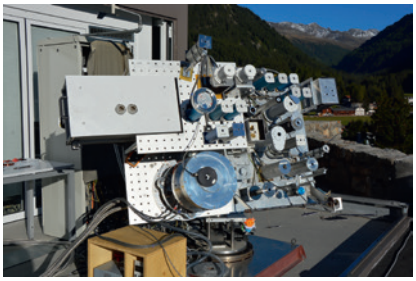

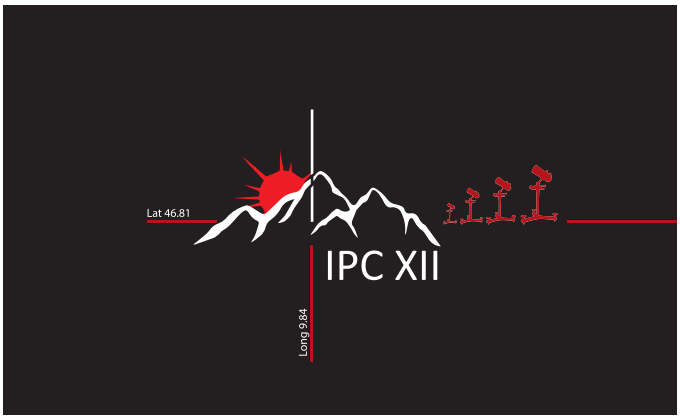







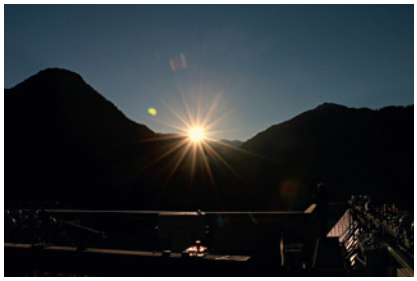







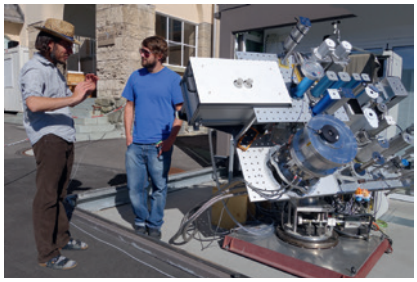


Pictures courtesy of Barbara Bücheler, Kathrin Anhorn, Stephan Nyeki

Operational Services

Quality Management System, Instrument Sales, and Calibration Services

Quality Management System

Silvio Koller and Ricco Soder

PMOD/WRC QMS

Four additional Calibration and Measurement Capabilites (CMC) of the WRC-WCC-UV calibration section were approved in January 2015. They are now listed in the BIPM key comparison database. These additional CMCs underline the relevance of the World Radiation Center.

Another important activity was the 12th WMO International Pyrheliometer Comparison IPC-XII, held at PMOD/WRC. This campaign is listed at the BIPM as a "Key and supplementary comparison" under the EURAMET.PR-S6 project. On the personnel side, the Quality Manager (QM) position was strengthened with the appointment of a deputy.

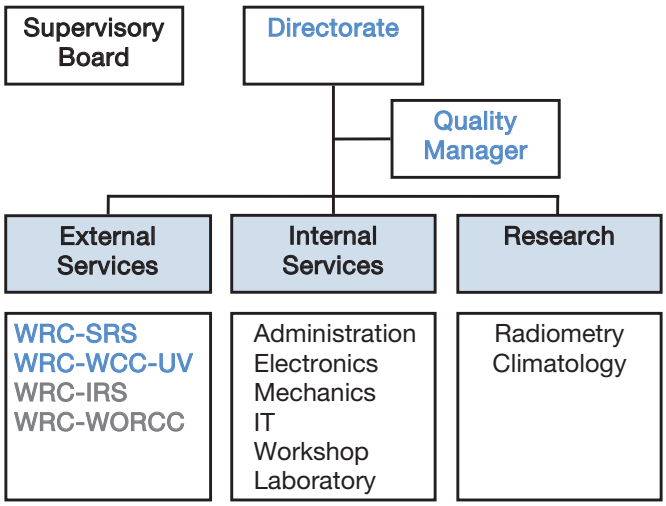

Figure 1. PMOD/WRC Quality Management System: Organisational chart. The WRC SRS and UV-WCC sections (in blue) perform calibrations according to the EN ISO/IEC standard 17025.

Quality Management System Activities

As mentioned in last year's Annual Report, a new software system was acquired to streamline administrative aspects of our Calibration Services. Shipping and accounting are now covered by an integrated tool, where accordingly, the relevant processes were updated.

The sections WRC-IRS and WRC-WORCC have not yet been fully integrated into the QM-system according to ISO-17025:2005 but work is ongoing to obtain the required documents and to update various procedures and protocols.

Instrument Sales

Daniel Pfiffner

In 2015, five PMO6-CC absolute radiometers were sold to the following customers:

- The National Metrology Institute of Germany (Physikalisch-Technische Bundesanstalt, PTB).
- Naval Research Institute, USA.
- Mc Master University, Hamilton, Canada.
- Prede, Japan.
- Central Institution for Meteorology and Geodynamics (Zentralanstalt für Meteorologie und Geodynamik, ZAMG), Austria.

Two Precision Spectroradiometers (PSR) were sold to:

- The Bureau of Meteorology (BOM), Melbourne, Australia.
- National Observatory of Athens (NOA), Greece.

A PSR cosine diffuser was also sold to the National Meteorological Service of Germany (Deutscher Wetterdienst, DWD). An overview of instrument sales statistics is shown in Figure 2. Overall sales in 2015 continued the upward trend since 2013. An increase in the number of PMO6-CC sold is particularly evident, and now once again reflects the volume of previous sales.

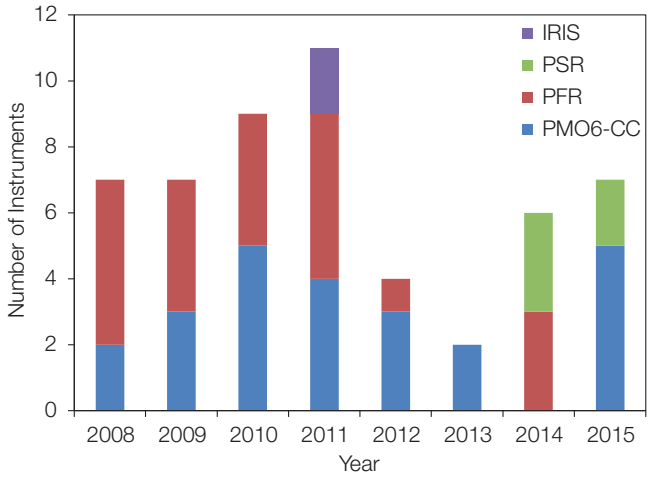

Figure 2. Number of PMOD/WRC instruments sold since 2008. IRIS = Infrared Integrating Sphere Radiometer, PSR = Precision Spectroradiometer, PFR = Precision Filter Radiometer, and PMO6-CC = absolute cavity pyrheliometer.

Calibration Services

Silvio Koller, Wolfgang Finsterle, Julian Gröbner

The overall number of calibrations reached an all-time record high in 2015 (Figure 3), mainly through calibrations conducted by the WCC-UV and IRS sections.

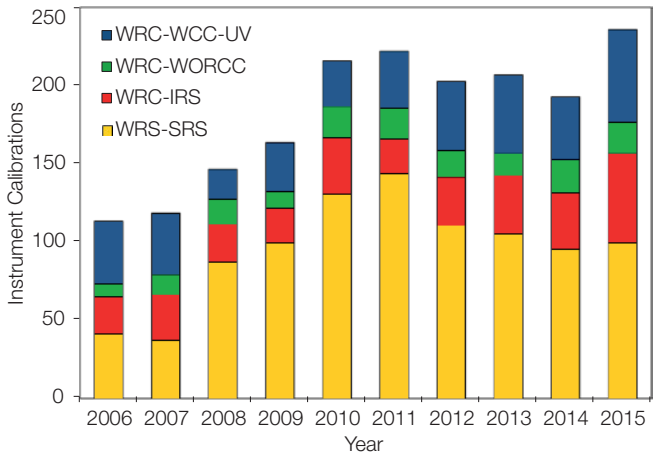

Figure 3. Statistics of instrument calibrations at PMOD/WRC for the 2006–2015 period.

Solar Radiometry Section (WRC-SRS)

In 2015, the WRC-SRS section calibrated 22 pyrheliometers and 78 pyranometers. All certificates were issued with the CIPM logo. The CLARA space instrument, an absolute radiometer on the Norwegian NORSAT-1 mission, was calibrated against the NIST traceable TSI Radiometer Facility (TRF). The TRF is a cryogenic radiometer, located at LASP, Boulder CO.

Infrared Radiometry Section (WRC-IRS)

The WRC-IRS section performed 53 pyrgeometer and 4 IRIS calibrations in 2015.

Atmospheric Turbidity Section (WRC-WORCC)

The WRC-WORCC section calibrated 15 precision filter radiometers (PFR) against the WORCC triad standard. In addition, five precision solar spectroradiometers (PSR) were calibrated against a reference standard, traceable to the National Metrology Institute of Germany. Since April 2015, Dr. Stelios Kazadzis has been in charge of the section WRC-WORCC.

World Calibration Center for UV Section (WRC WCC-UV)

The following number of radiometers were calibrated in 2015: 14 UVB, three UVA, two UV-Global, one dual channel (UVA/UVB) broadband. In addition, seven lamps/diodes were calibrated by the WCC-UV section. These calibrations resulted in 34 certificates, 8 of them with the CIPM logo. The WCC-UV section performed three quality assurance site audits of solar UV monitoring spectroradiometers at their respective field sites using the QASUME travelling reference spectroradiometers. Over the period May to June 2015, 21 Brewer spectrophotometers were calibrated relative to the QASUME spectroradiometer during the 10th RBCC-E campaign at INTA, El Arensillo, Spain.

Solar Radiometry Section (WRC-SRS)

Wolfgang FInsterle

The Solar Radiometry Section (SRS) of the WRC maintains and operates the World Standard Group of Pyrheliometers (WSG) which represents the World Radiometric Reference (WRR) for ground based total solar irradiance measurements. Apart from the ordinary calibration activities, the 12th International Pyrheliometer Comparison was organised and held in 2015.

In 2015, the SRS of the World Radiation Center calibrated 101 radiometers: 78 pyranometers, 16 pyrheliometers with thermopile sensor and 7 absolute cavity radiometers. The WSG was operated on 65 days and the Cryogenic Solar Absolute Radiometer and Monitor for Integrated Transmittance (CSAR/MITRA) on 20 days (see article by Benjamin Walter).

The SRS was also heavily involved with the calibration of the CLARA space radiometer. After CLARA had passed all mechanical, thermal and electrical tests, SRS scientist Benjamin Walter together with PMOD/WRC engineer Pierre-Luc Lévesque, took CLARA to the TSI Radiometer Facility (TRF) in Boulder, USA for end-to-end calibration against a NIST traceable cryogenic radiometer (Figure 2).

The versatile beam-tailoring offered by the TRF was then used to validate the diffraction correction as well as to determine the scattered light contribution. Following the TRF calibration campaign, CLARA was then delivered to the University of Toronto's Institute for Aerospace Studies Space Flight Laboratory (UTIAS-SFL) for integration into the NORSAT-1 satellite (Figure 1). The calibration of CLARA has been co-funded by the European Metrology Research Programme, EMRP-ENV53 "Metrology for earth observation and Climate, MetEOC-2".

Figure 1. PMOD/WRC engineer Pierre-Luc Lévesque installing the CLARA radiometer in the TRF vacuum tank in Boulder, USA.

In June, the absolute cavity radiometer for THz radiation was delivered to the Physikalisch-Technische Bundesanstalt (PTB), Berlin. The THz radiometer was developed within the EMRP-NEW07 project (Microwave and THz metrology for homeland security). The final meeting of this project took place at PMOD/WRC in conjunction with a workshop in May.

A new research project to understand sensor degradation of absolute cavity radiometers in Space and to develop an improved sensor coating was selected for funding by the Swiss National Science Foundation. Because it has taken longer than expected to fill the vacancy with a PhD student, the commencement of the project had to be postponed from November 2015 to June 2016. This project is in collaboration with the University of Zurich.

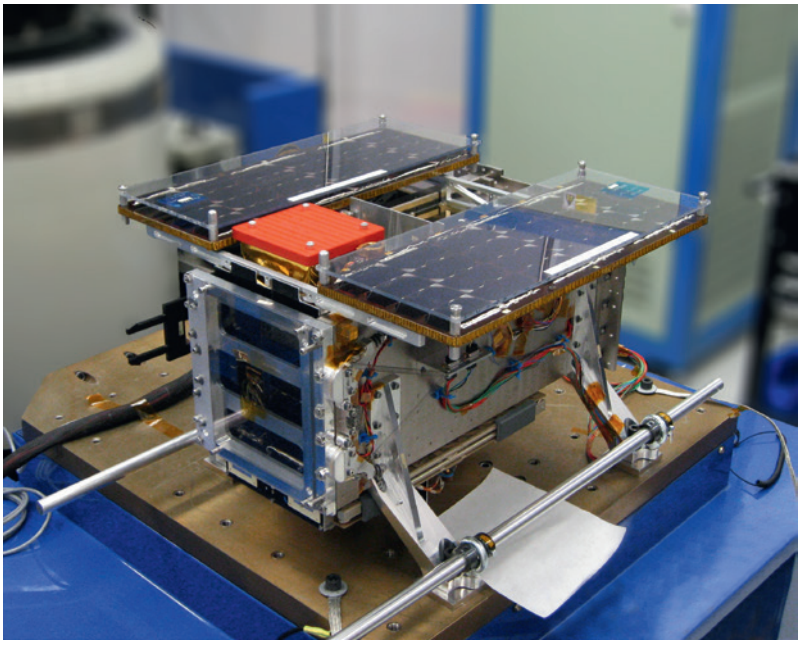

Figure 2. CLARA (seen with red protective cover) was integrated into the NORSAT-1 satellite at the University of Toronto, Canada, in October 2015.

Infrared Radiometry Section (WRC-IRS)

Julian Gröbner, Christian Thomann and Stephan Nyeki

The Infrared Radiometry Section of the WRC maintains and operates the World Infrared Standard Group of Pyrgeometers (WISG) which represents the world-wide reference for atmospheric long-wave irradiance measurements.

Most of the activities of 2015 centred on the organisation and operation of the second International Pyrgeometer Comparison (IPgC-II) which was held during IPC-XII, from 26 September to 15 October 2015. The intercomparison resulted in the issuance of 33 calibration certificates, providing formal traceability of atmospheric downwelling long-wave irradiance to 23 participants from 18 countries.

The four IRIS radiometers were operated on the roof platform of PMOD/WRC during 63 nights alongside the WISG, confirming the results previously published by Gröbner et al., 2014. Figure 1 shows the four IRIS radiometers in operation during the IPgC-II, as well as the Absolute Cavity Pyrgeometer (ACP) in the background. Currently, the World Infra-Red Standard Group (WISG) acts as the reference for atmospheric long-wave irradiance measurements. A Task Team on Radiation References was established by the Commission for Instruments and Methods of Observation (CIMO) in 2014, to address the implications of the observed differences between these radiometers providing traceable measurements of atmospheric long-wave radiation and the WISG.

In October 2015, a novel pyroelectric detector with a nanotube coating was installed in IRIS4, in a joint collaboration with Dr. John Lehman from the National Institute of Standards and Technology (NIST, USA) and Dr. Theo Theocharous from the National Physical Laboratory (NPL, England). The main advantage of this detector over those currently in use is the very high uniform spectral responsivity which is obtained by coating it with a black substance composed of a vertically aligned nanotube array (VANTA).

This detector was previously characterised in NPL's detector characterisation facilities, demonstrating its extremely uniform relative spectral responsivity over the 0.8 – 24 µm wavelength range (Theocharous et al., 2013). The VANTA detector was mounted on IRIS4 and evaluation started in the PMOD/WRC blackbody facility at the end of 2015. Measurements with the upgraded IRIS4 are expected to begin in 2016.

References: Gröbner J., Reda I., Wacker S., Nyeki S., Behrens K., Gorman J.: 2014, A new absolute reference for atmospheric longwave irradiance measurements with traceability to SI units, J. Geophys. Res. Atmos., 119, doi:10.1002/2014JD021630.

Theocharous E., Theocharous S.P., Lehman J.H.: 2013, Assembly and evaluation of a pyroelectric detector bonded to vertically aligned multi-walled carbon nanotubes over thin silicon, Appl. Opt., 52, 8054–8059.

Figure 1. IRIS radiometers in operation on the PMOD/WRC roof platform during IPgC-II. The Absolute Cavity Pyrgeometer (ACP) from the National Renewable Energy Lab. (NREL; USA) can be seen on the left-hand side, at the back of the platform.

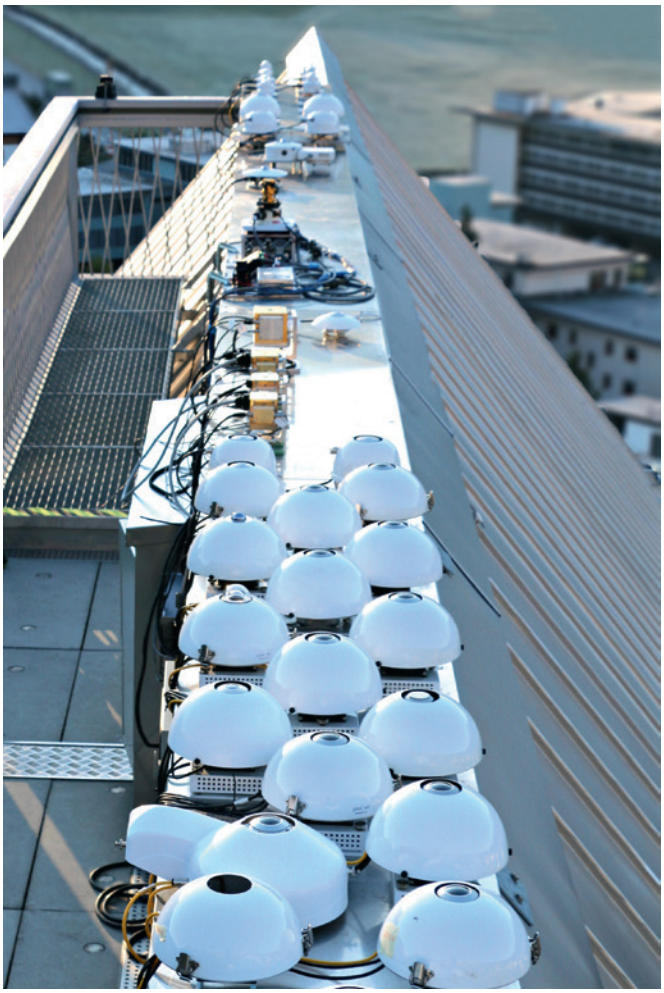

Figure 2. View of the PMOD/WRC roof-platform during IPgC-II, showing pyrgeometers in the foreground.

Atmospheric Turbidity Section (WRC-WORCC)

Stelios Kazadzis, Natalia Kouremeti, Julian Gröbner

The Atmospheric Turbidity Section of the WRC maintains a standard group of three Precision Filter Radiometers (PFR) that serve as a reference for Aerosol Optical Depth (AOD) measurements within the WMO. WORCC also operates the global GAW-PFR AOD network.

The PFR reference triad has been operating near continuously since early 2005. Two PFR instruments operating at Izaña (Canary Islands) and one at Mauna Loa (Hawaii) were used in an intercomparison with the triad during August–September, 2015. Two of the triad PFRs showed differences <0.5% at all wavelengths and the third from 1 to 1.1% for three out of four wavelengths. This latter PFR has been re-calibrated.

The Fourth Filter Radiometer Comparison FRC-IV was held at PMOD/WRC from 28 September to 16 October, 2015. Thirty filter radiometers and spectroradiometers from 12 countries and different global and national aerosol networks participated in this campaign. The WMO recommendations on AOD related intercomparisons were fulfilled. In summary, 26 and 24 instruments out of 29 at λ = 500 nm and 862 nm, respectively, were in good agreement with the WMO criterion (95% of measurements should be within ±0.005 + 0.01/*m*; where *m* = airmass) compared with the average triad AOD.

Annual quality assured data from 4 GAW-PFR stations were updated to 2015 and submitted to WDCA. Daily AOD results from 21 stations are submitted in (quasi) near real-time and are available through ebas.nilu.no within 24 hours. In 2015, six instruments of the extended GAW-PFR network were calibrated against the reference triad. In addition, customer instruments were re-calibrated in the course of repair works.

A lunar PFR was installed at Ny Ålesund from October 2014 to February 2015, to measure AOD using the moon as a light source. The lunar PFR was sent to Izaña in Spring 2015 and was re-calibrated. The PFR was then returned to the PMOD/WRC for instrument upgrade, related to the sensitivity increase of 3 out of 4 channels and the reduction of noise (modifications on the electronic board), as well as necessary modifications for the integration of the new acquisition system. In addition, the instrument was characterised by measuring its filter characteristics and the non-linearity using an ATLAS/ESA (newly purchased tunable laser system). The activity is being conducted within the framework of a project funded by the Svalbard Science Foundation in collaboration with partners from NILU (Norway), ISAC/CNR (Italy), AWI (Germany), NOAA/CIRES (US), and IGF/ PAS (Poland).

The WORCC section has commenced a collaboration with SKYNET Europe and SKYNET Asia by installing two PFR instruments at Valencia, Spain and Chiba, Japan. SKYNET is a network to study aerosol-cloud-radiation interactions in the atmosphere with most stations located in Asia and Europe. The collaboration aims to homogenise AOD measurements in different global networks. The instruments will perform synchronous measurements with sky radiometers belonging to the SKYNET and AERONET networks.

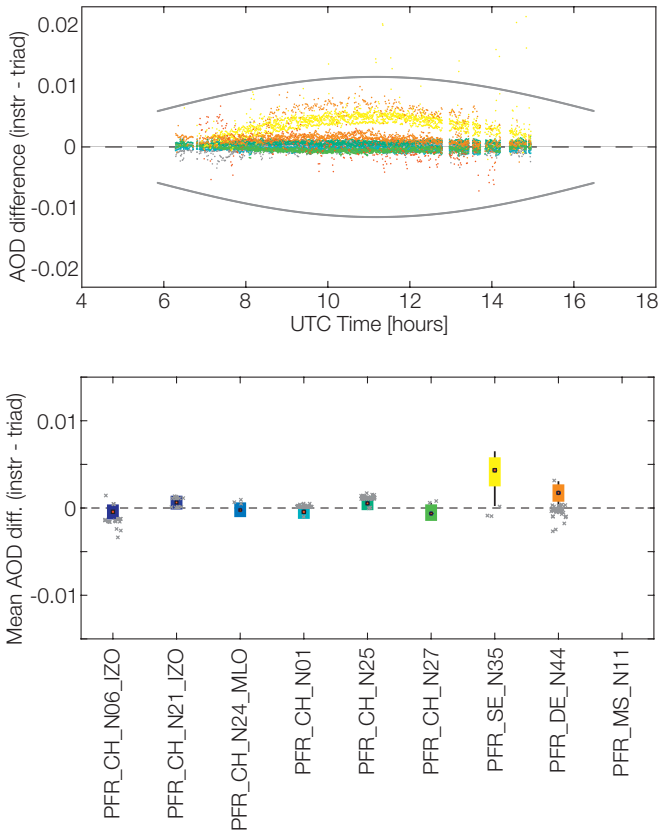

Figure 1. Performance of eight PFR instruments (λ = 500 nm) during the FRC-IV at 500 nm. Top: AOD differences with respect to the WORCC reference triad (grey lines represent the WMO limits). Bottom: AOD mean differences and 5th to 95th percentiles.

As part of the project, "A travel standard for Aerosol Optical Depth in the UV", the UV version of the PFR (UV-PFR) was tested as a reference instrument to calibrate Brewer spectrophotometers for the determination of AOD. After instrument modifications and calibration, the UV-PFR participated in a campaign as part of the Regional Brewer Calibration Center-Europe which was held in Huelva, Spain. During this campaign, 21 Brewer spectrophotometers belonging to the EUBREWNET, were calibrated for AOD against the UV-PFR.

Four Precision Spectroradiometers (PSR) were characterised and tested at PMOD/WRC. The instruments were sold and deployed in Germany (2), Australia and Greece. Three of them participated in the FRC-IV and provided spectral AOD. These three were modified to include a second solar input option for measuring global horizontal irradiance in addition to the direct sun measurements.

World Calibration Centre for UV (WRC-WCC-UV)

Julian Gröbner, Gregor Hülsen, and Luca Egli

The Global Atmosphere Watch (GAW) Ultraviolet (UV) calibration centre aims to improve data quality in the Global GAW UV network. It also aims to harmonise the results from different stations and monitoring programmes in order to ensure representative and consistent UV radiation data on a global scale.

The transportable reference spectroradiometer, QASUMEII, developed within the EMRP Project SolarUV, was extensively tested during Summer and Autumn 2015. A long-term intercomparison to QASUME revealed its outstanding performance for solar UV measurements. Only minor adjustments of the instrument and the measuring procedure were necessary to successfully validate the second WCC-UV reference spectroradiometer. A publication about this activity will be submitted in the near future (Hülsen et al., 2016). One of the conclusions is that a nearly two-fold reduction in the uncertainties of solar UV irradiance measurements is possible.

From May till June 2015, WRC-WCC-UV participated in the 10th Regional Brewer Calibration Centre - Europe (RBCC-E) campaign in El Arenosillo, Spain. The reference for solar UV irradiance measurements was made available to the participating spectroradiometers. During this intercomparison, 21 Brewer spectrophotometers were calibrated relative to the QASUME reference spectroradiometer.

QASUME was used during three additional quality assurance site visits which had all been previously visited. These included:

1) The solar UV monitoring site at Innsbruck, Austria, which serves as a reference site for the Austrian UV network (www.uv-index.at). A third visit occurred in 2015 (previous visits in 2002 and 2010).

Figure 1. Participants at the 10th RBCC-E in El Arenosillo, Spain.

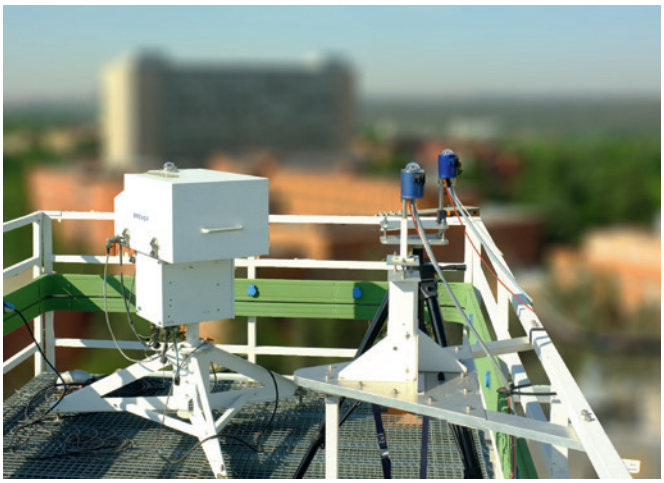

Figure 2. QASUME site audit in Madrid to assess the quality of the Brewer #186 spectrophotometer and the AEM Bentham DM300 double monochromator.

2) The Agenzia Regionale per la Protezione dell Ambiente in the Valle d´Aosta in Italy. A sixth visit occurred in 2015.

3) The Agencia Estatal de Meteorologia of Madrid, Spain. A fourth visit occurred in 2015 to perform a comparison of solar UV irradiance measurements between the local spectroradiometers and QASUME.

The main objective of the EMRP project ENV59-ATMOZ "Traceability for atmospheric total column ozone" is to provide a framework for traceable measurements of total column ozone measurements for standard ozone monitoring instruments, e.g. Brewer and Dobson, as well as modern diode-array based spectroradiometer systems. Apart from coordinating an international consortium of national metrology institutes, designated institutes and experts from the end-user community, PMOD/WRC is also developing models to determine the uncertainties inherent in total column measurements, as well as developing a high resolution spectroradiometer based on a CCD detector.

Results of all the QASUME site audits can be found on the WCC-UV web-site:

http://www.pmodwrc.ch/wcc_uv/wcc_uv.php?topic=qasume_audit.

References: Hülsen G., Gröbner J., Nevas S., Sperfeld P., Egli L., Porrovecchio G., Smid M.: 2016, Applied Optics, submitted.

The Cryogenic Solar Absolute Radiometer (CSAR)

Benjamin Walter, Wolfgang Finsterle, Nathan Mingard, and Ricco Soder

The Cryogenic Solar Absolute Radiometer (CSAR) aims to reduce the uncertainty of terrestrial direct total solar irradiance measurements from 0.3% to 0.01% and is intended to become the link between the World Radiometric Reference (WRR) and the International System of Units (SI) in the future. CSAR will provide direct traceability of worldwide solar irradiance measurements back to the SI system. CSAR was installed at PMOD/WRC in April 2015 to be extensively tested and prepare for participation in IPC-XII. CSAR measurements performed in 2015 agreed well with previous findings of a ~0.3% lower SI radiometric scale relative to the WRR scale with a comparison uncertainty of 0.053%.

Direct Solar Irradiance (DSI) measurements are traceable to the artefact-based World Radiometric Reference (WRR) hosted by PMOD/WRC in Davos. A recent comparison of the WRR-scale to the International System of Units (SI) scale showed a significant difference of about 0.34% ± 0.09% (k = 1) between both scales (Fehlmann, 2012). To reduce the measurement uncertainty of DSI measurements from 0.3% down to 0.01%, and to provide direct traceability back to the SI scale, the Cryogenic Solar Absolute Radiometer (CSAR; Winkler, 2012) was built by the National Physical Laboratory (NPL), METAS and the PMOD/WRC.

The radiation absorbing cavities of CSAR (Figure 1) are operated under vacuum at cryogenic temperatures (~20K) to eliminate various negative thermal effects. The solar radiation entering CSAR is partly reflected and absorbed by the window. The spectrally integrated window transmittance for the solar radiation needs to be monitored in parallel to correct the power reading of CSAR for these losses. The 'Monitor to measure the Integral TRAnsmittance of Windows' (MITRA) aims to measure the window transmittance with an uncertainty <0.01% (Walter, 2014).

CSAR was returned to DAVOS in April 2015 after four years of further development at the NPL. The main technical improvements include changes to the cooling system resulting in a more stable

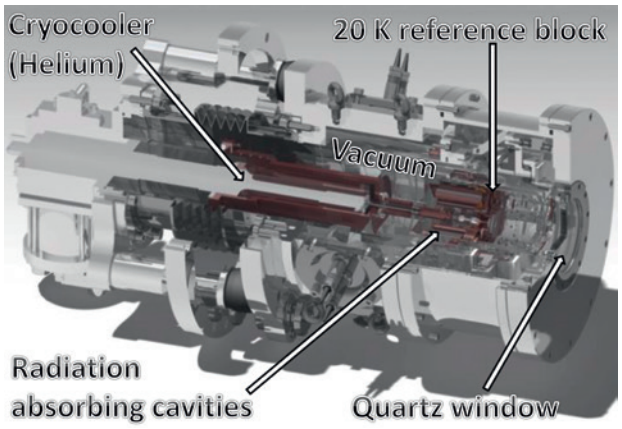

Figure 1. Drawing of the CSAR instrument. The cavities are heated by the absorbed solar radiation. The temperature rise of the cavities relative to the cooled 20 K reference block is proportional to the solar irradiance. Reflection and absorption losses of the quartz window are monitored using MITRA to correct the power readings of CSAR for these losses.

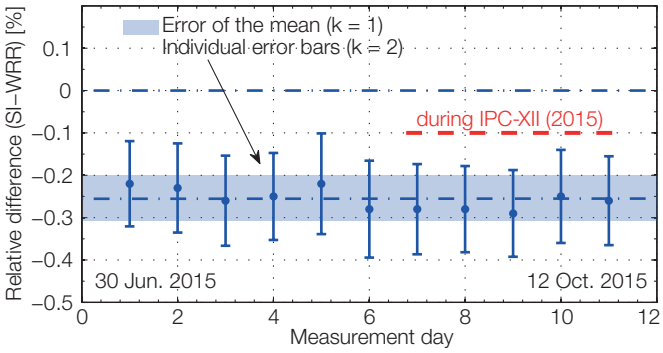

Figure 2. Daily averages of 11 WRR to SI intercomparisons performed at PMOD/WRC with CSAR. The last five intercomparisons were performed during the IPC-XII.

reference block temperature. After the installation and commissioning phase, CSAR was extensively tested on the sun-tacking platform to be ready for the 12th International Pyrheliometer Comparison (IPC-XII) in September 2015. Improvements to MITRA mainly include detailed testing and fine-tuning of the instrument and the implementation of a re-calibration procedure applied to the cavity thermometers to better account for instrument temperature drifts.

First results (Figure 2) indicate an SI scale difference -0.26±0.053% (k = 1) with respect to the WRR which agrees with past findings of a lower SI scale (Fehlmann, 2012). It is intended that CSAR regularly participates in SI cryogenic radiometer intercomparisons to guarantee its SI stability. An official transition from the WRR to the SI-scale for DSI measurements is expected to take place within the next 5–10 years.

The MITRA uncertainty (~0.36%) dominates the CSAR uncertainty (~0.39%) at present. Future improvements to MITRA will include a new heatsink design with three instead of two cavities. The third cavity will always be shaded and used to track parasitic heatflows between the cavities and the heatsink, resulting from instrument temperature drifts. Simulations have shown that these dark measurements can be used to finally eliminate any influence of instrument temperature drifts on the integral transmittance measurements, making a numerical correction or thermometer re-calibration unnecessary.

References:

Fehlmann A. et al., 2012: Fourth World Radiometric Reference to SI Radiometric Scale Comparison, Metrologia, 49, 34–38.

Walter B. et al., 2014: Spectrally integrated window transmittance measurements for a cryogenic solar absolute radiometer, Metrologia, 51, 344–349.

Winkler R.: 2012, Cryogenic Solar Absolute Radiometer - a potential replacement for the World Radiometric Reference, PhD Thesis, Univ. College.

Validation of the New Transportable Reference Spectroradiometer QASUMEII

Gregor Hülsen and Julian Gröbner

A second UV reference spectroradiometer QASUMEII was constructed and validated relative to its forerunner QASUME. A total of 1443 synchronised solar scans were within the uncertainty of 3.7%. The new hybrid detector of QASUMEII can be used to detect long-term sensitivity changes and diurnal variabilities.

Within the Joint Research Project, "Traceability for surface spectral solar ultraviolet radiation", a second portable reference spectroradiometer was constructed. It was fitted with an improved global entrance optic and a newly developed hybrid device, consisting of a photomultiplier and a solid-state detector (SSDS).

During a long-term campaign the new reference spectroradiometer QASUMEII was validated against QASUME in 2015. Synchronised scans were acquired from sunrise to sunset every half-hour for the wavelength range 290–500 nm with 0.25 nm increments. The validation campaign started on day of year (DOY) 196, 15 July, and lasted until DOY 300, 27 October. On clear sky days, QASUME data were corrected for the cosine error of the input optic.

Both data-sets were further processed using the matSHIC algorithm which applies a deconvolution technique based on a high resolution reference solar spectrum, to adjust the wavelengths of the measured solar spectrum to this reference spectrum. Finally, a solar spectrum with a nominal resolution of 1 nm is obtained by convolving the high resolution reference spectrum, and applying the spectral irradiances of the originally measured solar spectrum. The two QASUME systems were calibrated regularly during the comparison using portable 250 W lamps. QASUME stayed within ±1% whereas the responsivity of QASUMEII changed by 3% on DOY 245 due to a repair of the entrance optic.

The long-term stability of the SSDS Si-diode relative to the photomultiplier (SSDS ratio) was validated against the external lamp calibrations. Figure 1 shows the good agreement between these two monitoring schemes. Data from the spectral lamp calibrations (red line) were averaged for the comparison in the wavelength band 450±2.5 nm. The SSDS ratio measurement not only reveals the long-term responsivity change of the system, but also diurnal variability. During a clear sky day, the responsivity of the photocounter changed by up to 3%. The diurnal change of the SSDS ratio (Fig. 2) is used to compensate for this observed variability.

The statistics of the spectral average ratio of QASUMEII to QASUME summarise the results of the validation campaign. Up to 1443 out of 2060 synchronised solar irradiance scans are available for the calculation. The mean ratio has an offset of +0.7% and a standard deviation of ±1.5% for wavelengths greater than 305 nm. The performance throughout the intercomparison period is shown in Figure 3, which displays the mean spectral ratio between QASUMEII to QASUME for the wavelength bands 310, 350 and 495 nm for each individual scan. The bands have a width of ±2.5 nm. All comparison points are within a combined expanded uncertainty (*U*) of ±3.7% (*k*=2).

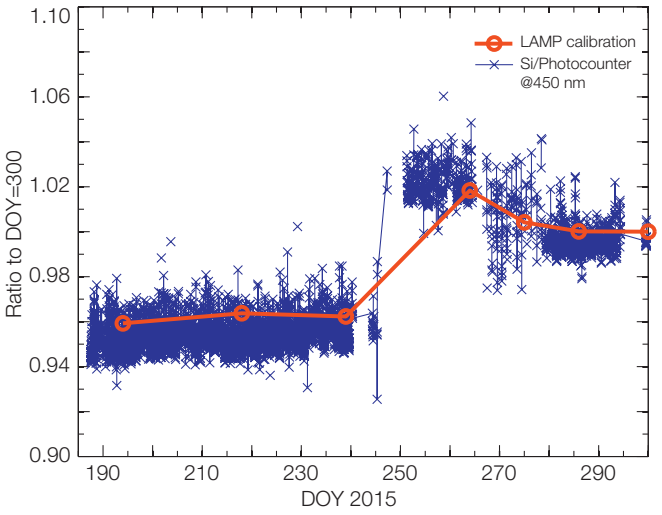

Figure 1. QASUMEII responsivity change as detected by Si-diode to photocounter ratio at 450 nm (blue) and the regular lamp calibrations (red).

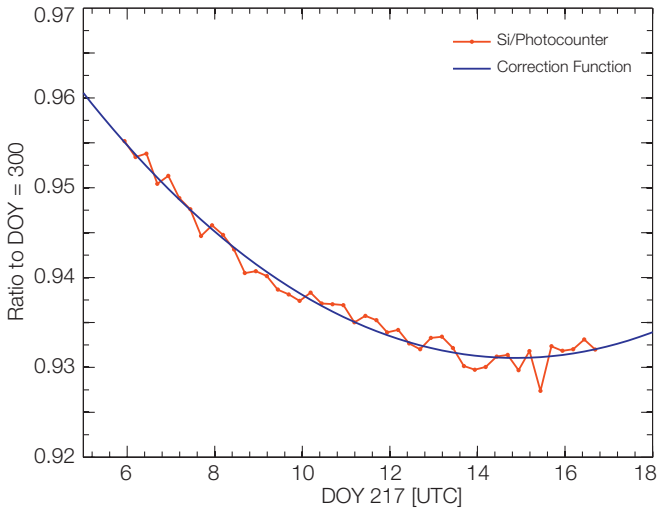

Figure 2. Diurnal variability of the ratio Si-Diode to photocounter ratio for a clear sky day with a large change in irradiance (UVI 0–8.5). The blue line shows the fitted correction function to compensate for photocounter hysteresis.

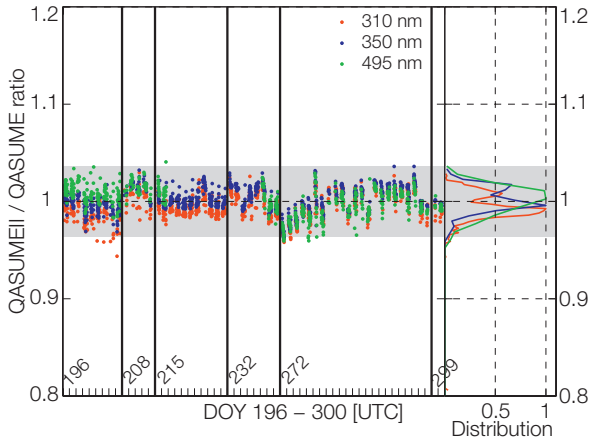

Figure 3. The mean ratios between the two reference spectroradiometers are within the combined measurement uncertainty (grey shading). The five thick vertical lines indicate interruptions during the intercomparison.

The Infrared Cloud Camera (IRCCAM)

Julian Gröbner, Christine Aebi, Ricco Soder, and Pascal Schlatter

The Infrared Cloud Camera (IRCCAM) measures the thermal emission of the atmosphere in the 8–14 µm wavelength range in order to determine the cloud-cover during the day and night.

The IRCCAM consists of a commercial thermal camera, which is sensitive in the 8–14 µm wavelength range, and a convex gold-plated mirror which images the whole upper hemisphere of the sky. The camera was calibrated in the PMOD/WRC reference blackbody over the -20–20°C temperature range, with an uncertainty of ±1 K.

Sky images are taken routinely every 1–minute during 24 hours in a day. An onboard microprocessor acquires the raw images and stores them for further analysis. The processing algorithm consists of the following steps:

- Conversion from raw counts to effective radiation temperature.
- Correct image distortion.
- Mask horizon and camera.
- Determine cloud mask.
- Save data.

Figure 1 shows an image taken with a traditional visible hemispherical camera at the top and an image by IRCCAM at the bottom. While the visible sky image (middle) shows the cloud structure at visible wavelengths, the IRCCAM thermal sky image not only shows the structure, but also the radiation temperature of the sky and clouds.

A cloud mask is generated for each image by choosing all pixels with a temperature above a background threshold based on: 1) clear sky radiative transfer calculations using Modtran, and 2) ambient temperature and integrated water vapor as input parameters.

The lower image in Figure 1 shows the corresponding image containing only the clouds and after removal of the background sky. The cloud fraction for this image is 79%, while the visible image gives a cloud fraction of 71%. Future developments will be to refine the algorithm to also detect cirrus clouds and cloud height, and to validate the cloud height retrieval using ceilometer data.

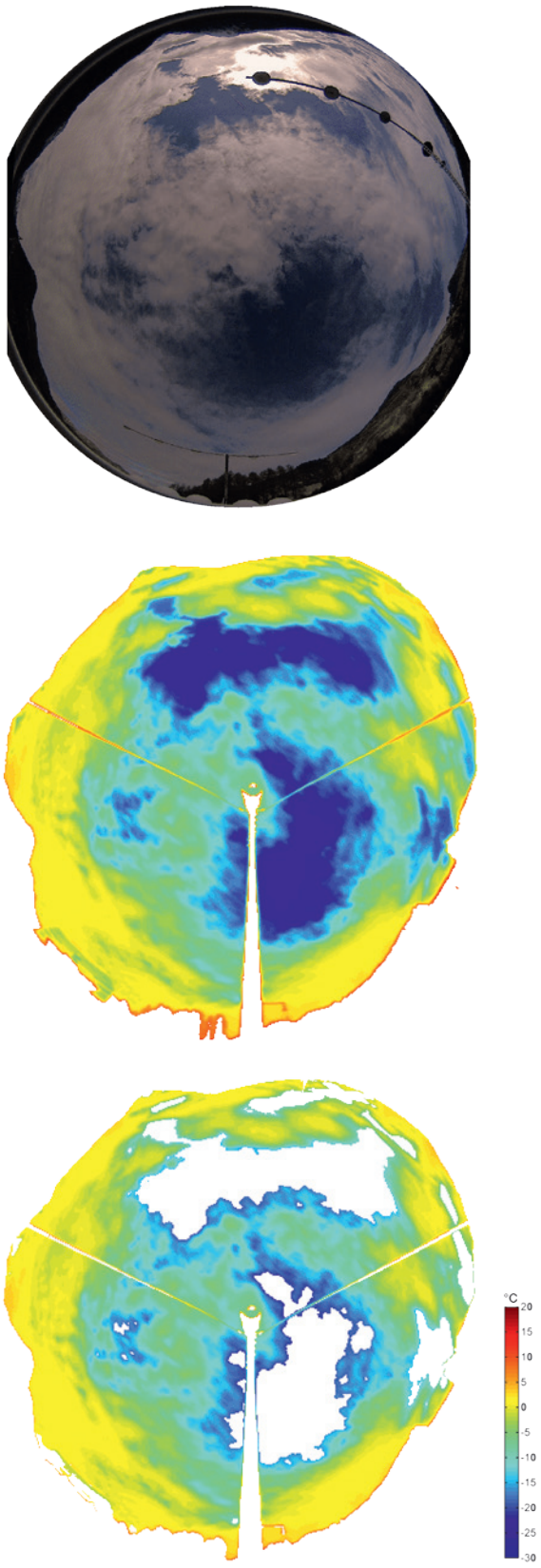

Figure 1. Sky image on 6 November 2015 at 11:15 UTC. The upper figure was taken with a visible camera mounted on a solar tracker with sun-shading. The middle figure was obtained with the IRCCAM and the lower figure shows only the clouds. The temperature scale ranges from -30°C (blue) to +20°C (red).

Development of a Lunar PFR

Natalia Kouremeti, Julian Gröbner, Stelios Kazadzis, Daniel Pfiffner, and Ricco Soder

The growing interest in night-time observations of aerosol optical depth (AOD) has led to the development of a lunar Precision Filter Radiometer (PFR) at PMOD/WRC. In addition to the retrieval of nocturnal AOD, the radiometric calibration of the lunar PFR aims to provide absolute lunar irradiance measurements with an expanded uncertainty of less than 5% (k=2).

Atmospheric aerosols are known to impact the climate, but they still represent one of the largest uncertainties in climate change studies. Night-time AOD measurements could provide valuable information on the climatology of aerosols at high latitude stations, where direct sun measurements are not possible throughout the year. For example, in the northern hemisphere they can be used to monitor the arctic haze during polar winter. In passive remote sensing techniques, the moon or the stars are used as the light source. The high intensity of the moon in comparison to stars (more than 5 orders of magnitude) makes it suitable for nocturnal observation without the necessity of using complex systems. However, the transition from Sun to lunar photometry is challenging due to the continuous change in lunar brightness, depending on the viewing geometry, as well as the fact that lunar irradiance is 5 to 6 orders of magnitude less than the Sun's.

PMOD/WRC participated in the Lunar Arctic Project (March 2014–June 2015) funded by the Svalbard Science Foundation, that aimed to close the gap in the annual cycle of the arctic aerosol climatology and to develop Svalbard as a satellite validation site. The role of PMOD/WRC in the project was the modification of an existing PFR and its deployment at Ny Ålesund. The lunar PFR is a standard PFR instrument that is used in the GAW-PFR network, with enhanced sensitivity, which measures at four wavelengths 412, 500, 675, and 862 nm with sensor stabilisation at 20°C. The instrument was installed at Ny-Ålesund (Norway; 78.9°N, 11.9°E), from October 2014 to February 2015, and measured six lunar cycles. During the Arctic Summer, it was installed at Izaña (Spain) to perform Langley calibrations, investigate its stability, and to evaluate its measurement limitations. A valuable data-set was retrieved during this period, providing the opportunity to improve a number of technical and measurement issues.

The prototype lunar PFR was upgraded in Oct. 2015 whereby the sensitivity was increased by a factor 10 in three of the four channels and a 22-bit data acquisition system (SACRAM) was installed. The instrument was characterised at PMOD/WRC: the filter functions (Figure 2) and instrument linearity were measured using the ATLAS tunable laser system. Differences of ~0.5 nm were found from the initial nominal central wavelength values. The absolute responsivity of the lunar PFR was measured on the direct irradiance calibration setup, consisting of a reference irradiance source (1000 W FEL type lamp source). The calibration factors were determined with an expanded uncertainty of 3.5% (k=2) including uncertainties in the reference plane determination, non-linearity correction, and the reference irradiance used. In 2016, the lunar PFR will be deployed at Ny-Ålesund to provide continuity in night-time measurements and later at Izaña for validation of the radiometric calibration.

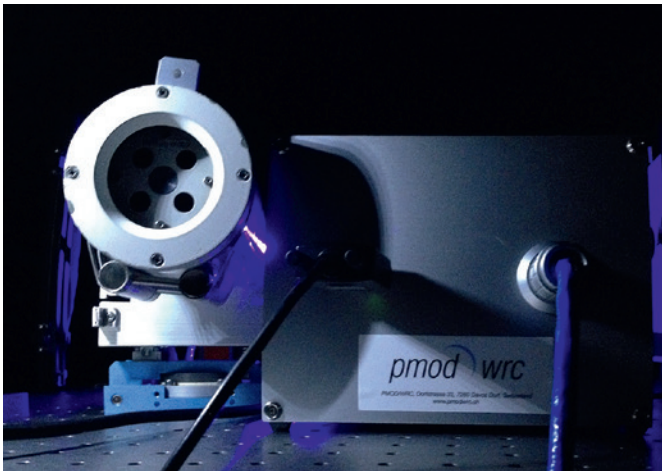

Figure 1. Lunar PFR and SACRAM data acquisition system.

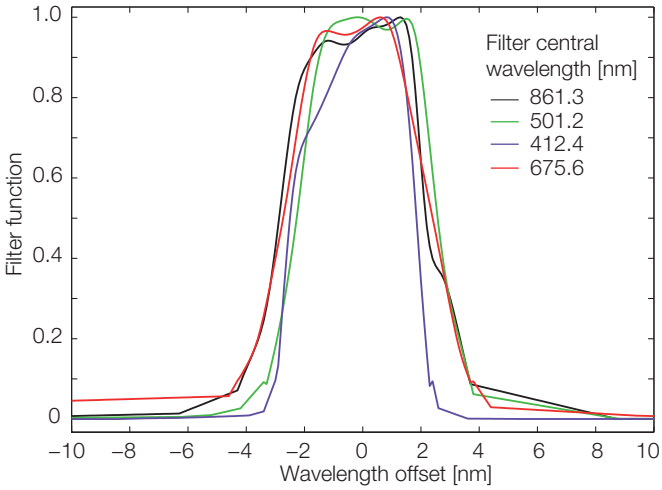

Figure 2. Filter functions of the 4 Lunar PFR channels measured with the ATLAS tunable laser system.

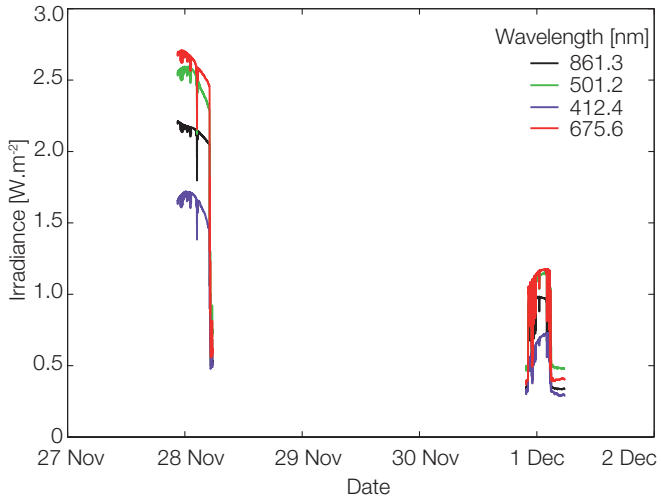

Figure 3. Lunar irradiance measurements performed in Davos after the calibration of the lunar PFR.

Space Experiments

Manfred Gyo, Valeria Büchel, Etienne de Coulon, Fabian Dürig, Wolfgang Finsterle, Nuno Guerreiro, Patrik Langer, Pierre Luc Lévesque, Margit Haberreiter, Johnathan Kennedy, Silvio Koller, Philipp Kuhn, Nathan Mingard, Andri Morandi, Dany Pfiffner, Pascal Schlatter, Marcel Specha, and Werner Schmutz

SPICE

The Spectral Imaging of the Coronal Environment (SPICE) experiment, a payload aboard the ESA/NASA Solar Orbiter Mission.

Low Voltage Power Supply (LVPS)

The LVPS has been designed and manufactured by PMOD/WRC (Figure 1). During the first three months of 2015, the electrical board with number "SN002", was assembled in the PMOD/WRC cleanroom. For inspection, we sent SN002 to the Rutherford Appleton Laboratory (RAL). The outcome of the board inspection was that various modifications were required which were completed by RAL. Once finished, environmental tests on the board were conducted at several laboratories in Switzerland during Summer 2015. After all tests were successfully completed, including extensive electrical tests, we shipped board SN002 to the Southwest Research Institute (SwRI), Boulder, USA.

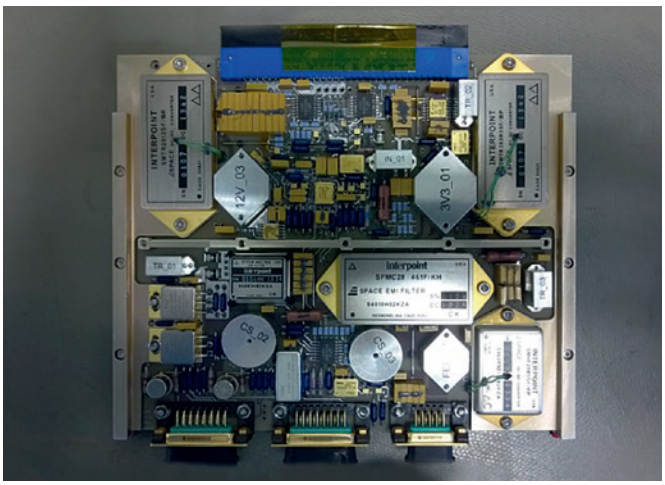

Figure 1. Low voltage power supply (board number SN002).

During testing of board SN002, RAL decided that SN003 should be assembled by SWRI. All components were therefore packed and shipped to SWRI for assembly. After successful production, board SN003 was sent to PMOD/WRC for testing in late 2015.

SPICE Door Mechanism (SDM)

The SDM is designed to prevent instrument contamination while on the ground and in space. It also allows the instrument to be purged through a labyrinth seal during Assembly Integration and Test (AIT) activities and the launch. The manufacture of QM, FM and flight spare (FS) was finished in June 2015, and thus the qualification and acceptance test campaign have started (Figure 2).

During life-time testing, blocking of the motor was observed. Detailed assessments have shown that the cause was a test set-up which was not being conducted in a completely dry vacuum

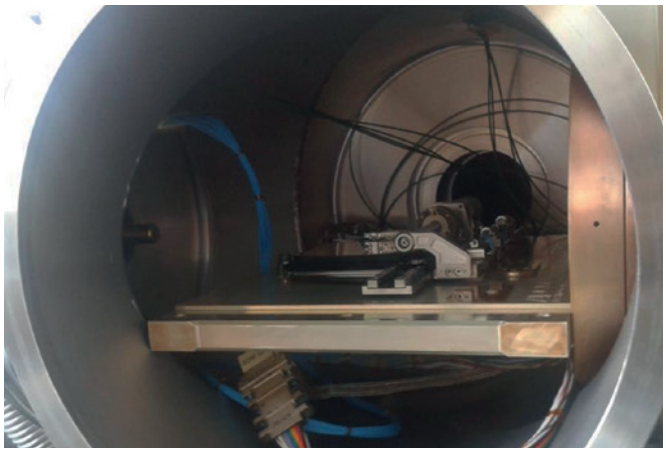

Figure 2. SDM QM in the PMOD/WRC vacuum chamber in preparation of the functional test.

chamber. The QM motor therefore needs to be replaced and the life-time testing repeated. Based on the long delivery time of the motor, the final qualification will be conducted in Summer 2016.

All other tests were successful. The acceptance tests for the FM and FS is on-going. The delivery of the FM is planned for Spring 2016 before the end of the life-time test, in order that instrument integration is not delayed.

Slit Change Mechanism (SCM)

The SCM is a vital mechanism designed to position one of four slits of differing widths during measurement. Almatech, our industry partner based at Lausanne, has been assembling, testing, and verifying the QM (Figure 3).

The construction of an assembled QM was one of the main objectives in 2015. The target was met with some delay, early in 2016, and is now ready for testing. Assembly of the Flight Model is on-going while the qualification test campaign has also started.

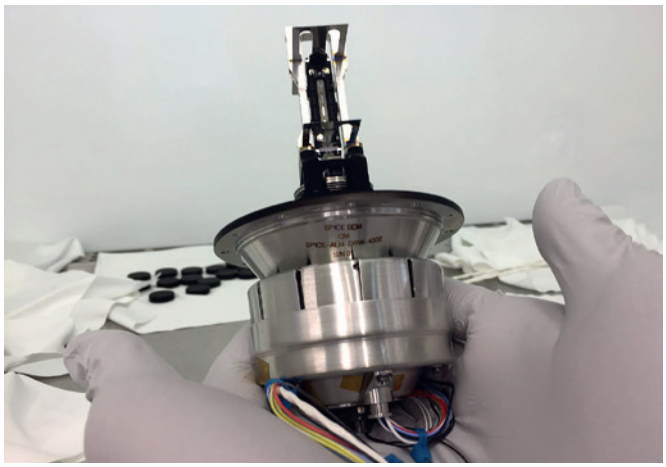

Figure 3. Assembled QM model of the slit change mechanism.

EUI

The Extreme UV Imager (EUI) experiment, a payload aboard the ESA/NASA Solar Orbiter Mission.

PMOD/WRC is responsible for the optical bench structure (OBS) of the EUI instrument. In Spring 2015, late design changes requested from by the spacecraft consortium were implemented into the EUI OBS. The material and process qualifications were finished simultaneously. After the manufacturing readiness review (MRR) of the qualification model (QM), the latter was manufactured and delivered in November 2015. Figure 4 shows the OBS during inspection before delivery.

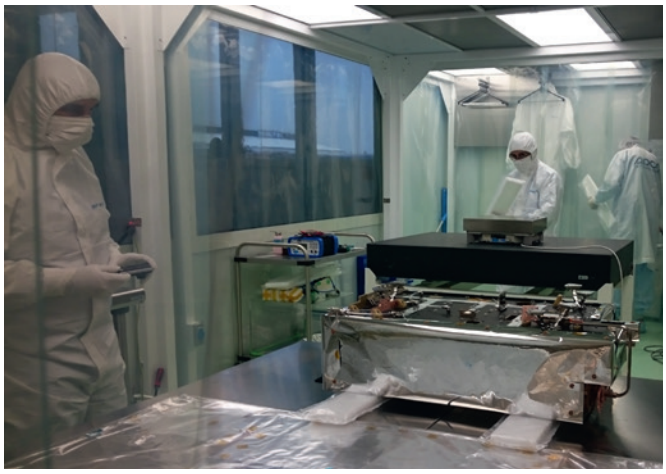

Figure 4. EUI OBS Qualification Model during inspection before delivery.

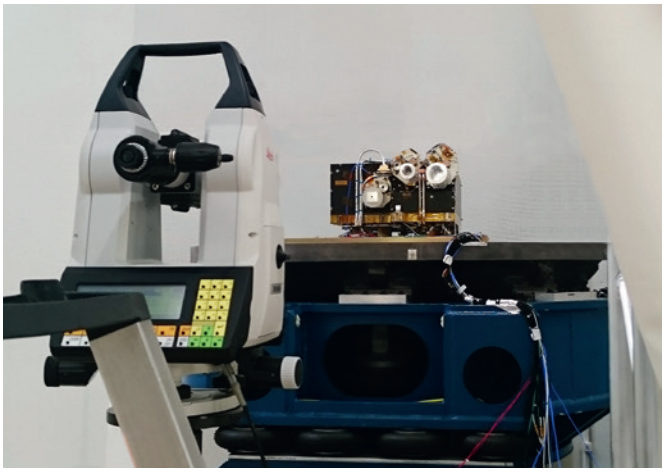

Figure 6. EUI QM mounted on a shaker for QM vibration test at the Centre Spatial de Liège (CSL), France.

The integration of the other sub-systems (Figure 5) was conducted at CSL and the QM was ready in February 2016 for the qualification test campaign of the entire instrument (Figure 6). In addition, the MRR of the EUI OBS flight model was held in November 2015. Final manufacturing has started.

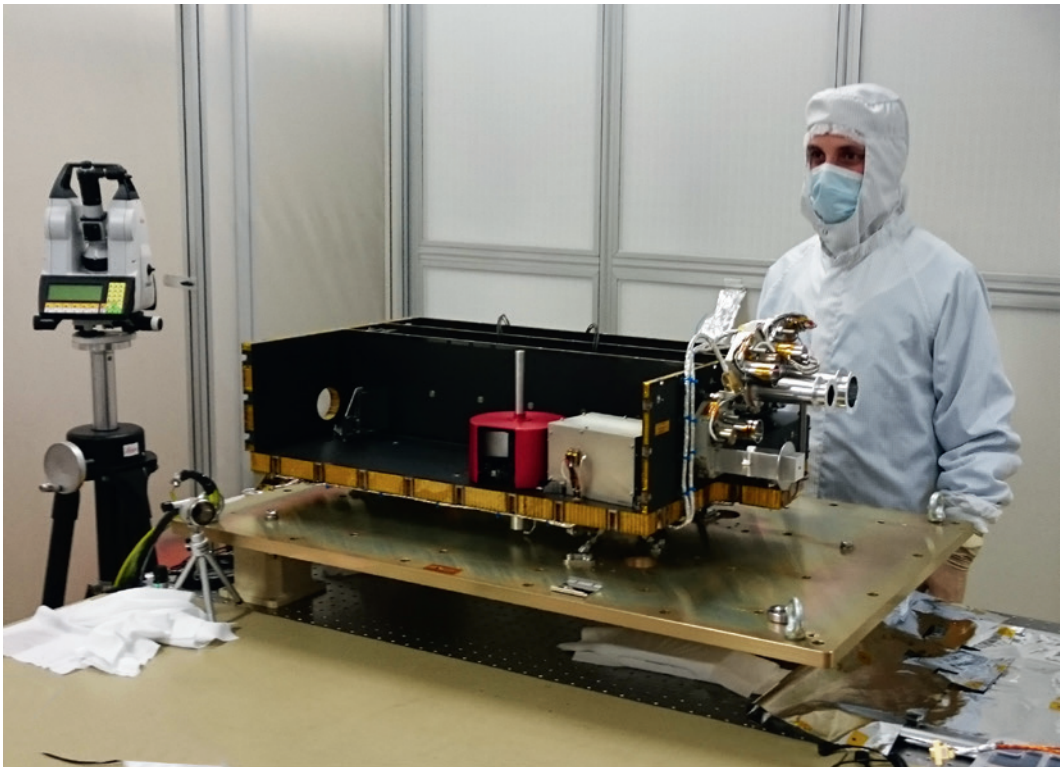

Figure 5. EUI QM Integration of sub-systems.

CLARA

The Compact Lightweight Absolute Radiometer (CLARA), a payload aboard the Norwegian micro-satellite, NORSAT-1.

CLARA is the latest radiometer in a line of pyrheliometers, developed at PMOD/WRC, which continues its long heritage of space-borne Total Solar Irradiance (TSI) measurements. Similar to most radiometers built at PMOD/WRC, CLARA uses electrical substitution in its black-body cavity to measure TSI, and has three cavities that can be used either as a measuring cavity, reference cavity or for degradation measurements. Based on the success of the engineering model in 2014, the FM design (Figure 7) and Flight Spare (FS) were finalised. The overall instrument concept and electronics were developed by PMOD/WRC.

CLARA's development has also benefited from the knowledge and expertise of many Swiss industry partners. The on-board software and the Electrical Ground Support Equipment (EGSE) were designed by DLAB. RUAG Space in Zürich reviewed the mechanical design, performed mechanical and thermal analysis, provided all structural and thermal components, and conducted most of the environmental tests on the FM. We also had the privilege of using the infrastructure of the Fachhochschule Nordwestschweiz to perform vibration tests.

Being an absolute radiometer by design, each of CLARA's components was calibrated in-house against traceable SI units. CLARA was compared against the TSI World Standard Group of pyrheliometers at PMOD/WRC, Davos, as well as the TSI Radiometer Facility (TRF) in Boulder, USA. These calibrations ensure consistency with previous TSI measurements and SI traceability to the National Institute of Standards and Technology (NIST, USA). In September 2015, the CLARA FM was delivered to the University of Toronto Institute for Aerospace Studies (UTIAS) for integration on the Norwegian NORSAT-1 micro-satellite.

Figure 7. Silvio Koller (left) and Pierre-Luc Lévesque (right) with the CLARA Flight Model.

DARA

The Digital Absolute Radiometer (DARA), a payload aboard ESA's formation flying mission, PROBA-3.

Based on the CLARA design and expertise gained during Assembly, Integration and Test (AIT) activities, the DARA instrument design was adapted in order to cover internal and external requirements (ESA and prime contractor SENER). With the preliminary design as a contractual basis, three Swiss industry contracts were placed in the context of ESA's PROgramme de Développement d'Expériences scientifiques (PRODEX):

- Mechanical and thermal analysis and testing.
- Onboard and ground support software development.
- Design, development and manufacturing of the digital control board.

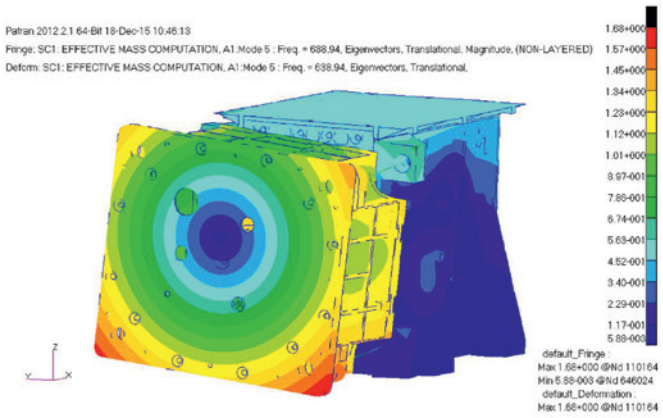

Figure 8. Visualised displacement at an eigenfrequency of 639 Hz.

These three contracts were signed in the 3rd and 4th quarters of 2015. First preliminary results from the thermal and mechanical analysis were provided just shortly before the end of the year (Figure 8). The high vibration loads during launch (VEGA rocket), transmitted to the DARA mounting interface, will require a re-design of the mechanics.

The design work of the electronics (Figure 9) started in 2015 at the PMOD/WRC. Special care was required when considering the high radiation dose which will be accumulated during the lifetime of the mission. The harsh environment in Space has a fundamental influence on the selection of electrical and mechanical components. For instance, the drawbacks of radiation-tolerant materials are their extremely high costs and long delivery times. Although the overall concept of the electronics system is similar to that for CLARA, a complete re-design was considered necessary due to mechanical constraints, the implementation of improvements, and the replacement of certain electrical components.

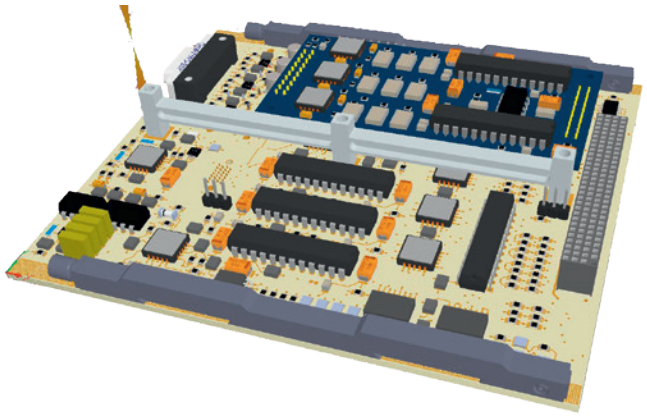

Figure 9. DARA data acquisition board (3-D model).

A further achievement has been the preparation of a life-cycle test for the radiometer shutter mechanism. Five motors will be tested under thermal vacuum conditions. The stepper motors will have to survive 4.5 million movements. The goal is not only to withstand the high number of activations, but also to prevent possible contamination of the instrument through the release of particles or molecules.

In 2016, it is planned to manufacture and test the Engineering Model (EM). A critical design review will detail design changes and the following manufacturing phase of the flight units.

JOIM

Joint Solar Irradiance Monitor (JOIM), a payload aboard the Chinese FY-3 mission.

In late 2015, the PMOD/WRC began the technical part of the JOIM experiment. This will be the first cooperation on a satellite mission with a Chinese Institute, the Changchun Institute of Optics, Fine mechanics and Physics (CIOMP). It is intended to develop a pyrheliometer based on DARA, which was designed, built and characterised at PMOD/WRC starting in 2009. To fulfill the strict time-table, as few design changes as possible are required. The technical feasibility will be proven in the first phase in 2016.

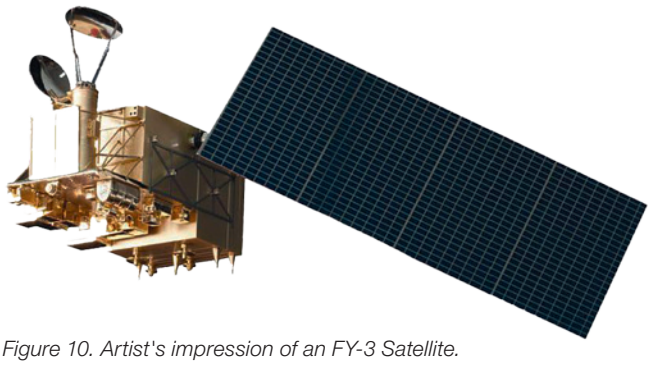

Figure 10. Artist's impression of an FY-3 Satellite.

JOIM will consist of three absolute cavity pyrheliometers of different design and manufacturer to form a Space Standard Group. CIOMP (China), IRMB (Belgium), and PMOD/WRC will each supply a radiometer. The standard group concept has been extremely successful on the ground, where the World Standard Group (WSG) was defined in 1977. The WSG has served to provide an accurate and stable reference for world-wide solar irradiance measurements. In many respects, the situation of TSI measurements in space is similar to that of the solar irradiance measurements on the ground 40 years ago. The reproducibility of the absolute value of TSI measurements is too low to guarantee long-term stability, resulting in inhomogeneous time-series. A standard group of three pyrheliometers will allow the required stability over decades to be maintained, as proven by the ground-based WSG.

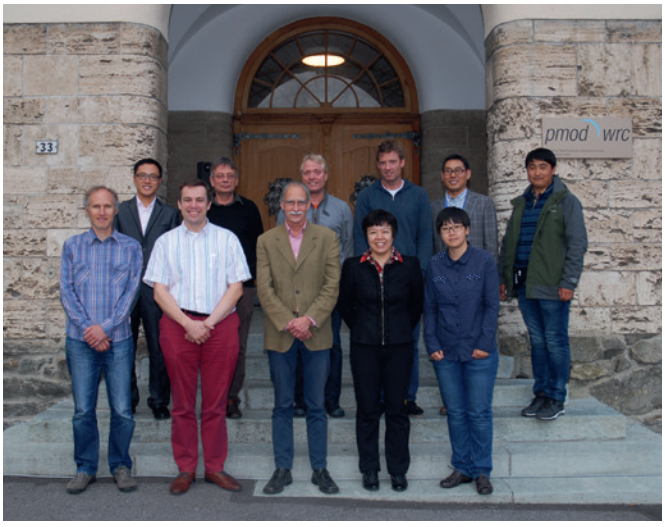

Figure 11. JOIM Kick-off meeting at the PMOD/WRC. Bottom left: Wolfgang Finsterle, Steven Dewitte (RMI), Werner Schmutz, Wei Fang (CIOMP), Jin Qi (CMA); Top left: Hongrui Wang (CIOMP), André Chevallier (IRMB), Manfred Gyo, Philipp Kuhn, Yupeng Wang (CIOMP), Yang Luo (CIOMP). See text for institute abbreviations.

JOIM will be the first TSI experiment to not only transfer the WRR standard, but the entire concept and methodology of a standard group in Space. It will thus achieve unprecedented levels of stability. The Space Standard Group will serve to homogenise existing and future TSI measurements.

JOIM will be placed on a Chinese Satellite. The FY-3 series of CMA/NSMC (China Meteorological Administration/National Satellite Meteorological Centre) represents the second generation of Chinese polar-orbiting meteorological satellites (follow-on of FY-1 series) (Figure 10). The FY-3 series represents a cooperative programme between CMA and CNSA (China National Space Administration). It was initially approved in 1998 and entered full-scale development in 1999. Key aspects of the FY-3 satellite series include collecting atmospheric data for intermediate- and long-term weather forecasting and global climate research. The Kick-off Meeting for the JOIM collaboration took place during the 12th IPC 2015 in Davos (Figure 11).

Scientific Research Activities

Overview

Werner Schmutz

Projects at PMOD/WRC are related to solar radiation in which we address questions regarding the radiation energy budget in the terrestrial atmosphere, as well as problems in solar physics to understand the mechanisms concerning the variability of solar irradiance. Hardware projects at our institute are part of investigations into Sun-Earth interactions by providing measurements of solar irradiance.

The choice of projects to be conducted at the institute is governed by the synergy between the expertise obtained from the Operational Services of the World Radiation Center and other research activities. Basically, the same instruments are built for space-based experiments as are utilised for ground-based measurements.

The research activities can be grouped into three themes:

- Climate modelling
- Terrestrial radiation balance
- Solar physics

Research activities are financed through third-party funding. Last year, six projects were supported by the Swiss National Science Foundation, three projects by Swiss participation in the EU COST actions, one project by MeteoSwiss, two projects by the 7th European Framework Program FP7, and three projects by the European Metrology Research Programme. These funding sources have supported four PhD Theses and seven post-doctoral positions. The Swiss participation in ESA's PRODEX (PROgramme de Développement d'Expériences scientifiques) programme, funds the hardware development for space experiments. The institute's four PRODEX projects paid for the equivalent of eight technical department positions. The latest involvement with the European Space agency is a contribution to the ESA project IDEAS+ concerning calibration expertise at the PMOD/WRC.

During the last three years, the PMOD/WRC has led the FP7 SOLID (First European Comprehensive Solar Irradiance Data Exploitation) project. SOLID has successfully compiled spectral solar irradiance data from the past decades using observations. The goal was to create a homogeneous data set with the instrumental differences removed and scaled to the best-known absolute calibration. This allows the magnitudes of solar irradiance variations to be assessed, which are an important driver of the chemistry, temperature, and dynamics of the Earth's atmosphere and ultimately of the Earth's climate. While the involvement of the institute, beside its management effort, was only a 90% research position, the outcome is nevertheless of importance to climate research at the institute.

Understanding the solar forcing and its impact on the climate is the main theme of the SNSF Sinergia project "Future and Past Solar Influence on the Terrestrial Climate" (FUPSOL), which is a collaborative multi-institute research with partners from EAWAG, IAC ETHZ, Bern University, and the Oeschger Centre for Climate Change Research. This 3-year project has now completed its second year, and establishing a solar forcing database was an important achievement in order to begin climate simulations, which are at the core of the project.

A considerable number of publications result from research activities of the World Radiation Center at the PMOD/WRC. These papers usually do not get a high number of citations. Nevertheless, it is fundamentally important that research connected with calibration is conducted because only through active research can we be a leading institute for radiation calibration. The number of cited publications has stabilised in the last three years at around 1200. This high citation level and the overall increasing trend in previous years as illustrated in Fig. 1 statistically testifies the good reputation of PMOD/WRC scientific staff and the interest of the science community in results published by the institute.

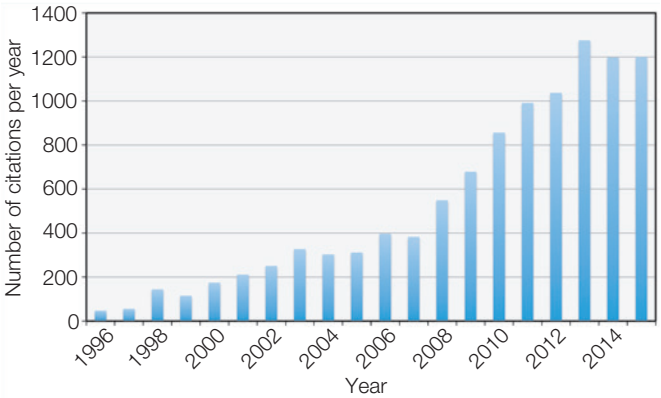

Figure 1. Number of annual citations of publications which include an author with a PMOD/WRC affiliation. A total of 11,105 citations to 508 publications were included in Thomson Reuter's Web of Science up to April 2015. The articles have been selected using the search criteria address = (World Rad C*) OR (PMOD* NOT PMOD Technol*) OR (Phys* Met* Obs*).*

SOLID – First European Comprehensive Solar Irradiance Data Exploitation – Technical and Scientific Management

Margit Haberreiter and Werner Schmutz in collaboration with the SOLID consortium

The SOLID project ran from December 2012 to November 2015, and has formally finished. The 3rd year of SOLID included a number of activities that are summarised here.

The Third Annual Meeting of the SOLID consortium was held on 5–8 October 2015 at the Aristotle Univ. of Thessaloniki, Greece.

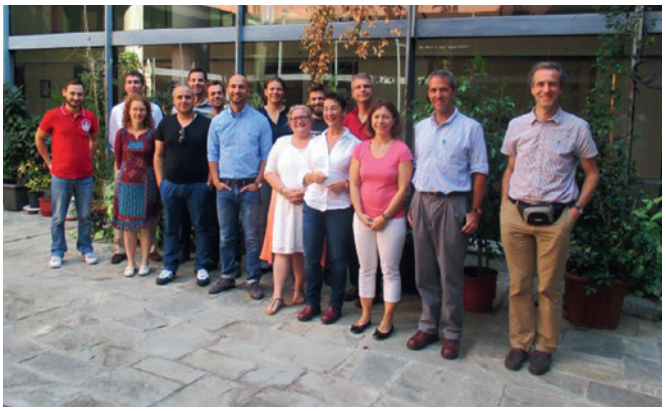

Figure 1. Group Photo of the Third Annual SOLID Meeting: back row from left to right: Alexandros Emmanouilides, Farzad Kamalabadi, Stergios Misios, Matthieu Kretzschmar, Margit Haberreiter, Andreas Chrysanthou, Mark Weber; front row from left to right: Veronique Delouille, Wissam Chehade, Omar Ashamari, Laure Lefevre, Klairie Tourpali, Katja Matthes, Matt DeLand, Thierry Dudok de Wit. Not in the picture: Ilaria Ermolli, Alice Cristaldi, Giulio Del Zanna, Micha Schöll, Yvonne Unruh.

Review of 3rd Periodic Report: A successful second review meeting of SOLID was held on 22 January 2016 in Brussels, where the third Reporting Period covering the period from 1 December 2014 to 30 November 2015 was reviewed and approved.

Annual Newsletter: An annual newsletter has been published each year with the third and final newsletter being available online at ftp://ftp.pmodwrc.ch/pub/margit/FP7_SOLID/Newsletter/SOLID_Newsletter_3.pdf.

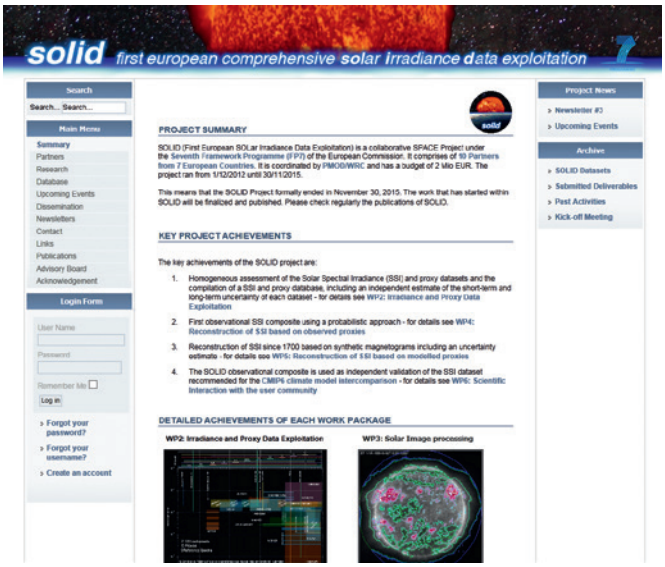

Figure 3. Sceenshot of the current status of the SOLID webpage and its elements.

SOLID and CMIP6: The SOLID observational Solar Spectral Irradiance (SSI) composite is used to validate the recommended SSI data-set for the CMIP6 intercomparisons. Figure 2 shows the comparison of the SOLID data composite with the CMIP6 recommendation. Further details can be found in Matthes et al. (2016).

SOLID Webpage and Database: The SOLID webpage provides a summary of the achievements of the project, and is being continuously updated.

Acknowledgement. This work has received funding from the EC's 7th Framework Programme (FP7 2012) under grant agreement no 313188 (SOLID).

References: Matthes K. et al.: 2016, CMIP6 solar forcing, submitted to Geosci. Model Dev.

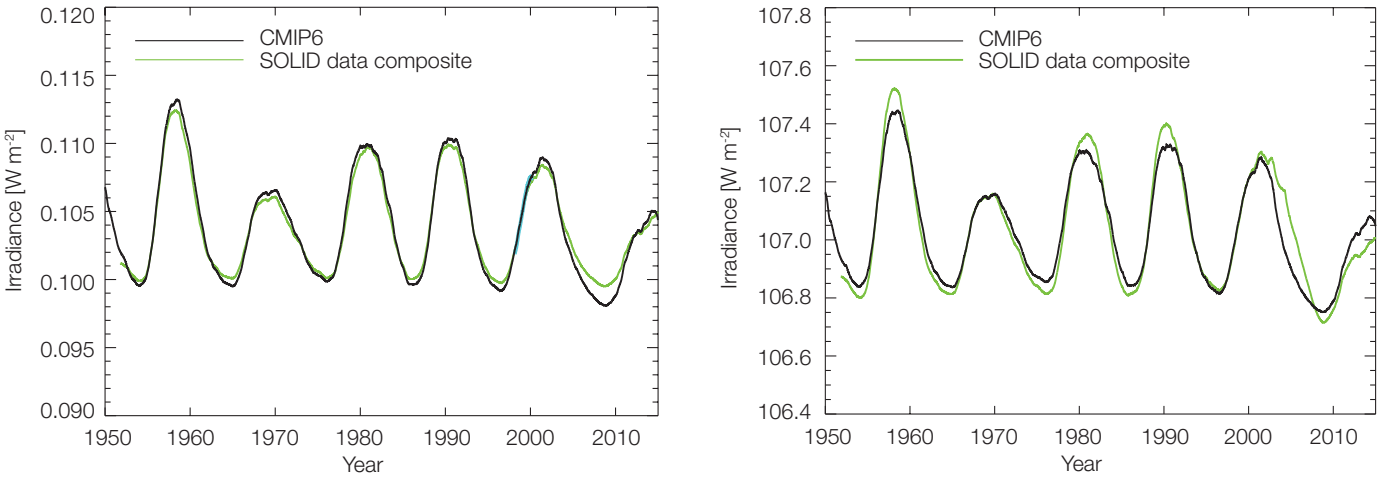

Figure 2. CMIP6 recommended SSI time-series (black) from 1950 to 2015 together with the SOLID data composite (green) and relevant instrument observations for the following wavelength bins: 120–200 nm (left), 200–400 nm (right). The SOLID and instrument time-series have been adjusted to match the average level of the CMIP6 time-series. All time-series are running averages over two years (adapted from Matthes et al., 2016).

Future and Past Solar Influence on the Terrestrial Climate (FUPSOL-2)

Werner Schmutz (PI), Eugene Rozanov (project manager) in collaboration with teams from EAWAG, IAC ETHZ, KUP and GIUB of University of Bern, and Oeschger Centre for Climate Change Research

The FUPSOL-2 project involves partners from the Institute for Atmosphere and Climate Sciences of the ETH Zürich (IAC ETH), the Swiss Federal Institute of Aquatic Science and Technology, Dübendorf (EAWAG), the Physics Institute (KUP) and Institute of Geography (GIUB) of the University of Bern, and the Oeschger Centre for Climate Change Research. It aims to study solar forcing and its influence on the Earth's atmosphere, ozone layer and climate in the past and future.

During 2015, we completed the implementation of an alternative set of solar structure models. The new set of models is based on improvements in representing the solar irradiance emitted by the quiet Sun and improves the reconstruction of the solar irradiance. Using the new set of solar models and updated solar modulation potential reconstructions based on the time-series of cosmogenic isotope series, we produced the SSI data covering 1600–2010. Figure 1 compares the total solar irradiance (TSI) used in FUPSOL-1 (Shapiro et al., 2011) and new reconstructions.

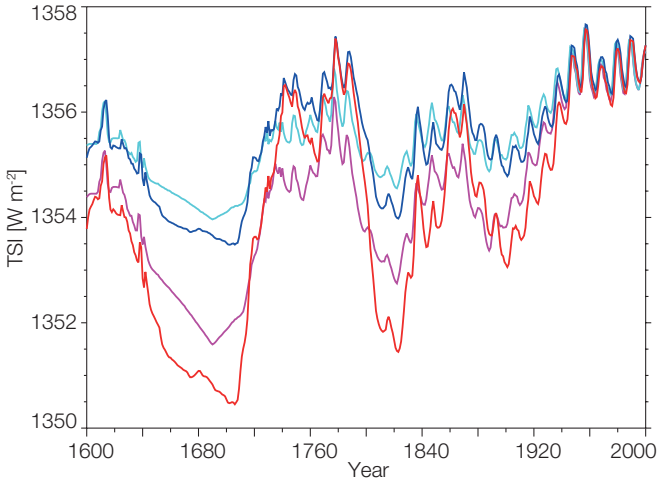

Figure 1. Evolution of the Total Solar Irradiance (TSI; Wm^{-2}) used in FUPSOL-1 (red and blue) and reconstructed using updated solar modulation potential and solar structure models (pink and light blue).

We completed the planned improvement of the gravity-wave drag (GWD) parameterisation, introducing the missing latitudinal dependence of the gravity-wave source strength. The inclusion of the new GWD parameterisation decreases the strength and increases the variability of the Northern Hemisphere polar vortex, leading to better agreement with re-analysis data. We also investigated the influence of Middle Range Energy Electron (MEE, 30–300 keV) precipitation on the atmosphere. The results show that during geomagnetically active periods, MEE can substantially enhance the difference in ozone anomalies between geomagnetically active and quiescent periods. The comparison with MIPAS NO_y observations indicates that the additional source of NO_y from MEE improves the model performance. However, above 50 km the model still substantially underestimates observed NO_y concentrations in the polar area during the cold seasons. These results are presented by Arsenovic et al. (2015) in greater detail. As a result of our efforts, the model with an improved GWD parameterisation and introduction of MEE is ready, and planned simulations of 20th century climate are ongoing.

Another topic during the last year has been the analysis of sensitivity simulations during a solar minimum. The major research question is the influence of chemistry-climate interactions on the response of the oceanic circulation when solar forcing is strongly reduced. We identified two mechanisms that control the behaviour of the Atlantic meridional overturning circulation (AMOC). The first mechanism driven by thermal changes intensifies the convection and leads to an acceleration of the AMOC. The second is driven by the interaction of UV radiation with the tropospheric circulation, which increases the probability of a negative phase of the North Atlantic Oscillation (NAO), causing a weakening of the AMOC. Using sensitivity simulations with and without chemistry-climate interactions, we show that the second mechanisms leads to a significant AMOC weakening only if stratospheric chemistry is allowed to respond to the solar minimum. A manuscript summarising the findings is currently in preparation (Muthers at al., 2016).

Using a new classification of weather types, we analysed the influence of solar activity on European weather. We discovered an increase in the number of days with an easterly flow over Europe during the periods of low solar activity and demonstrated that the mean sea level pressure field over the North Atlantic has different patterns relative to the 11 year cycle characterised by lower values of high solar activity (Schwander et al., 2016).

References:

Arsenovic P. et al.: 2015, The influence of middle range energy electrons on atmospheric chemistry and climate, JASTP, SI: Solar wind and climate, submitted.

Muthers S., Raible C., Stocker T.F.: 2016, Response of the AMOC to solar forcing and the modulating role of atmospheric chemistry, in preparation.

Schwander M. et al.: 2016, Impact of solar activity on European weather patterns from 1763 to 2009, in preparation for Ann. Geophys.

Shapiro A.I. et al.: 2011, A new approach to the long-term reconstruction of the solar irradiance leads to large historical solar forcing, A&A, 529, A67, doi:10.1051/0004-6361/201016173.

The Influence of Middle Range Energy Electrons on Atmospheric Chemistry and Regional Climate

Eugene Rozanov in collaboration with Pavle Arsenovic, Andrea Stenke, Fiona Tummon and Thomas Peter (IAC ETHZ); Bernd Funke (IAA, CSIC, Spain), Jan-Maik Wissing (Univ. Osnabrück, Germany), and Kalevi Mursula (ReSoLVE Centre of Excellence, Oulu, Finland)

In the framework of the SNF FUPSOL-2 project, we studied the influence of Middle Range Energy Electrons (MEE). Our results show that during the geomagnetically active period, MEE result in enhanced concentrations of NO_Y and HO_X in the polar winter mesosphere, resulting in local ozone depletion by up to 35%. These perturbations propagate down, affecting circulation patterns in the entire atmosphere. A surface air temperature response is detected in several regions, with the most pronounced warming in the Antarctic during austral winter. Surface warming of up to 2 K is also seen over continental Asia during boreal winter.

MEE (30–300 keV) originate from the outer radiation belt. They penetrate Earth's atmosphere and deposit their energy in the mesosphere and upper stratosphere, producing NO_X and HO_X, which destroy ozone (Rozanov et al., 2012).

To study their influence, we applied the Atmosphere-Ocean CCM SOCOL3-MPIOM (Muthers et al., 2014), adding the daily mean ionisation rates of MEE calculated with the Atmospheric Ionisation Module developed at the University of Osnabrück (AIMOS, v1.6). We performed two 10-year long, six-member ensemble runs with and without MEE (NOMEE) keeping the other boundary conditions unchanged, and analysed the difference of ozone and temperature fields between the simulations during the geomagnetically active period 2002–2005 period.

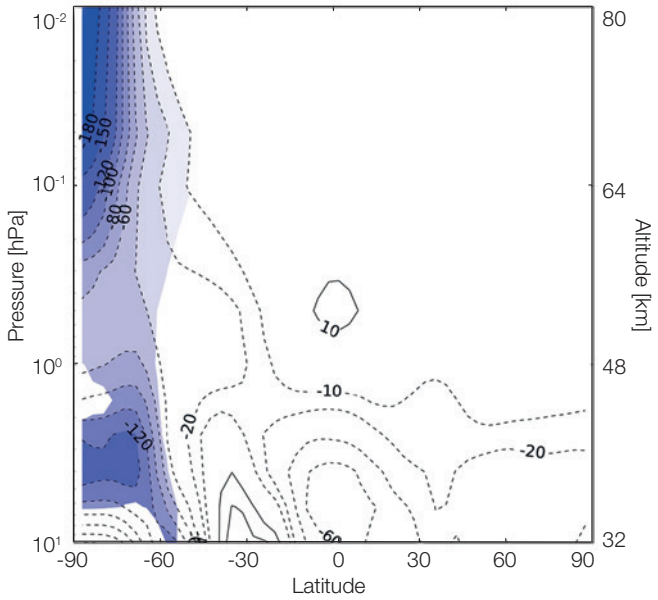

Figure 1. Zonal mean ozone difference (MEE - NOMEE) in ppbv for JJA averaged over 2002–2005. Colour marks the area where the results are significant at a 95% confidence level.

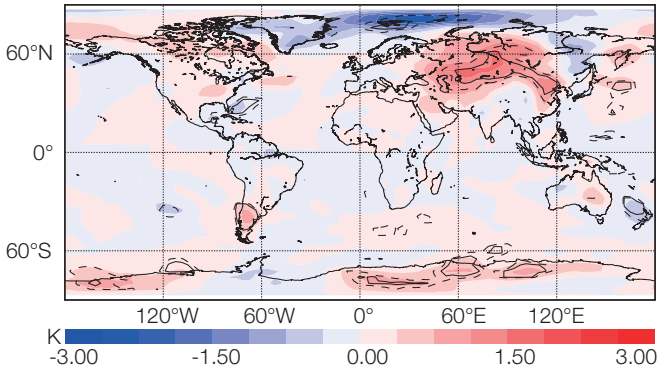

Figure 2. Spatial distribution of the 2 m temperature difference (MEE - NOMEE) in Kelvin for DJF. The dashed and solid lines circle regions with a 90% and 95% confidence level, respectively.

We show that MEE strongly impact ozone in the Southern Hemisphere (SH) during the austral winter (JJA). Figure 1 illustrates that the ozone depletion in the SH can reach up to 200 ppbv (about 40%) in the upper mesosphere and up to 120 ppbv (~2.5%) in the upper stratosphere.

In the Northern Hemisphere (NH) during boreal winter, ozone depletion is slightly less, reaching 150 ppbv (about 25%) in the upper mesosphere. The ozone depletion is also visible down to the upper stratosphere, but is not statistically significant below 1 hPa. The precipitation of MEE influences not only the chemistry and climate in the upper atmosphere, but also the surface climate.

Surface temperature changes are depicted in Figure 2. During the boreal winter season, statistically significant increases in the surface temperature are seen mostly in the NH, with a warming of up to 2 K over continental Asia. During the austral winter, an increase in sea level pressure over Antarctica leads to a deceleration of westerly winds around 60°S, which induces significant (up to 3 K) warming over Antarctica (not shown).

References: Muthers S. et al.: 2014, The coupled atmosphere-chemistry-ocean model SOCOL-MPIOM, Geosci. Model Dev., 7, 2157–2179.

Rozanov E. et al.: 2012, Influence of the precipitating energetic particles on atmospheric chemistry and climate, Surv. Geophys, 483–501.

SOVAC – Solar Variability and Climate Change During the First Half of the 20th Century

Tatiana Egorova, Eugene Rozanov, and Werner Schmutz in collaboration with the FUPSOL-2 project team.

The project aims to understand the causes of climate warming during the first half of the 20th century. To address this problem we simulated the climate evolution from 1900 to 1950 with the state-of-the-art Atmosphere-Ocean-Chemistry-Climate model (AOCCM) SOCOL-MPIOM driven by the most recent compilation of all relevant climate forcing data, and compare the obtained results with observations and other model results.

During the final phase of the project, we continued extensive comparisons of simulated results with observations and other models using different statistical approaches. Figure 1 illustrates the annual mean surface air warming from 1900 to 1940 calculated from the NCDC temperature time-series. The results reveal a pronounced warming over Northern Europe and North America.

The simulated temperature trends are shown in Figure 2 for the cases when strong and weak solar irradiance forcing was applied. The comparison with the observed pattern shows that AOCCM SOCOL-MPIOM (Muthers et al., 2014) is able to mimic the observed pattern of climate warming during the first half of the 20th century only if we apply large changes of solar irradiance during this period. For the weaker forcing, the warming over North America is almost absent.

The agreement in the temperature change pattern is not so convincing on a seasonal scale, because the model does not produce large warming over Northern Europe during the cold seasons. The main issue here is the rather low efficiency of the top-down mechanism of the influence of solar activity on the climate in AOCCM SOCOL-MPIOM (see Anet et al., 2014). This problem cannot be resolved with the present version of AOCCM SOCOL-MPIOM and requires a new version of the core GCM. More detailed analysis of the long-term model behaviour to filter out the very low frequency variability from the trend analysis is also necessary.

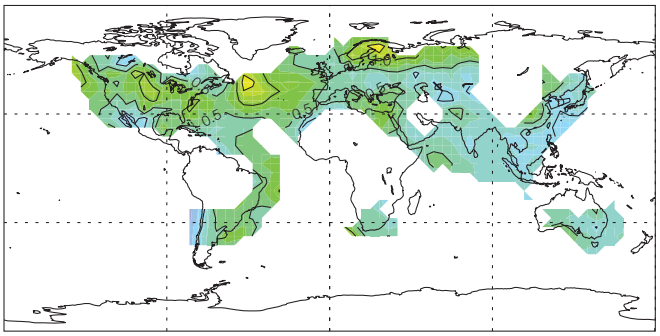

Figure 1. Trend in surface air temperature warming (K) during the period 1900–1940, obtained with observations (NCDC data-set), and simulated with the AOCCM SOCOL-MPIOM and other models which participated in the CMIP-5 activity.

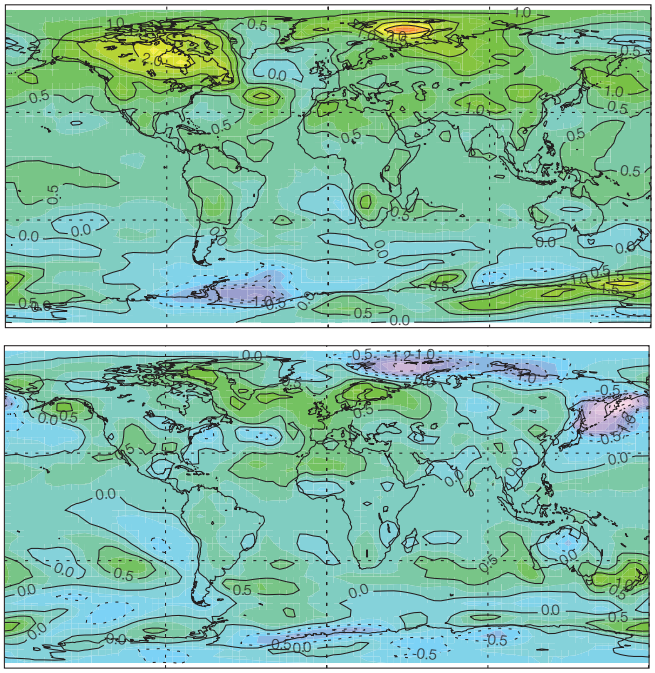

Figure 2. Trend in surface air temperature warming (K) during the 1900–1940 period, simulated with AOCCM SOCOL-MPIOM using strong (upper panel) and weak (lower panel) solar irradiance forcing.

We also analysed the climate and ozone responses to the decadal scale solar irradiance variability simulated with models participating in IPCC CMIP-5. The comparison of AOCCM SOCOL-MPIOM simulations with CMIP-5 models and observation results will be described in a paper to be submitted to the EGU journal 'Climate of the Past'.

We also participated in the SPARC SolMIP project whose goal is the analysis of model performance in reproducing the climate and ozone layer responses to past solar variability (e.g., Hood et al., 2015).

References:

Anet J. et al.: 2014, Impact of solar vs. volcanic activity variations on tropospheric temperatures and precipitation during the Dalton Minimum, Clim. Past, 10, 921–938.

Hood L.L. et al.: 2015, Solar signals in CMIP-5 simulations: The ozone response, QJRMS, doi:10.1002/qj.2553.

Muthers S. et al.: 2014, The coupled atmosphere-chemistry-ocean model SOCOL-MPIOM, Geosci. Model Dev., 7, 2157–2179.

Cosmogenic ^{10}Be Signatures of the Extreme Solar Energetic Particle Event of 774–775 AD

Timofei Sukhodolov, Eugene Rozanov, William Ball, and Werner Schmutz in collaboration with ReSoLVE Centre of Excellence and Sodankyla Geophysical Observatory, University of Oulu, Finland

The SOCOLv3 Chemistry-Climate Model (CCM) is used to study the strongest solar particle event of the last 11,000 years. We show good agreement of the modelled and observed ^{10}Be deposition fluxes which allows the strength of the event to be properly characterised, and suggests the most probable season in which the event occurred.

Earth is continuously bombarded by energetic particles from galactic cosmic rays (GCR) and by solar energetic particles (SEPs) emitted during sporadic solar flares and coronal mass ejections. Such energetic particles are the main source of cosmogenic radionuclides and of atmospheric ionisation, affecting dynamics and chemistry of the middle atmosphere. An exceptionally strong SEP event around 775 AD was discovered recently in observations of different cosmogenic isotopes (Usoskin et al., 2013; and references therein). The discovered event appears to be the strongest during at least the last 11,000 years, but its exact strength is not clear. It has therefore been problematic to estimate atmospheric effects caused by this event and, hence, potentially by any such events in the future.

To clarify the strength of the event, we modelled ^{10}Be production, transport and deposition using SOCOLv3 CMM (Stenke et al., 2013), and the production rates estimated by Usoskin et al. (2013) (very hard energy spectrum, 45 times stronger than the largest directly observed event on 23 February 1956), and compared the modelled deposition fields to ice core observations. The GCR-induced ^{10}Be is modelled assuming moderate 11-year solar cycles with phases derived from ^{10}Be observations. All other model boundary conditions were set to the conditions of the 8th century based on paleo-reconstructions of sea surface temperatures and geomagnetic field. After 5 years of spin-up, we initiated a 5-member, 35-year long ensemble run from 766 to 800 AD. We also tried to estimate the season when the event occurred, which is important to correctly determine dynamical consequences, and therefore established four ^{10}Be injection scenarios with identical parameters except for the date of particle injection, being set to four different seasons.

Figure 1 shows the simulated background ^{10}Be concentration, which is in good agreement with other modelling studies and observations. Figure 2 shows a comparison of the simulated and observed ^{10}Be deposition fluxes averaged over four different locations in Greenland and Antarctica. The model reproduces the SEP-induced spike almost perfectly and reproduces the 11-year cycle well, both in phase and amplitude. Analysing the Pearson correlation between the measured and modelled signals and the shape of the peak, we found that the event occurred most likely in boreal autumn, with spring being inconsistent with the Greenland data. In summary, we characterised the strength, identified the season, and were able to correctly model atmospheric transport. Based on this, we then assessed the event's impact upon stratospheric ozone, nitrate deposition fluxes, and surface climate. The obtained results have been submitted to the Nature journal (Sukhodolov et al., in review) and can be used as an upper bound to study the effects of possible SEP events in the future.

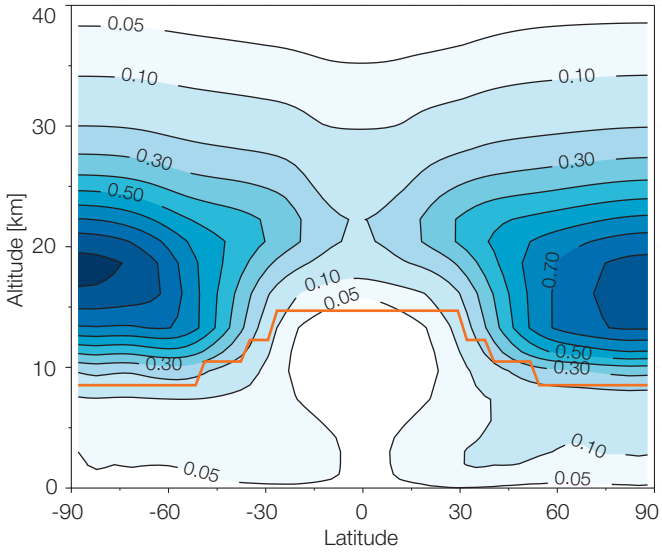

Figure 1. Simulated annual mean concentration of ^{10}Be (atoms per cm^3) for the year 774 AD (ϕ ~ 600 MV). The orange line shows the approximate location of the tropopause.

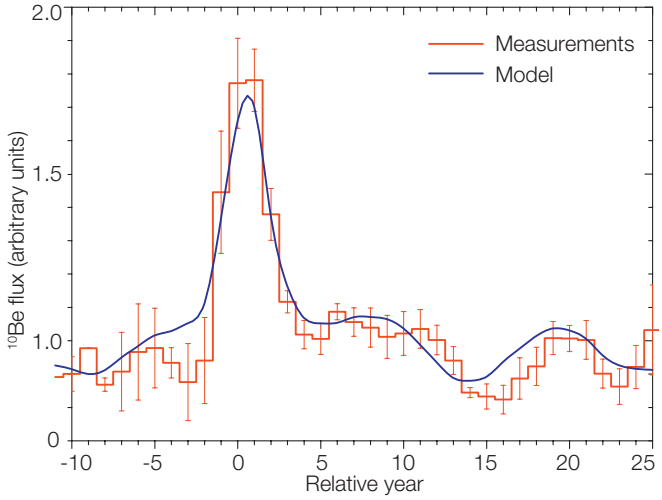

Figure 2. Annual variability of the relative (normalised to the period after 777 AD) ^{10}Be flux. The time scale is relative to 775 AD. The red curve is a 3-yr running mean of the ensemble average over the four measured series studied here (error bars are standard error of mean). The blue curve is the ensemble average of the modelled data over five model runs for the same locations as the data sites for the period 766–800 AD. The dashed line is an extension of the modelled curve by duplicating the cycle.

References:

Stenke A. et al.: 2013, Geosci. Model Dev., 6, 1407–1427.

Sukhodolov T. et al.: 2016, Atmospheric impacts of the strongest known solar particle storm in 775 AD, Nat. Geosci. Letters, in review.

Usoskin I.G. et al.: 2013, The AD 775 cosmic event revisited: the Sun is to blame, Astron. Astrophys., 552, L3.

Evaluation of the Simulated Photolysis Rates and Their Response to Solar Irradiance Variability

Timofei Sukhodolov, Eugene Rozanov, William Ball, and Werner Schmutz in collaboration with IAC ETHZ and other institutes

Photochemical processes are crucial to maintain the ozone layer and temperature structure of the middle atmosphere. We performed a comparison of eight, widely used, photolysis codes against two reference schemes to evaluate their performance in terms of absolute values and solar signal representation.

Chemistry-climate models (CCMs) are common tools to explain observations and to understand the details of the processes involved in the Sun's influence on the Earth's climate. However, even when using the same solar spectral irradiance (SSI) data, different CCMs show a variety of results in amplitude and sign of stratospheric ozone and temperature responses (Ermolli et al., 2013), indicating that there are differences between models in representation of solar-induced stratospheric changes. The treatment of the solar signal in CCMs starts with changes in the heating and photolysis rates, which are usually calculated separately using different parameterisations. Our understanding of these two sources is not the same because the uncertainties in heating rates have been widely discussed in the literature, whereas the response of photodissociation rates to solar variability has not yet been examined.

We analysed the performance of eight parameterisations against two reference models (libRadtran and FLBLM) with an accurate solver of the radiative transfer and very high spectral resolution. First of all, we performed a sensitivity test with a 1-D radiative-convective photochemical model (RCPM, Egorova et al., 1997) by reducing the photolysis rates of various species separately by 30%, and showed that the most important aspect with regard to ozone is the photodissociation reactions of O_2, O_3 and H_2O in the mesosphere. Calculations were then performed on these three photolysis reactions using eight parameterisations and two reference codes. For calculations, we used a standard tropical atmosphere, solar zenith angle of 10°, albedo of 0.1 and SSI data provided by the NESSY model for moderate solar minimum and maximum conditions. To estimate the importance of the obtained differences between the results of each code and reference models, we then applied these differences to the standard RCPM photolysis profiles, and calculated the associated changes in temperature and ozone.

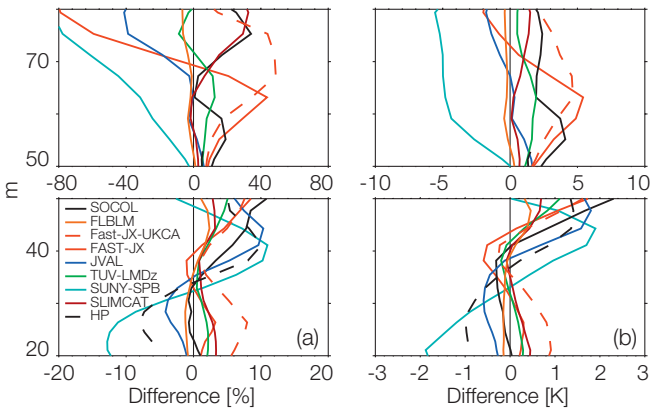

Figure 1. Response of ozone (left column) and temperature (right) profiles to the errors provided by each parameterisation in the representation of O_2, O_3 and H_2O photolysis rates simulated with RCPM for the solar minimum case. Errors are estimated as relative differences between photolysis rates calculated by each parameterisation and libRadtran.

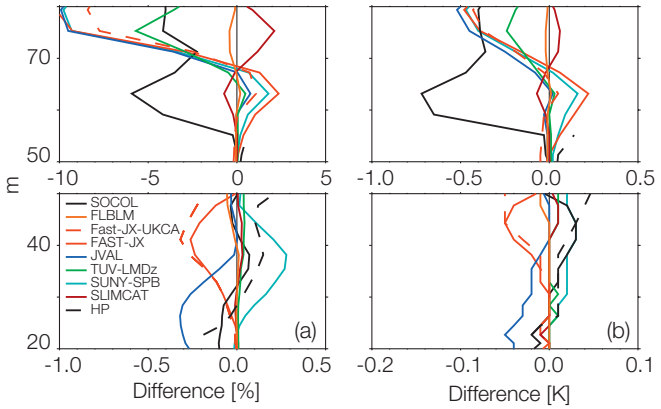

Figure 2. The difference between the solar signals in 1D-modelled ozone (left) and temperature (right) due to the errors provided by each parameterisation in the representation of O_2, O_3 and H_2O photolysis rates. Errors are estimated as relative differences between photolysis rates calculated by each parameterisation and libRadtran.

Figure 1 shows temperature and ozone changes due to deficiencies in photolysis parameterisations for solar minimum conditions, which represents the possible effects these photolysis parameterisations might have on the climatological state of global models. Figure 2 shows which part of the solar signal, induced by the changes in the photolysis rate, is underestimated or overestimated due to problems in certain photolysis schemes. As one can see, errors in photolysis rate parameterisations can largely affect both the state of the middle atmosphere and the solar signal representation. These results, together with the detailed discussion of the possible sources of uncertainties, have recently been published (Sukhodolov et al., 2016) and are useful to interpret CCM results.

References:

Egorova T., Karol I., Rozanov E.: 1997, The influence of ozone content loss in the lower stratosphere on the radiative balance of the troposphere, Phys. Atmos. Ocean (Russ. Acad. Sci.), 33, 492–499.

Ermolli I. et al.: 2013, Recent variability of the solar spectral irradiance and its impact on climate modelling, Atmos. Chem. Phys., 13, 3945–3977, doi:10.5194/acp-13-3945-2013.

Sukhodolov T. et al.: 2016, Evaluation of simulated photolysis rates and their response to solar irradiance variability, J. Geophys. Res. Atmos., 121, doi:10.1002/2015JD024277.

SILA – Study of Factors Influencing Ozone Layer Evolution

William Ball, Eugene Rozanov, Timofei Sukhodolov, and Anna Shapiro in collaboration with IAC ETHZ

The SILA project, now complete, sought to understand unforced ozone variability and its interplay in response to Spectral Solar Irradiance (SSI) variability. During the project we successfully: (i) identified which SSI data-set gave the best agreement between modelled and measured stratospheric ozone responses to the 11-year solar cycle; (ii) determined whether there is a link between spontaneous ozone variability and effects caused by SSI variability; (iii) reproduced the January 2009 SSW event for the international model-measurement intercomparison activity HEPPA - II; and (iv) joined the international Chemistry-Climate Model Initiative (CCMI) to study troposphere-stratosphere coupling with different Chemistry-Climate Models (CCMs).

Our main tool was the state-of-the-art atmospheric CCM SOlar Ozone Climate Links (SOCOL) model, a fully coupled ocean-atmosphere model with a detailed stratospheric chemistry scheme developed at PMOD/WRC and IAC/ETHZ. The successful inclusion of nudging, necessary for completion of this study, was also a major task and will contribute to studies beyond this project (e.g. see the SIMA project on the following pages for further details).

The use of nudging has led to a key result and publication (Ball et al., 2016). We calculated the solar cycle changes in ozone from 1991 to 2012, encompassing two solar cycles. We considered the SORCE SSI data that shows ultraviolet solar cycle variability two to three times larger than two solar models typically considered in climate modelling, which we also employed in this study. Critically, we also simulated a case without solar variability. Since the dynamics were forced to be the same in each simulation, the subtraction of the constant simulation from the three with varying SSI reveals the photolytic response.

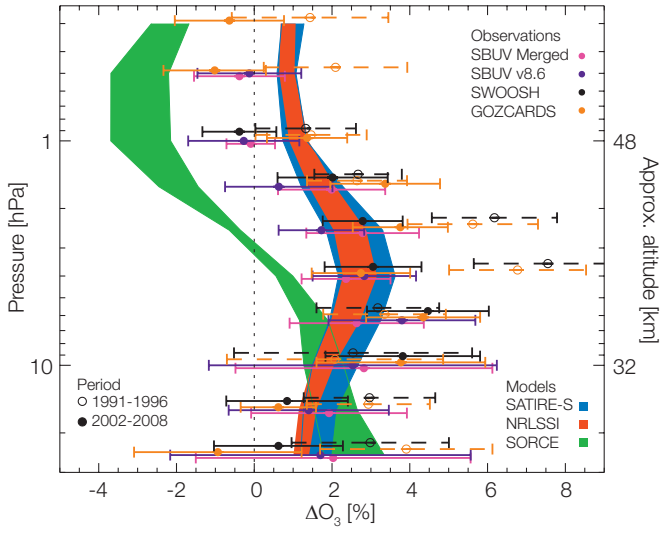

Figure 1. The photolytic response to solar cycle changes extracted from ozone composites of observations (dot-bars), and CCM simulations using a varying solar irradiance (shading). Extraction of the signal was achieved by subtracting a CCM run with no varying solar component. Figure from Ball et al., 2016.

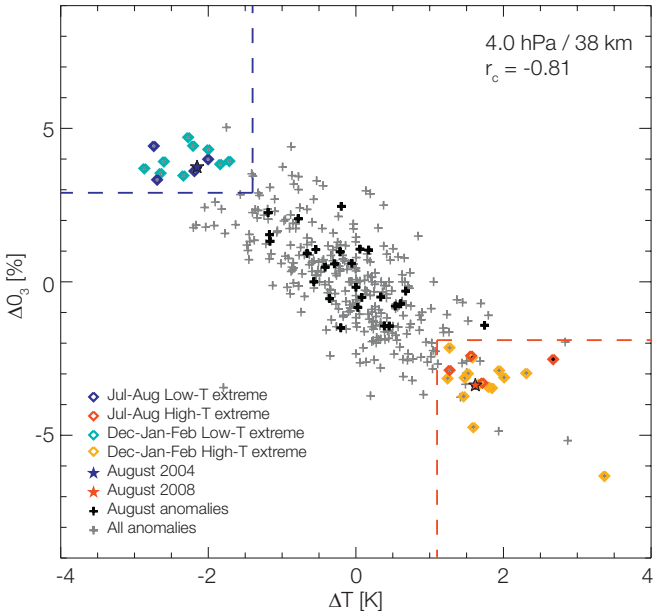

Figure 2. Monthly ozone and temperature anomalies at 4 hPa (~38 km) from 1983–2012. August anomalies are highlighted in black, while extreme events are highlighted with coloured diamonds, which represent different seasons.

Further, since the nudging reproduces realistic historical variations in ozone, except for the solar photolytic component, we were able to subtract the constant simulation from observations of ozone. The results strongly suggest that SORCE is unlikely to be correct and, indeed, solar cycle changes are more like the models (see Figure 1).

In another study, also using nudging, we have identified multiple spontaneous, short-term and large dynamical events between 1983 and 2012, following the work of Shapiro et al., 2013 (see Figure 2). We find that these are related to changes in the large-scale, meridional circulation of the stratosphere, likely responding to variations in waves propagating up from the troposphere. The consequence of this finding is that we have developed a dynamical proxy that explains a large fraction of the remaining unaccounted variability within the equatorial middle atmosphere, driving down uncertainties in ozone and temperature by up to 45%. A publication describing these results, and the development of the proxy for use by the research community, has been submitted for review.

References: Ball W.T. et al.: 2016, High solar cycle spectral variations inconsistent with stratospheric ozone observations. Nature Geoscience, 9, 206–209, doi: 10.1038/ngeo2640.

Shapiro A. et al.: 2013, The role of the solar irradiance variability in the evolution of the middle atmosphere during 2004–2009, J. Geophys. Res. Atmos., 118 doi: 10.1002/jgrd.50208.

SIMA – Study to Determine Spectral Solar Irradiance and its Impact on the Middle Atmosphere

William Ball, Eugene Rozanov, and Werner Schmutz in collaboration with ETHZ/IAC and Imperial College London

The aim of the project Spectral Solar Irradiance and its Impact on the Middle Atmosphere (SIMA), which began in Oct. 2015, is to determine the magnitude of the solar cycle spectral irradiance variability. This will be achieved simultaneously while quantifying chemistry, temperature, and dynamical responses to solar changes.

Within a Bayesian framework, the project seeks to holistically combine available observations and knowledge from climate and solar models. SIMA follows work packages (WPs) that build upon each other. The first two WPs are nearing completion and WP3 will begin later this year. Here we discuss current progress and the outcomes of WPs 1 and 2.

WP1 is to build upon Ball et al. (2014), where the general framework to infer spectral solar irradiance ultraviolet variability from ozone observations was developed and tested upon two different ozone profiles (grey/black lines, Figure 1). To advance this work, we are using ozone data from four new ozone composites, spanning 1985–2012. However, there are differences between the four composites that lead to very different extracted ozone profiles (coloured lines, Figure 1). We have developed a methodology that is being employed to correct the ozone data-sets, with the simple following step that will be to extract a robust ozone profile to determine the solar irradiance variability (see an example in Figure 2). This work is currently being prepared for publication.

WP2 takes WP1 a step further, integrating temperature observations with ozone, which will constrain further our inference of spectral solar irradiance variability. The algorithm extension to include temperature has already been completed and tested, which we apply to infer solar irradiance and ozone, based on temperature, and equally temperature and solar irradiance from ozone. The paper detailing this extension and the results is currently in preparation. However, the final estimate will depend on the new ozone estimates we derive (see above).

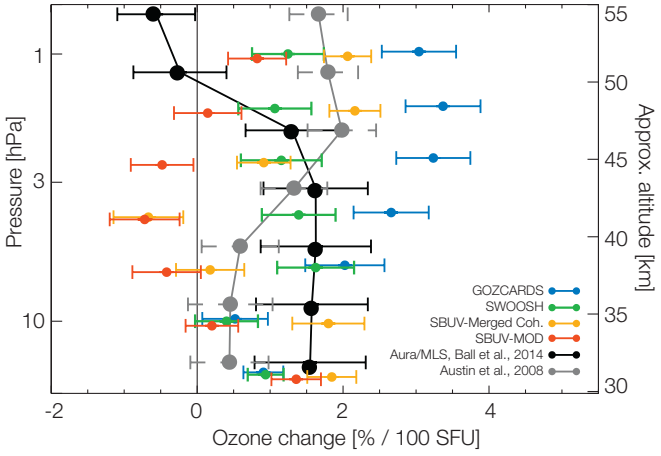

Figure 1. Profiles (black, grey; Ball et al., 2014), used to test the framework of the inversion of ozone observations to infer solar cycle spectral irradiance changes. Coloured profiles are the solar cycles extracted from four ozone composites spanning 1985–2012, which are currently being analysed and corrected before solar irradiance changes are determined.

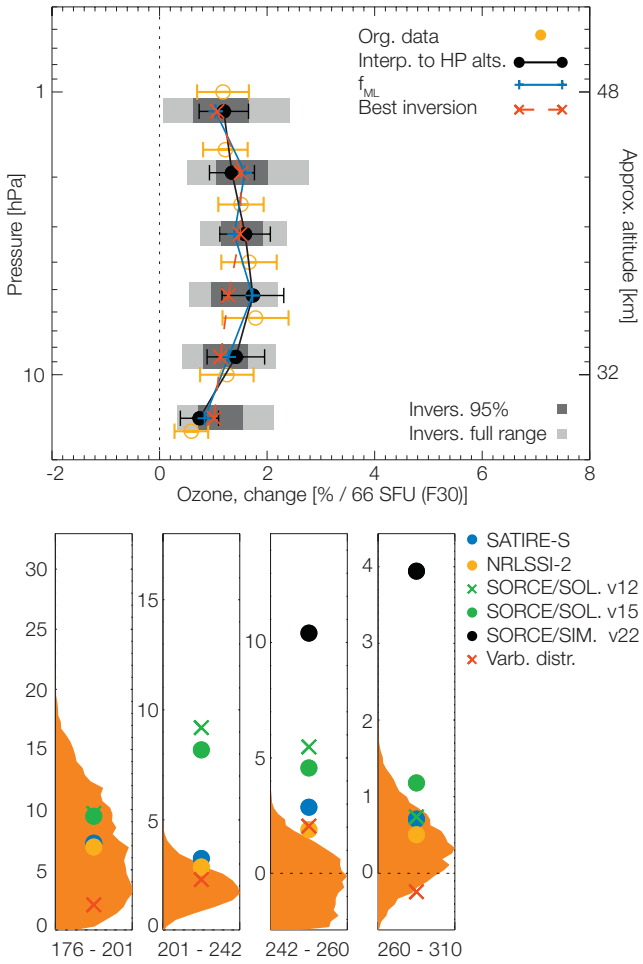

Figure 2. Inversion example: (upper) the range (light grey, 3-σ; dark grey, 1-σ) of sampled ozone profiles from GOZCARDS (orange, original; interpolated, black) ozone composite spanning 1991–2012 (from Ball et al., 2016), the best fit inversion (red) and the most likely profile; (lower) the distributions (orange) of solar irradiance from the upper plot samples for four spectral bands, compared to SATIRE-S, NRLSSI-2, SORCE SOLSTICE and SIM. Red crosses show the best inversion result from the upper plot.

WP3 will develop priors for the inversion. Completion of WPs 1–3 will open up WPs 4–6, which will move from a 2-D to a 3-D climate model, including the CCM SOlar Ozone Climate Links (SOCOL) model developed at PMOD/WRC and IAC/ETHZ. Ultimately this work will lead to a new estimate of spectral irradiance variability and a spectral irradiance time-series data-set.

References: Ball W.T., Mortlock D., Egerton J., Haigh J. D.: 2014, Assessing the relationship between spectral solar irradiance and stratospheric ozone using Bayesian inference, J. Space Weather Space Clim. 4 A25, doi: 10.1051/swsc/2014023.

Ball W. T. et al.: 2016, High solar cycle spectral variations inconsistent with stratospheric ozone observations. Nature Geoscience 9, 206–209, doi:10.1038/ngeo2640.

Modelling of Nitrogen Oxides in the Polar Middle Atmosphere

Eugene Rozanov in collaboration with B. Funke, AAS, Spain, and N. Tsvetkova, CAO, Moscow, Russia

We evaluated the performance of the Chemistry-Climate Model (CCM) SOCOL v3 in the simulation of nitrogen oxides (NO_Y) over the polar areas using the results of several model runs, and comparison with MIPAS observations. We show that a new parameterisation for the NO_Y production and downward propagation from the thermosphere is necessary.

Auroral electrons continuously deposit their energy in the lower thermosphere producing substantial amounts of NO_Y which can further propagate down to the mesosphere and stratosphere affecting the ozone balance, with further implications for the thermal regime, circulation, and climate. The influx of NO_Y is parameterised in CCM SOCOL v3 as a specified function of the geomagnetic activity index, Ap, (Rozanov et al., 2012).

Recent MIPAS observations of NO_Y allow: 1) the performance of the applied parameterisation to be evaluated, 2) the new parameterisation recently proposed by B. Funke (personal communications) to be tested, and 3) the contribution of middle range energy electrons (MEE) to be considered, which is not represented in the standard run. To do so, we performed two transient model runs covering 2002 – 2010 with standard and a new treatment of the upper boundary conditions. The results of the model run with MEE were provided by P. Arsenovic (private communications).

Figure 1 shows the evolution of the observed and simulated NO_Y mixing ratio at 60 km over the northern and southern polar caps. The seasonal cycle of NO_Y with two maxima in summer and winter is well pronounced. The summer maximum reflects the influx of NO_Y-rich air from the mid-latitudes after breaking up of the polar vortex. The regular winter time peak is explained by the downward propagation of thermospheric NO_Y caused by the descent of air inside the polar vortex. The difference in the magnitude of winter time peaks is explained by the variability of the polar vortex state, and the emergence of sudden stratospheric warming, which enhance downward propagation. Irregular spikes occur as a result of strong solar proton events such as the Halloween storm in October 2003 or the ground level enhancement event in January 2005.

The standard model successfully simulates summer peaks. However, it also substantially underestimates the observed NO_Y mixing ratio during the winter season. The introduction of MEE slightly improves the situation, but the underestimation still constitutes a problem. The application of new boundary conditions on the basis of MIPAS measurements helps to increase the magnitude of the winter maxima.

However, in this case the simulated NO_Y in the lower mesosphere is substantially overestimated, especially in the Southern Hemisphere. The problem can be related to some errors during the introduction of new boundary conditions or to downward propagation of NO_Y from the mesopause which is too rapid.

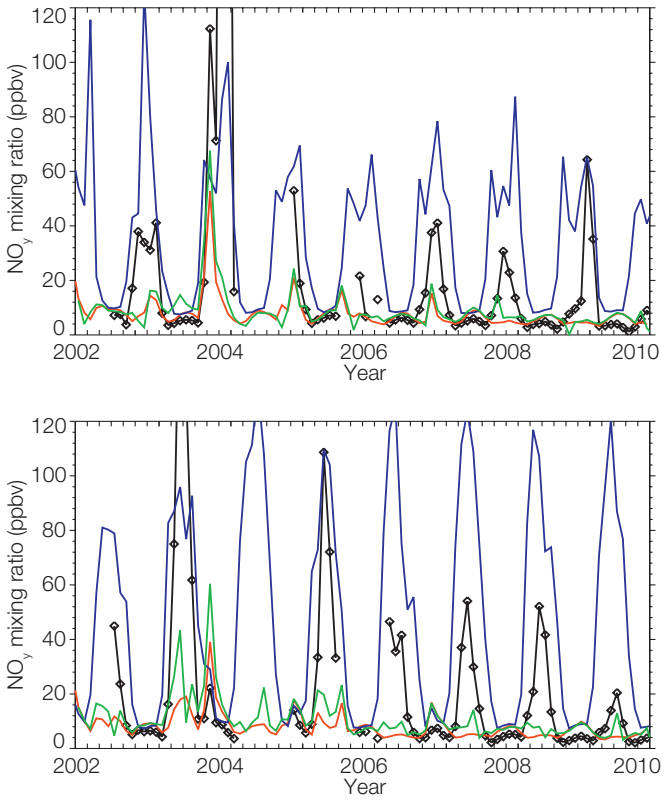

Figure 1. Evolution of the NO_Y mixing ratio (ppbv) at 60 km averaged over the northern (upper panel) and southern (lower panel) polar caps (70°-90°). The results from CCM SOCOL are shown in red (standard run), blue (new boundary conditions) and green (standard run with MEE). MIPAS data are shown in black.

Further work is necessary to resolve the problems and properly simulate NO_Y in the entire middle atmosphere.

The results have important implications for the simulation of the future climate in case of a decline in solar activity. Should this occur, the new parameterisation will give a larger difference in NO_Y and hence ozone between the present and the future, leading to stronger changes in temperature, circulation, and climate, especially on seasonal and regional levels than previously simulated (Anet et al., 2013).

References:

Anet J. et al.: 2013, Impact of a potential 21st century "grand solar minimum" on surface temperatures and stratospheric ozone, Geophys. Res. Lett., 40, 4420–4425.

Funke B. et al.: 2014, Hemispheric distributions and interannual variability of NOy produced by energetic particle precipitation in 2002–2012, J. Geophys. Res. Atmos., 119, 13,565–13,582.

Rozanov E. et al.: 2012, Influence of the precipitating energetic particles on atmospheric chemistry and climate, Surveys in Geophysics, 33, 3, 483–501.

Response of Atmospheric Chemistry to a Solar Proton Event in January 2005

Eugene Rozanov in collaboration with Irina Mironova, SPbU, St. Petersburg, Russia

The impact of solar energetic protons (SEP) on the chemical composition of the polar middle atmosphere is studied when comparing the simulated and observed responses of hydroxyl radical to the ionisation caused by a solar proton event on January 2005. We show that proper representation of the ionisation rates is crucial.

This study is motivated by unexplained cooling and stratospheric aerosol formation during stable mid-winter conditions after strong solar proton events on 17 and 20 January 2005. To address this question we use the SOCOL chemistry-climate model (CCM) and compare the modelled effects with different available observations. One of the main problems is the choice of the ionisation rates. The widely used approach (Jackman et al., 2011) does not account for very energetic protons emerging during the January 2005 event, while the available version of the Monte-Carlo based code, developed by Usoskin et al. (2010), does not include solar protons with an energy less than 10 MeV.

The importance of these deficiencies can be evaluated using the observations of very short-lived hydroxyl radical (OH), obtained by the Microwave Limb Sounder (MLS) instrument onboard the EOS AURA satellite. The observed OH mixing ratio is shown in Figure 1. The response of hydroxyl to an enhanced proton flux is clearly visible starting on 10 January with two pronounced maxima during the sub-events on 17 and 20 January 2005. The features of these sub-events were completely different. The protons during the first event had lower energies and mostly affected the upper atmosphere, while more energetic protons occurred during the second, providing more pronounced effects in the lower atmosphere. Both SEP events resulted in OH production in the polar mesosphere. However, the event on 17 January had slightly stronger effects.

The OH evolution, simulated using both available ionisation rate data-sets, is shown in Figures 2 and 3. The results demonstrate

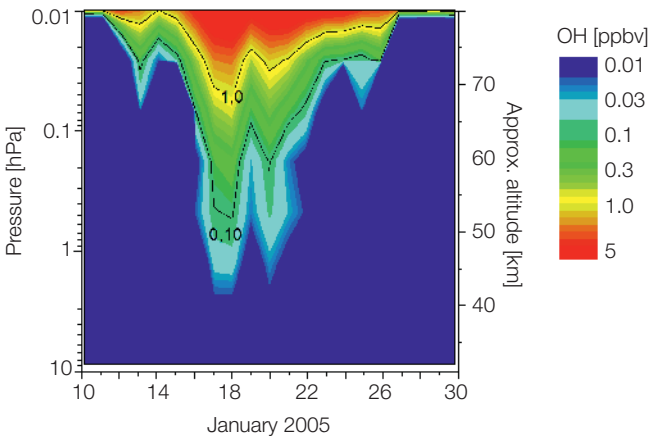

Figure 1. Polar cap mean OH mixing ratio (mol/mol) for the northern hemisphere (75°–82°N) in January 2005, observed by MLS onboard EOS AURA satellite (Damiani et al., 2008).

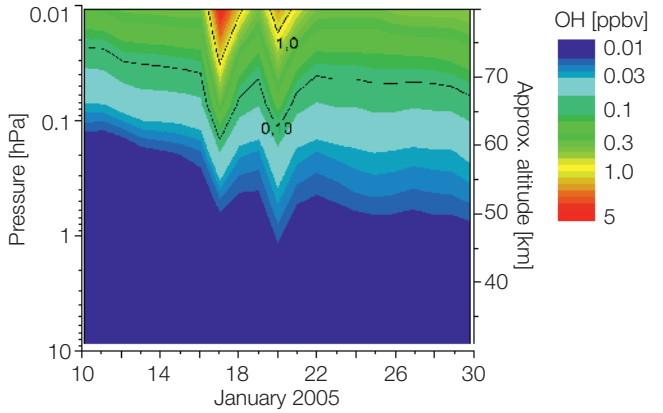

Figure 2. Polar cap mean OH mixing ratio (mol/mol) for the northern hemisphere (76°–83°N) in January 2005, simulated with CCM SOCOL v2 driven by ionisation rates calculated using the approach by Usoskin et al. (2010).

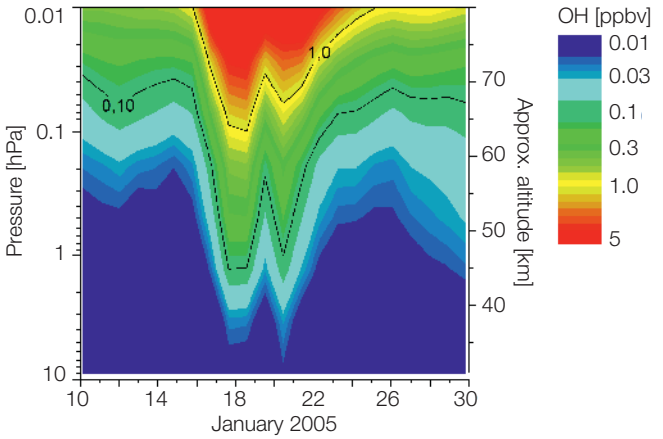

Figure 3. Polar cap mean OH mixing ratio (mol/mol) for the northern hemisphere (76°–83°N) in January 2005, simulated with CCM SOCOL v2 driven by ionisation rates calculated using the standard approach.

that the absence of low energy (below 10 MeV) protons does not give good agreement with observational data in the mesosphere. On the other hand, a problem with the treatment of solar protons by Jackman et al. (2011) leads to some overestimation of OH production below 1 hPa for the sub-event on 20 January. The latter can have implications for the ozone balance in the stratosphere. From these results we conclude that: (i) a new ionisation rate model is necessary to treat particles with a wide energy range, and (ii) a comparison of simulated and observed OH is a good method to characterise the quality of the ionisation rate data.

References: Jackman C. et al.: 2011, Northern Hemisphere atmospheric influence of the solar proton events and ground level enhancement in January 2005, Atmos. Chem. Phys. 11, 6153–6166.

Usoskin I. et al.: 2010, Cosmic ray induced ionisation model CRAC:CRII: An extension to the upper atmosphere. J. Geophys. Res. 115, D10302.

ATLAS – A Pulsed Tunable Laser System for the Characterisation of Spectrometers

Julian Gröbner, Natalia Kouremeti, and Stelios Kazadzis

"A pulsed Tunable laser system for the characterisation of spectrometers" (ATLAS) is an ESA funded project which started in March 2015. ATLAS's main aim is the improved characterisation of array spectroradiometer systems that are widely used for satellite validation of various atmospheric products.

Surface-based optical radiation measurements are a key requirement for the validation of remote-sensing products from Earth observing satellites. State-of-the-art systems consist of array spectroradiometers measuring solar radiation in the UV-VIS-NIR range in order to determine a large range of parameters, from surface radiation to atmospheric composition products. Such products are: total concentrations of trace gases as well as their profiles. In order to fulfil their role as reference systems for the validation of satellite products, traceable surface-based measurements to the international system of units are required. This includes a comprehensive uncertainty budget based on an extensive characterisation of the measuring system. One key aspect in this chain is the radiometric characterisation of the optical system, including its stray-light characteristics and non-linearities in order to produce correction functions for these parameters.

The ATLAS project aims to improve the accuracy of array spectroradiometers that are widely used for satellite validation of various atmospheric products. More specifically, the aim is: 1) to measure the stray-light and linearity of spectroradiometers, and 2) to develop algorithms and post-correction functions in order to deal with these major instrumentation uncertainties. The methodology is going to be initially applied to two systems belonging to two different surface networks of atmospheric trace gas measurements, viz.: 1) a Phaethon system, and 2) a Pandora spectroradiometer belonging to the Pandonia network (http://www.pandonia.net/).

The project consists of two main tasks:

Figure 1. The ATLAS tunable laser from EKSPLA.

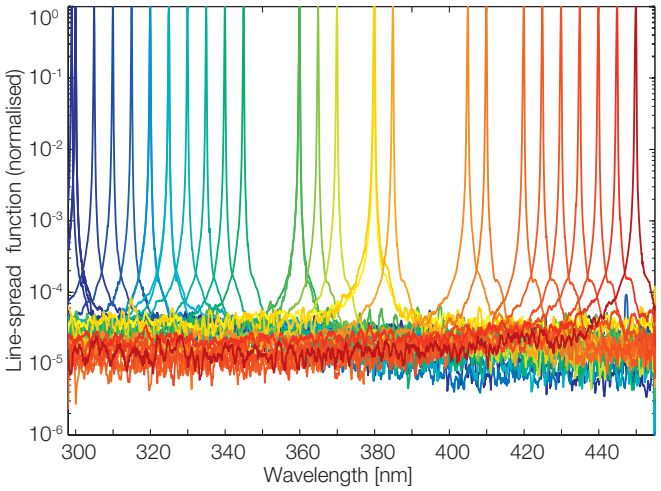

Figure 2. Line-spread function measurements from a Phaeton System, obtained with the ATLAS setup.

- The commissioning of the tunable laser system.

PMOD/WRC has purchased a tunable laser from the manufacturer EKSPLA that was installed in August 2015. Tunable laser systems have become the tool-of-choice for measuring the response of a spectroradiometer to radiation at a given wavelength. Until recently, such systems were only available from very few national metrology institutes.

After setup, the controlling software for operating both the laser system and the external optical elements used for each characterisation were developed at PMOD/WRC and became operational in December 2015.

- Radiometric characterisation of array spectroradiometers using tunable laser sources.

The line-spread function measurements across the wavelength range of the array spectroradiometer can be used to determine the stray-light correction to apply to radiation measurements using a simple matrix inversion (Zong et al., 2006). These measurements will be performed on two spectroradiometer systems used for the validation of Earth observing satellites. Figure 2 shows preliminary results from line-spread function measurements of the Phaeton system using the ATLAS setup (Figure 1).

Similar measurements will be performed with a system belonging to the PANDONIA network in the Spring 2016. The final objective of the project will be to develop procedures to apply these characterisations to the operational products from both systems.

ATLAS is an ongoing project ending in July 2016.

References: Zong Y. et al.: 2006, Simple spectral stray light correction method for array spectroradiometers, Appl. Opt. 45, 1111–1119.

Global Aerosol Mixtures and Their Multi-Year and Seasonal Characteristics

Stelios Kazadzis with collaboration with M. Taylor, NOA, and R. A. Kahn, NASA Goddard Space Flight Centre

The optical and microphysical characteristics of distinct aerosol types, and especially aerosol mixtures in the atmosphere, are not yet specified at the level of detail required for climate forcing studies. Using the GOCART model and surfaced based aerosol data, the approach presented here provides gridded mean compositions of aerosol mixtures as well as tentative estimates of mean aerosol optical and microphysical parameters on a global scale.

It is now known that aerosols contribute strongly to the change in radiative climate forcing and prediction uncertainty (IPCC, 2013). However, much is still unknown about the optical and physical properties of the aerosol components. Given the current limitations on surface-based aerosol coverage, we presented a method for identifying, naming and visualising global mixtures of aerosols from the output of global circulation or chemical transport models. In this study, we use the GOCART (Georgia Tech/Goddard Global Ozone Chemistry Aerosol Radiation and Transport) model to spatially partition the globe into zones of aerosol mixtures of distinct characteristics. Afterwards, we used values of optical and microphysical parameters provided by AERONET sites in each cluster, and then assessed the characteristics of the global partitioning in the context of existing strategies for aerosol classification.

The first task was to perform cluster analysis on the percentage contributions of each aerosol type provided by GOCART multi-year data, using a k-means clustering algorithm. This calculates the norm of the Euclidean distances from cluster centres to every point in the 4-D space of percentage contributions. The result of applying this methodology was a vector of cluster indices in each case. Each row of this vector assigns each pixel to a distinct cluster and has a direct 1:1 mapping with the matrix of unfolded aerosol type percentages (i.e., each pixel has a specific and distinct proportion of aerosol from biomass burning, sulphur, dust, and sea salt). The analysis ended up with 10 clusters, each with a different type of aerosol mixture, as seen in Figure 1.

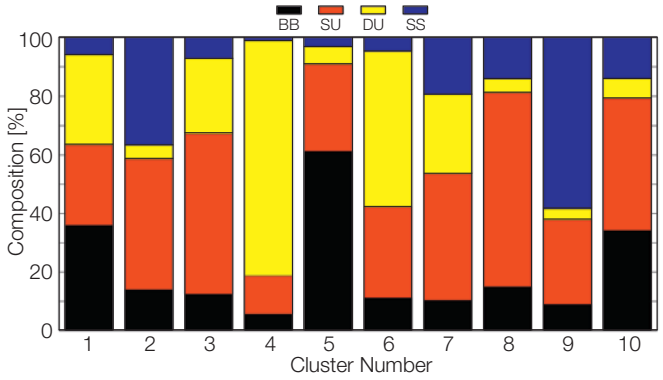

Figure 1. Stacked bar chart displaying the aerosol composition of each cluster from GOCART data. Biomass burning (BB), sulfur (SU), dust (DU) and sea salt (SS) to the total AOD.

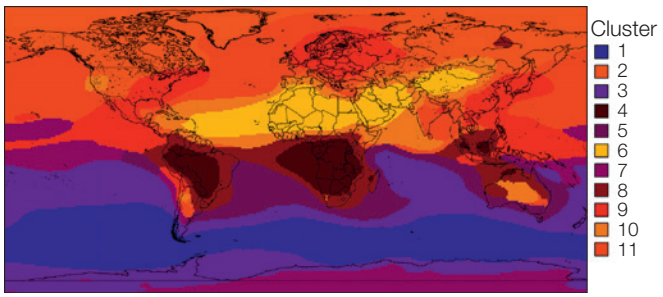

Figure 2. The spatial distribution of aerosol mixtures resulting from application of the k-means clustering algorithm to the seasonal mean of global GOCART chemical data for the summer season (JJA).

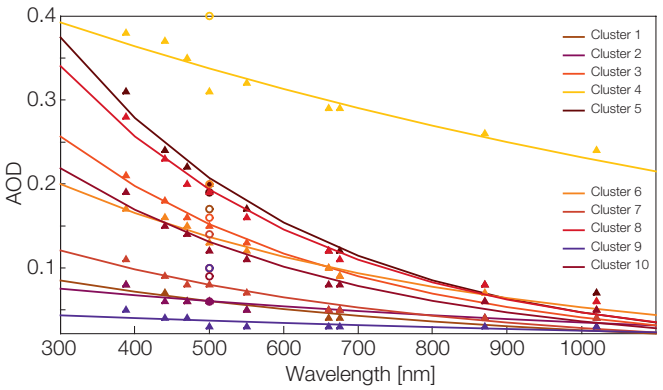

Figure 3. AOD for each cluster at the central wavelengths: 380, 440, 470, 500, 550, 660, 675, 870 and 1020 nm (triangles). The circles at 500 nm are the mean cluster values of AOD obtained by GOCART.

Having identified the composition of global mean aerosol mixtures on the multiyear and seasonal timescales, we visualised the clusters as partitions of gridded (1° x 1°) global maps to see how they are spatially distributed worldwide. With regard to aerosol mixtures for seasonal means, it can be seen in Figure 2 that the basic features of their spatial distribution are largely similar. Note that these maps represent the mixture of aerosol types and not the amount, which varies seasonally to a much greater extent.

Averaging AERONET optical parameter data (AOD, asymmetry parameter, absorption AOD, single scattering albedo) from stations belonging to each cluster, we build a global aerosol climatology (e.g. Figure 3 for AOD). Global chemical transport models and/or circulation models have prognostic capacity but tend to be most reliable on the regional scale due to their dependence on chemical and meteorological boundary conditions. It would be interesting to assess whether source inventories currently used to specify model inputs can be supported by new parameterisations of aerosol, particularly those inputs related to aerosol microphysics which can be a large source of uncertainty.

References: IPCC: 2013, Climate Change 2013, The Physical Science Basis, Cambridge Univ. Press, New York.

Correction of BSRN Short and Long-Wave Irradiance Data: Methods and Implications

Stephan Nyeki, J. Gröbner and W. Finsterle in collaboration with Stefan Wacker, Asiaq, Greenland, and Martin Wild, ETHZ, Switzerland

Previous studies suggest that the World Standard Group for short-wave irradiance and World Infra-red Standard Group for long-wave irradiance at the PMOD/WRC may need to be corrected. Implications with respect to the archive of the Baseline Surface Radiation Network are discussed.

The Baseline Surface Radiation Network (BSRN) archive of surface observations is used worldwide to validate satellite products and global climate models (GCM). Most BSRN records are traceable to the World Standard Group (WSG) for short-wave irradiance and World Infra-red Standard Group (WISG) for long-wave irradiance, hosted by the PMOD/WRC. However, the WSG and WISG have recently been found to over- and underestimate irradiance values, respectively (Fehlmann et al., 2012; Gröbner et al., 2014). In view of a possible correction to both standard groups, and hence to the BSRN radiation archive, this study investigates possible methods towards this goal which will then form the basis of recommendations to be decided on by the WMO Commission for Instruments and Methods of Observations (CIMO).

A correction of the WSG by 0.3% can be readily applied to network radiometers (pyrheliometers and pyranometers) which measure the direct beam of the sun and the total (global) short-wave irradiance, as proposed by Wild et al. (2013). While a simple scale correction is possible for the WSG, this is not the case for the WISG. Long-wave irradiance studies (Gröbner et al., 2014; Nyeki et al., 2016) made during the calibration of pyrgeometers suggest that Eppley PIR and pre-2003 K&Z CG4 pyrgeometers will require a scale correction as well as a correction accounting for the integrated water vapor (IWV) content of the atmosphere when IWV < 10 mm (Gröbner and Wacker, 2013). On the other hand, post-2003 K&Z CG4 pyrgeometers will only require a scale correction. Based on a comparison with two independent long-wave radiometers, the WISG scale would have to be provisionally increased by +5.1 $W m^{-2}$ when IWV > 10 mm (Gröbner et al., 2014). As regards the IWV correction, this only applies to periods when IWV < 10 mm at the BSRN station.

The modified pyrgeometer equation, as recommended by BSRN (McArthur et al., 2004), will be used for both corrections which will require the raw time-series from each BSRN station. A provisional assessment of previous pyrgeometer calibrations at the PMOD/WRC indicates a stable and predictable IWV dependence. Hence, a "generic" correction for Eppley PIR and pre-2003 K&Z CG4 could be used in most cases. A more extensive characterisation of BSRN pyrgeometers (>6 months) at PMOD/WRC would nevertheless be useful but depends on whether the original pyrgeometer can be spared or whether it is still functional.

Table 1. Overview of pyrgeometers, which have submitted long-wave irradiance times-series to BSRN since 1992. Total traceable = number of direct and indirect (i.e. via travelling standard) traceable pyrgeometers.

	Eppley PIR	K&Z CG(R)4	Total
N	188	35	223
N (total traceable)	87	35	122
%	46	100	55

An overview of pyrgeometers, which have submitted long-wave irradiance times-series to BSRN, was made in order to assess the possible effect of the above-mentioned corrections. Data since 1992 from the BSRN website (www.awi-bsrn.de) is summarised in Table 1. Of a total of 223 pyrgeometers, 188 are Eppley PIR and only 35 are K&Z CG(R)4 instruments. When the calibration traceability (direct and indirect) to the WISG is examined, only 87 of the Eppley PIR and all 35 of the K&Z CG(R)4 were traceable. These 122 traceable pyrgeometers represent only 55% of the total, suggesting that a maximum of 45% have calibrations based on black-body sources or from other institutes.

The possible methods and procedures which are to be implemented as well as the absolute values of the corrections to the BSRN archive are at present deemed to be of equal importance. The findings from this study will be presented to CIMO who will make their own recommendations in the near future. However, this is dependent on a number of aspects. For instance: i) the necessity of an extensive multi-instrument inter-comparison campaign and/or ii) the development of additional independent absolute long-wave radiometers.

The effect of the above-discussed corrections may then potentially affect the global radiation budget. Recent studies have shown that GCM short-wave fluxes are over-estimated while GCM long-wave fluxes are under-estimated (e.g., Wild et al., 2013). Correction of the WSG and WISG scales would then result in even larger discrepancies between model outputs and observations than estimated in recent years. These aspects will be provisionally examined in greater detail for the time-series at several stations in the last year of this two-year study.

References:

Fehlmann A. et al.: 2012, Metrologia, 49, S34–S38, doi: 10.1088/0026- 1394/49/2/S34.

Gröbner J., Wacker S.: 2013, AIP Conf. Proc., vol. 1531, pp. 488–491, Dahlem Cube, Free Univ., Berlin, doi:10.1063/1.4804813.

Gröbner J. et al.: 2014, J. Geophys. Res. Atmos., 119, doi:10.1002/2014JD021630.

McArthur B.: 2005, Baseline Surface Radiation Network (BSRN), Operations Manual Version 2.1, WCRP 121, WMO/TD-No. 1274.

Nyeki S. et al.: 2016, Atmos. Meas. Tech, to be submitted.

Wild M. et al: 2013, Clim. Dyn., 40, 3107–3134, doi:10.1007/s00382-012-1569-8.

Stability of the Precision Solar Spectroradiometer

Natalia Kouremeti and Julian Gröbner in collaboration with Lionel Doppler, DWD, Germany

The first production series of Precision Solar Spectroradiometers (PSRs) has been in operation since 2014. Their stability over time is investigated using the two instruments with the longest dataset. The absolute calibration showed a stability within 3% over 1.5 years while the comparison with a co-located spectral radiometer (Cimel, AERONET network) showed a mean agreement in AOD of between 0.002 and 0.006**,** and a correlation coefficient 0.997 at 500 nm over the same period.

The Precision Solar Spectroradiometer (PSR) has been developed at PMOD/WRC to eventually replace current filter-based sunphotometers. The PSR is a temperature stabilised grating spectroradiometer with a 1024 pixel Hamamatsu diode-array detector, operated in a hermetically sealed nitrogen flushed enclosure. The spectroradiometer is designed to measure the solar spectrum in the 300–1020 nm wavelength range with a spectral resolution varying from 1.5–5 nm (full-width-at-half-maximum). The optical bench made of a carbon alloy is optimised to minimise the temperature dependence of solar measurements to less than 0.1% K^{-1} for ambient temperatures in the range -20°C to +40°C.

The first PSR series consisted of four instruments. Two PSRs are at DWD in MOL-RAO, Lindenberg, Germany since June 2014, one is at the Australian Bureau of Meteorology in Melbourne since July 2015, and the fourth is at the National Observatory of Athens (NOA) in Athens, Greece since November 2015. All instruments have been absolutely calibrated in the PMOD/WRC laboratory using reference standards traceable to PTB in order to measure direct spectral solar irradiance with an expanded uncertainty of ±3%. PSR-004 and PSR-006 (DWD) have been in continuous operation for almost 2 years, and their data set has been used to evaluate their stability over time. Both PSRs participated in the FRC-IV campaign and they were re-calibrated. The differences in the responsivity of both instruments was within the uncertainty of the calibration ±3% (Figure 1) with a small deviation of less than 1% in the 900–1020 nm wavelength range for PSR-006.

The AOD was calculated using the measured absolute direct irradiance, corrected for stray-light, and the literature extra-terrestrial spectrum (MHP_COKITH; Egli et al., 2012). Comparison with a co-located Cimel spectral radiometer (AERONET network) for the period June 2014–Dec. 2015 (~5000 points) showed a mean agreement in AOD at all Cimel wavelengths ranging from -0.01 (870 nm) and 0.006 (500 nm) for PSR-006, and from -0.02 (870 nm) to 0.01 (440 nm) for PSR-004. The correlation coefficients at 500 nm are equal to 0.997 for both instruments. Most importantly, the relative change in AOD between Cimel and PSRs is 0.014+0.014 (2σ) and 0.012+0.007 (2σ) per year for PSR-004 and PSR-006, respectively. Therefore, changes in the responsivity of both PSR of less than 2% in the 1.5 year deployment can be inferred from both the spectral AOD comparison and the absolute irradiance calibration.

References: Egli L., Gröbner J., Shapiro A.: 2012, Development of a new high resolution extraterrestrial spectrum, PMOD/WRC Annual Report 2012.

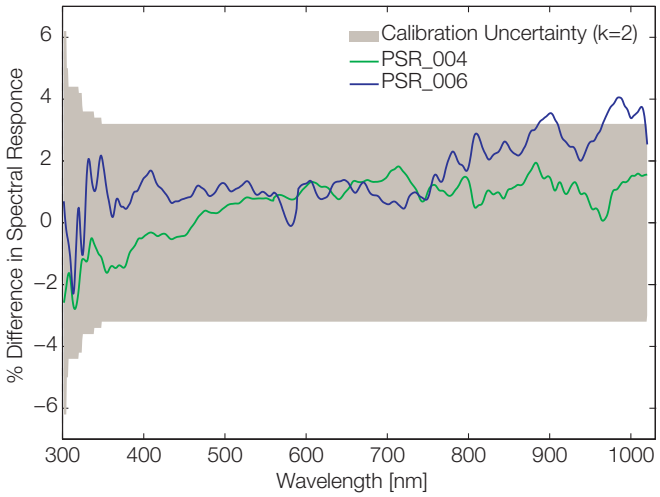

Figure 1. Percentage difference (RES(2014)/RES(2015)-1) of spectral response functions measured on May 2014 and October 2015 for PSR-004 and PSR-006.

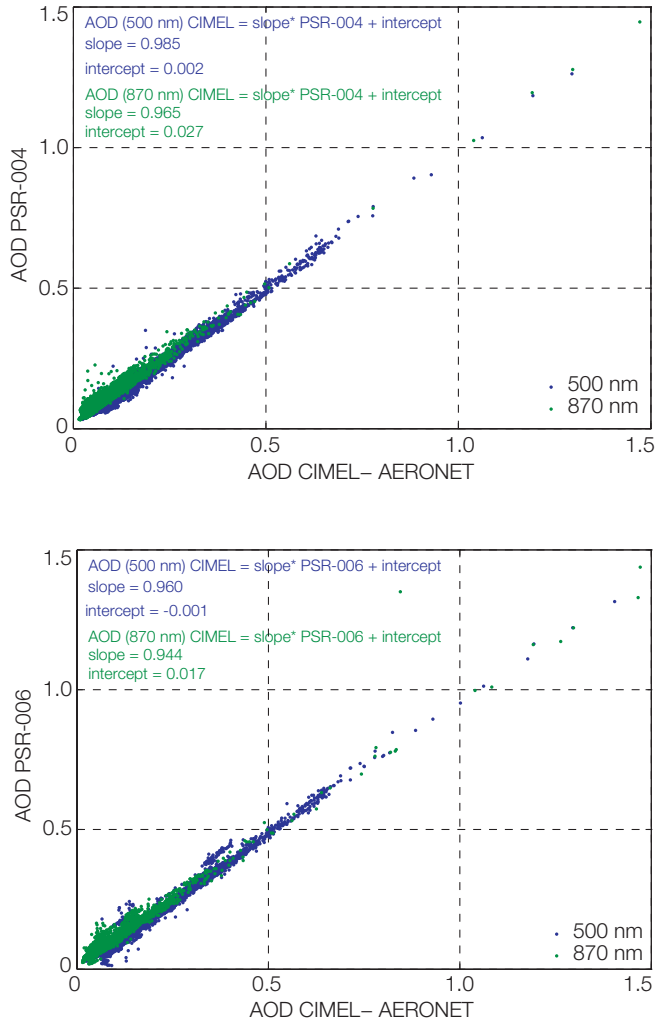

Figure 2. AOD comparison between PSR-004, PSR-006 and a Cimel at 500 (upper panel) and 870 nm (lower panel) during their operation at MOL-RAO, Lindenberg, Germany during the period from June 2014–December 2015.

Cloud Radiative Effect Depending on Cloud Properties and Atmospheric Parameters

Christine Aebi and Julian Gröbner in collaboration with University of Bern and MeteoSwiss

Within the project "A Comprehensive Radiation Flux Assessment" (CRUX), the role of clouds on the surface radiation budget is analysed in order to quantify the long-wave, short-wave and the total cloud radiative effect (CRE), depending on atmospheric parameters, cloud type and cloud fraction.

A climatology of the cloud radiative effect (CRE) is calculated for two stations in Switzerland (Payerne and Davos). The CRE is calculated for short-wave (SW; 0.3–3 µm) and long-wave (LW; 3–100 µm) separately. The sum of the short-wave and long-wave cloud radiative effects (SCE, LCE) is defined as the total cloud radiative effect (TCE). In the current study, the CRE is calculated by the difference of a measurement minus a clear sky model. The measured radiation data are taken from pyranometers (SW) and pyrgeometers (LW). The clear sky model for SW is a look-up table, based on LibRadtran plus different input parameters such as solar zenith angle, total ozone content, integrated water vapor and aerosols. The clear sky model for LW is an empirical model using measurements of water vapor and surface temperature with a climatology of the atmospheric temperature profile (Wacker et al., 2014).

The aim of this analysis is also to determine the sensitivity of the CRE on the surface radiation budget to cloud cover, cloud type, atmospheric water vapor, surface temperature and cloud base height. The cloud cover and cloud types are determined on the basis of pictures taken by visible all-sky cameras. Defined cloud classes include cirrus-cirrostratus, cirrocumulus-altocumulus, stratus-altostratus, cumulus, stratocumulus and cumulonimbus-nimbostratus.

Figure 1 shows the correlation between the LCE and cloud coverage in Davos. The larger the fractional cloud coverage, the larger the LCE. There is a non-linear correlation between both parameters. This non-linear behaviour cannot be explained at present. The other cloud types show similar behaviour. Low-level and optically thick clouds (SC, CU, ST-AS and CN-NS) have LCE values of ~60 Wm^{-2}; for mid-level clouds (CC-AC) LCE = 40–50 Wm^{-2}; and for high-level and thin clouds (CI-CS) LCE = 15–25 Wm^{-2}.

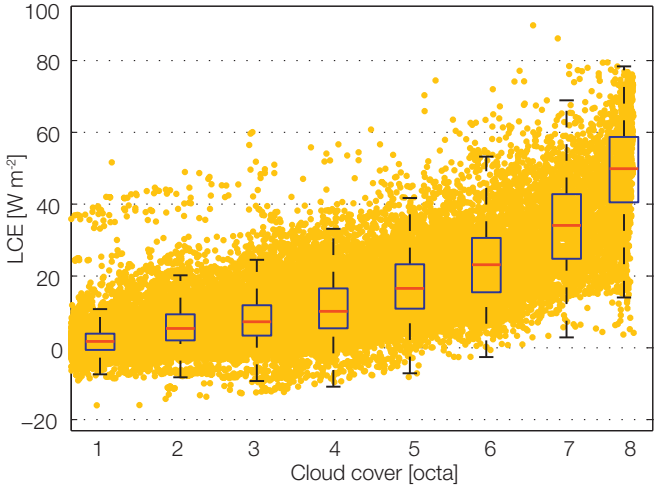

Figure 1. Graph of LCE against cloud coverage at Davos (7 Aug. 2013 – 31 Dec. 2015) for the cirrocumulus-altocumulus cloud class. Data points (yellow dots) and box plots are shown per octa with the median (red line), 25 and 75 percentiles (blue box), and the spread without outliers.

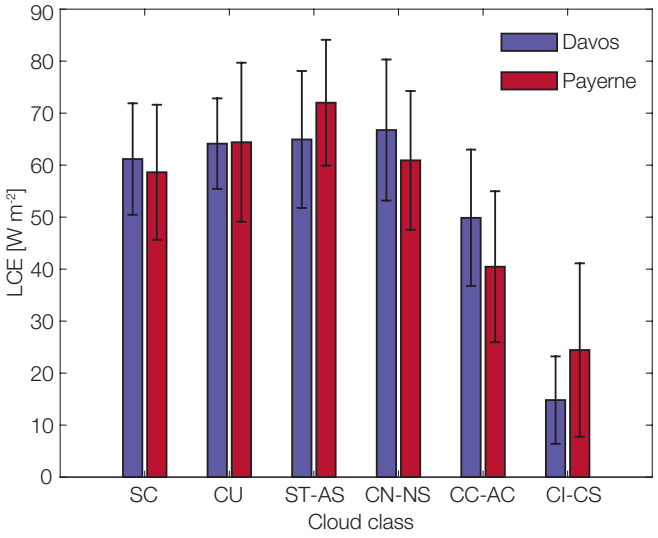

Figure 2. Comparison of the LCE between Davos (blue) and Payerne (dark red) for a cloud coverage of 8 octa (more than 95% cloud coverage) and its standard deviation (yellow). SC: stratocumulus, CU: cumulus, ST-AS: stratus-altostratus, CN-NS: cumulonimbus-nimbostratus, CC-AC: cirrocumulus-altocumulus, CI-CS: cirrus-cirrostratus.

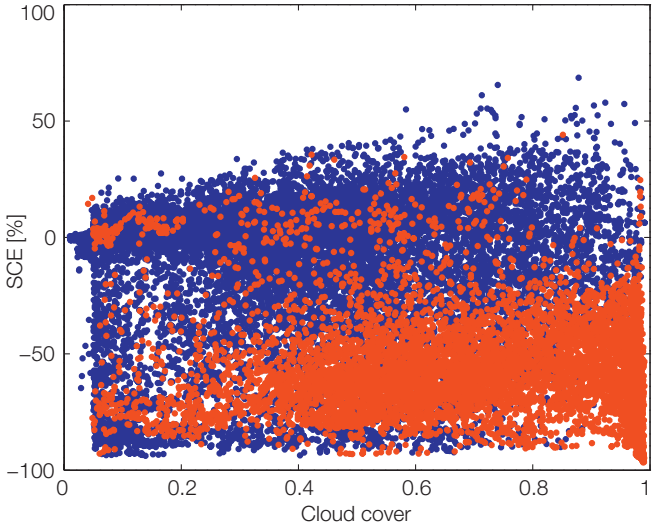

Figure 3. Correlation between cloud coverage and SCE for Davos and the time period 7 August 2013 – 31 December 2015 for the cirrocumulus-altocumulus cloud class. The Sun is covered by a cloud (red) or not covered (blue). SCE [%] = SCE [Wm^{-2}] divided by the SW clear sky model value.

Figure 3 shows the correlation between cloud cover and SCE for Davos and the cirrocumulus-altocumulus cloud class. There are two main groups of data points, one with an SCE at ~0% and the other from about -60 to -70%. These two groups correspond to the sun being covered or not covered by a cloud.

References: Wacker S., Gröbner J., Vuilleumier L.: 2014, Theor. Appl. Climatol., 115, 551–561, DOI: 10.1007/s00704-013-0901-5.

Sensitivity Analysis of Ozone Retrieval Using UV Measurements from an Array Spectroradiometer

Luca Egli and Julian Gröbner in collaboration with partners from the EMRP-ENV59 project ATMOZ

Within the European EMRP project, Traceability for Atmospheric Total Column Ozone (ATMOZ), a comprehensive uncertainty budget for total column ozone retrieval will be produced. The first step toward this goal is a sensitivity analysis of different parameters on the overall uncertainty of ozone determined with array spectroradiometers using a newly developed software tool.

The depletion of the stratospheric ozone layer has been reported since the 1970s, and is commonly monitored by ground-based manual Dobson instruments (Molina and Rowland, 1974) or automatic Brewer spectrophotometers. These instruments measure direct solar irradiance at only four wavelengths. However, array spectroradiometers, as operated at the WCC-UV section of PMOD/WRC, allow total column ozone (TOC) to be retrieved by measuring an entire spectrum in the UV ozone absorption band with a temporal resolution of seconds.

The European EMRP-ENV59 ATMOZ project, coordinated by PMOD/WRC, aims to determine the sources of uncertainty and an overall uncertainty budget of TOC retrieval from: 1) Dobson and Brewer instruments, and 2) array spectroradiometers. The first step towards this goal is to investigate the sensitivity of TOC uncertainties on different parameters, which stem from two main sources:

- UV measurement uncertainties originate from the instrument such as: 1) Noise equivalent irradiance of the instrument detector, 2) wavelength uncertainties, and 3) spectral resolution of the instrument in terms of full-width-half-maximum (FWHM).

- Retrieval model uncertainties: 1) Stratospheric temperatures used for the retrieval method, 2) different ozone absorption cross sections and their uncertainties, 3) uncertainties of the extra-terrestrial spectrum.

To understand the impact of the aforementioned parameters on the uncertainty budget of TOC estimation, a software tool to investigate the sensitivity on the different parameters was developed at PMOD/WRC. The algorithm generates different solar UV spectra in the 300–340 nm wavelength band for a range of atmospheric conditions in terms of air-mass and ozone content. The spectra are modelled with an atmosphere ozone attenuation model and are used as input for a least-squares fit model for TOC retrieval, which is able to retrieve TOC with less than 0.01% uncertainty, if no uncertainty was included in the generated spectrum.

The sensitivity is studied by using a Monte-Carlo based simulation, allowing variation of: 1) the generated spectrum in terms of instrument parameter uncertainty, and 2) input parameters of the retrieval model. All parameters were randomly varied in 500 ensemble runs for each parameter and all atmospheric conditions separately. The uncertainty from these runs is calculated which then allows the overall uncertainty to be determined.

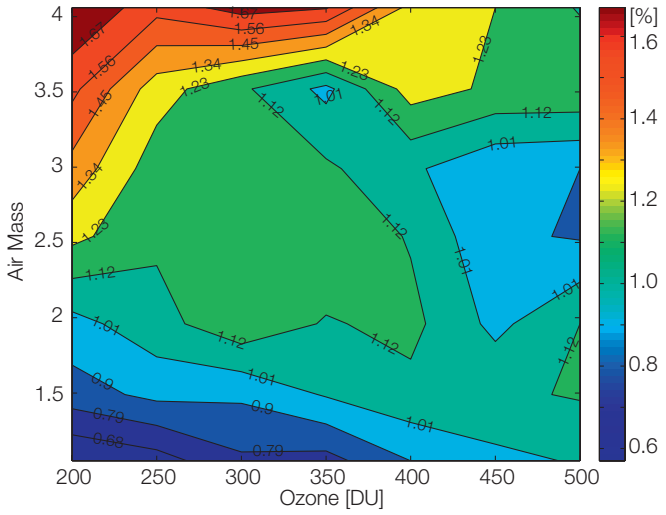

Figure 1. Uncertainty of ozone retrieval (in percent) with variation of stratospheric temperature between -60° -to 30° C. The noise equivalent irradiance of the instrument was simulated to be 0.1 mW.

Figure 1 shows the uncertainty arising from simulated measurements of an array spectroradiometer with an FWHM of 0.5 nm, a spectral resolution of 0.15 nm and a noise equivalent irradiance of 0.1 mW. The stratospheric temperature which is used for the ozone absorption cross section of the retrieval model was assumed to vary from -60° to -30° C. The graph shows that the uncertainty under these assumptions ranges from 0.6% for low air-masses (blue regions) during noon and 1.6% at high air-masses (yellow-red regions) during sunrise and sunset, which is almost independent of the ozone amount.

Further analysis has shown that the sensitivity on the overall uncertainty is minor when considering wavelength uncertainties or when varying the ozone absorption cross-section or the extra-terrestrial spectrum of the retrieval model. The TOC estimated uncertainty is dominated by the sensitivity of the detector (noise equivalent irradiance; Blumthaler et al., 2013), which limits the range of usable wavelengths. A lower noise equivalent irradiance allows a wider range of wavelengths to be used, which decreases the uncertainty of the overall ozone retrieval. Finally, a better knowledge of the stratospheric temperature will substantially improve the uncertainty of TOC determination.

The software tool developed here will further be used to determine the overall uncertainty of Dobson and Brewer instruments and to optimise the design of new developments of array spectroradiometers to detect ozone and other atmospheric gases.

References: Blumthaler M., Gröbner J., Egli L., Nevas S.: 2013, A guide to measuring solar UV spectra using array spectroradiometers, AIP Conf. Proc. 1531, doi: 10.1063/1.4804892.

Molina M.J., Rowland F.S.: 1974, Stratospheric sink for chlorofluoromethanes-chlorine atom catalysed destruction of ozone, Nature, 249, 810–812.

Spatial Coverage of Effective Solar UV Albedo During Snowmelt Around Davos

Luca Egli, Julian Gröbner, and Gregor Hülsen in collaboration with WSL Institute for Snow and Avalanche Research

By observing the effective UV albedo at PMOD/WRC, the seasonal course of the snow-covered area during the ablation period in the Davos region can be monitored. The spatial extent of effective albedo is investigated with three broadband radiometers, and snow-covered area data derived from satellite remote sensing and models calculations. The results show that global solar UV albedo is a complementary source to investigate the development of snow-water resources at larger scales.

Global solar UV radiation is influenced by the surrounding terrain. The multiple backscattering between the atmosphere and the high UV reflectance of snow at the Earth's surface affect single point UV measurements (Lenoble, 2000). This spatial effect is known as the effective UV albedo, which can be quantified under clear sky conditions by broadband or spectral global UV measurements and a radiative transfer model. During the snowmelt season, effective albedo is observed to be lower due to a decreasing fractional snow-covered area (SCA). SCA is an important parameter in monitoring snow-water resources and is commonly observed by space or airborne remote sensing techniques or spatially distributed snow models. However, effective UV albedo is an alternative ground-based method to detect areal SCA from a single point measurement, which is independent of the line-of-sight to the observed snow-cover, and is a measure of the average SCA with a high spatial sampling rate (Egli et al., 2013). This study presents further efforts to quantify the dimensions of the affected area using a 1-D radiative transfer model.

In order to investigate the dependency of effective UV albedo in complex mountainous terrain at different locations, three broadband solar UV radiometers were set-up in the Davos region, namely: 1) on the roof-top measurement platform at the PMOD/WRC (1622 m asl) in the main valley of Davos Dorf, 2) at the SLF experimental site on the Weissfluhjoch (2550 m asl), about 4 km from the PMOD/WRC, and 3) the middle of the Dischma valley

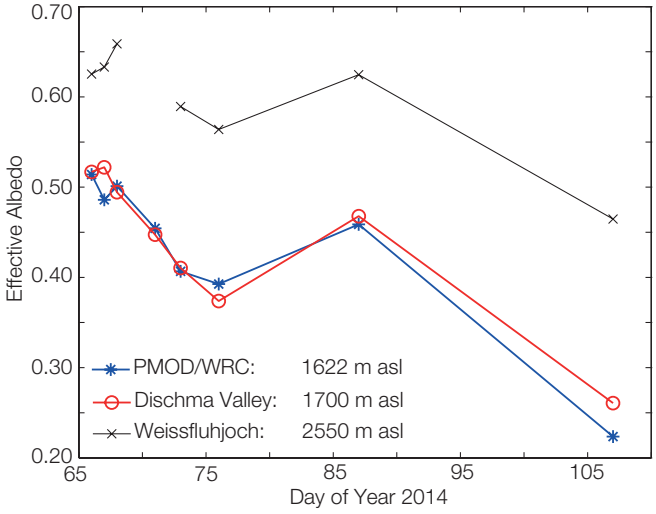

Figure 1. Temporal development of the effective UV albedo, derived from UV broadband radiometers at three different locations around the Davos region. Days without albedo estimates are cloud-covered days.

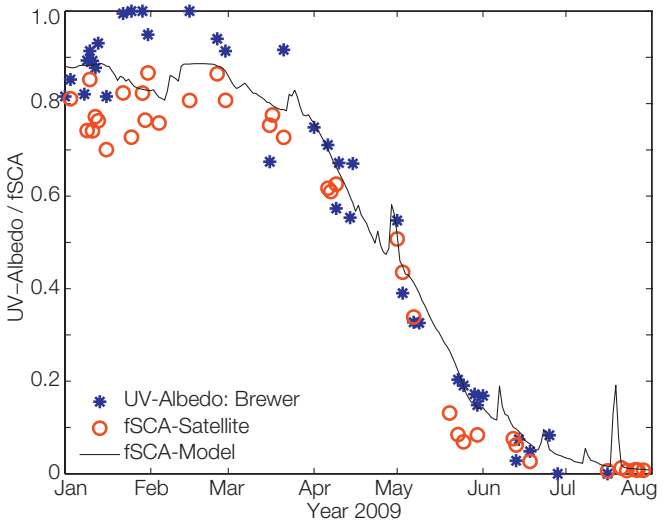

Figure 2. Effective UV albedo compared with the fractional snow-covered area (fSCA) as derived from satellite and model data within a 90 km radius of Davos.

(~1700 m asl), about 7 km from Davos Dorf. This valley is a small narrow side valley perpendicularly oriented to the main Davos valley. Figure 1 shows the temporal development the effective albedo for all three sites during the melting period in 2014. Interestingly, the UV measurements at similar altitudes display a congruent graph indicating that the effective albedo is independent of the geographical orientation and exposure of mountainous valleys. Furthermore, Figure 2 indicates that higher elevation sites are affected by a larger area than those on the valley floor.

In order to determine the maximum radius of effective albedo affecting the measurements around Davos, the temporal evolution of snow-covered area maps are correlated with effective albedo derived from spectral data from the Brewer double monochromator for six snow-melt seasons from 2007 to 2013.The SCA maps are taken from: a) freely available optical satellite data with a spatial resolution of 500 m (http://cryoland.eu) and b) from the spatially distributed operational snow hydrological model operated at SLF in Davos, with a 1 km grid size (http://www.slf.ch/ueber/organisation/gebirgshydrologie/schnee_hydro/oshd/index_EN). Figure 2 shows the good agreement between effective UV albedo and snow-covered area derived from satellite and model data within a 90 km radius of Davos. The best correlation between the data-sets was calculated for different extents, ranging from a radius of 5 km to 500 km, and for all available melt-seasons. The best agreement was found at a radius of 86±9 km. This large diameter may not necessarily be attributed to the multiple scattering behavior of UV radiation, but may hint at difficulties of sub-pixel parametrisations in satellite or model based SCA estimations. The advantages of effective albedo observations may support and complement other SCA monitoring techniques.

References: Egli L, Gröbner J., Hülsen G.: 2013, PMOD/WRC Annual Report.

Lenoble J.: 2000, Appl. Opt., 39, 24, 4247–4254.

A Travel Standard for Aerosol Optical Depth in the UV

Thomas Carlund, Natalia Kouremeti, and Julian Gröbner

One of the main objectives of the European Brewer Network (EUBREWNET; COST Action ES1207) is the retrieval of aerosol optical depth (AOD) in the ultraviolet (UV) spectral range. A UV-PFR developed at PMOD/WRC was used as a travelling standard for AOD measurements, in order to facilitate the necessary calibrations of the EUBREWNET participating instruments.

Currently, Brewer spectrophotometers measure total column ozone using a well-established measurement procedure for direct solar irradiance (Kerr et al., 1981). The same measurements can be used to retrieve AOD at UV wavelengths in the range 306–320 nm, if the instrument is suitably calibrated. For this reason, AOD retrievals in the UV from the European Brewer Network (EUBREWNET) is one of the three main objectives of COST Action ES1207. However, a calibration standard does not exist at present that could also be used to homogenise the calibration and AOD retrieval of Brewer spectrophotometers.

The UV Precision Filter Radiometer (UV-PFR) has been developed for the measurement of direct UV irradiance at 4 narrow-band channels using custom-made interference filters with centres in the 305–332 nm range and bandwidths of less than 2 nm. This instrument is based on the well-known PFR, developed at PMOD/WRC, which is used in the global WMO/GAW network for AOD in the visible-NIR wavelength range. The main goal of this project is to investigate the possibility to use such an instrument, and eventually establish the UV-PFR as a travelling standard for AOD-related calibrations of European Brewer instruments.

So far, the first activities in the project include: 1) Modification of the UV-PFR to reject out-of-band stray-light, 2) spectral characterisation of the instrument in the laboratory, 3) theoretical modelling of uncertainties introduced by the finite spectral bandwidth, and 4) a first calibration at the Izaña high altitude site, Spain.

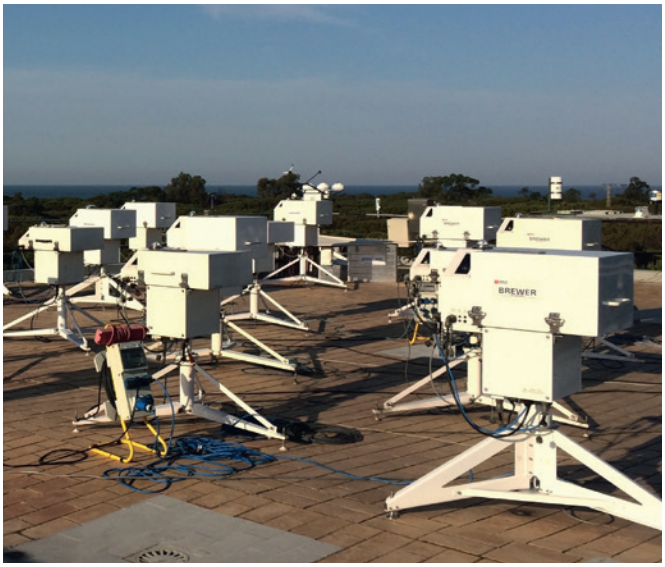

Figure 1. Brewer spectrophotometers (UV-PFR towards the back) during the 10th Regional Brewer Calibration Centre - Europe (RBCC-E) campaign at the El Arenosillo station, Spain.

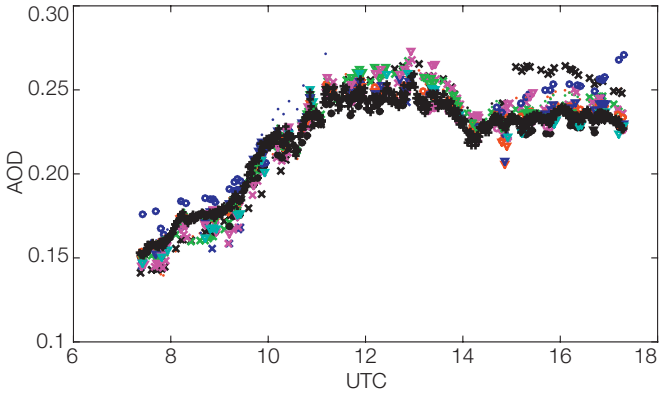

Figure 2. Aerosol optical depth (AOD) at 316.8 nm from the reference UV-PFR (black "plus" symbols) and 17 Brewer instruments (other symbols) on one day during the 10th RBCC-E campaign at El Arenosillo in southern Spain.

After the characterisation and calibration phase, the UV-PFR participated in the 10th Regional Brewer Calibration Centre for Europe (RBCC-E) campaign which was conducted from 25 May – 4 June 2015 at the El Arenosillo sounding station in southern Spain. During this campaign, 21 Brewer instruments were calibrated for AOD against the UV-PFR. The results of the RBCC-E campaign are promising, indicating that for a well-characterised and well-maintained Brewer instrument, AOD can be retrieved with a precision of 0.01 over the 306–320 nm wavelength range.

Brewer spectrophotometers are more complex to calibrate for absolute measurements because of several aspects, including uncertainties in neutral density (ND) filter transmission and internal polarisation effects. It was possible to obtain agreement to within 2% between the independently calibrated (Langley technique) travelling standard Brewer #185 and the UV-PFR when using: 1) spectrally dependent ND filter transmissions, determined during the RBCC-E campaign, and 2) an experimentally determined polarisation correction as recommended by Cede et al. (2006).

References:

Cede A. et al.: 2006, Correction of direct irradiance measurements of Brewer spectrophotometers due to the effect of internal polarisation, Geophys. Res. Letters, 33, L02806, doi:10.1029/2005GL024860.

Kerr J.B., McElroy C.T., Olafson R.A.: 1981, Measurements of ozone with the Brewer ozone spectrophotometer. Proc. Quadrennial Ozone Symp. (J. London, ed.), Boulder, Colorado, pp. 74–79.

A New Observational SSI Composite

Micha Schöll, Margit Haberreiter, and Werner Schmutz in collaboration with CNRS, France

Variations of the spectral solar irradiance (SSI) are an important driver for the chemistry, temperature and dynamics of the Earth's atmosphere and ultimately the Earth's climate. Due to sparse and scattered SSI data-sets it is important to establish tools to derive a consistent SSI composite, including realistic uncertainties.

A new SSI composite is presented by applying a probabilistic method that takes into account the scale-wise uncertainty of each individual SSI data set. The making of this composite is based on SSI data as listed in Table 1, and involves the following steps. First, the raw data are pre-processed, homogenised, and their short-term and long-term uncertainties are estimated (Schöll et al., 2016). Second, each individual time-series is decomposed into different time-scales from daily to decadal periods. Third, for each time-scale and wavelength, the uncertainty of the SSI data-sets is estimated. Then, the decomposed time-series, as well as the scale-dependent uncertainties, are re-combined by computing their weighted average.

It should be noted that the foremost aim has been to use the observations at their face value. This means that no SSI model has been used to correct the observational data. We compare the effects of the SOLID composite, the NRLSSI2 and SATIRE-S reconstruction on the Earth's atmosphere (for details see Haberreiter et al., 2016).

Acknowledgement: This work has received funding from the EC's 7th Framework Progr. under grant agreement no 313188 (SOLID).

Table 1. List of instruments included in the composite (for details see Haberreiter et al., 2016).

Instrument Name	Wavelength range (nm)	Observation period
GOES13/EUVS	11.7–123.2	07/2006–10/2014
GOES14/EUVS	11.7–123.2	07/2009–11/2012
GOES15/EUVS	11.7–123.2	04/2010–10/2014
ISS/SolACES	16.5–57.5	01/2011–03/2014
NIMBUS7/SBUV	170.0–399.0	11/1978–10/1986
NOAA9/SBUV2	170.0–399.0	03/1985–05/1997
NOAA11/SBUV2	170.0–399.0	12/1988–10/1994
NOAA16/SBUV2	170.0–406.2	10/2000–04/2003
SDO/EVE	5.8–106.2	04/2010–10/2014
SME/UV	115.5–302.5	10/1981–04/1989
SNOE/SXP	4.5	03/1998–09/2000
SOHO/CDS	31.4–62.0	04/1998–06/2010
SOHO/SEM	25.0–30.0	01/1996–06/2014
SORCE/SIM	240.0–2412.3	04/2003–05/2015
SORCE/SOLSTICE	115.0–309.0	04/2003–05/2015
SORCE/XPS	0.5–39.5	04/2003–05/2015
TIMED/SEE-EGS	27.1–189.8	02/2002–02/2013
TIMED/SEE-XPS	1.0–9.0	01/2002–11/2014
UARS/SOLSTICE	119.5–419.5	10/1991–09/2001
UARS/SUSIM	115.5–410.5	10/1991–08/2005

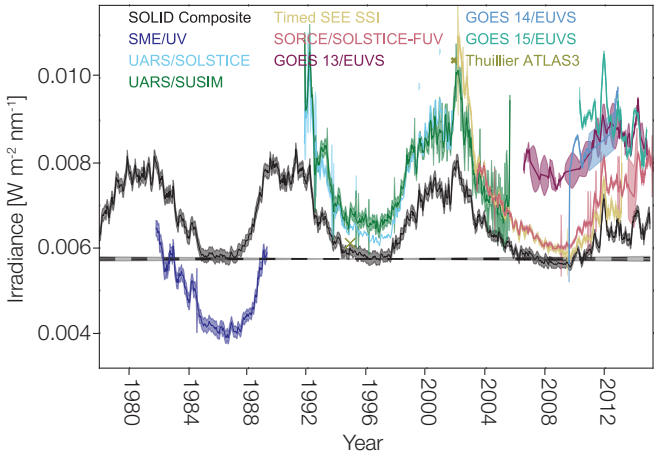

Figure 1. SOLID composite (black line) for 121.5 nm along with all available SSI data-sets (coloured lines) that are the input for the composite. The shaded areas indicate the uncertainty of each data-set for each individual time point.

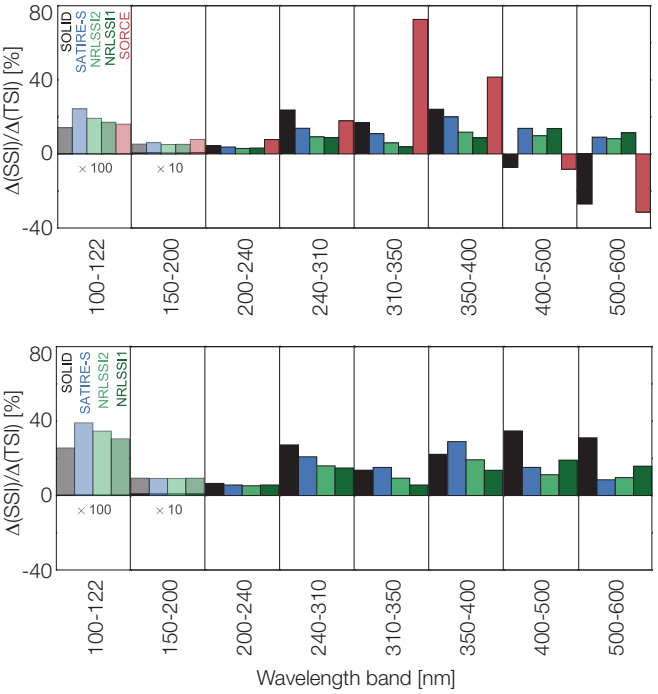

Figure 2. Upper panel: Change of the annual mean SSI in different spectral bins from 2003 to 2008 with respect to the variation in TSI for the same time interval. Shown are the relative changes for SOLID (black), SATIRE-S (blue), NRLSSI1 and NRLSSI2 (dark and light green), and the SORCE composite (red). For better illustration, the first and second spectral bins, i.e. for 121–122nm and 150–200nm are multiplied by a factor of 100 and 10, respectively, shown in partly transparent colour. Lower panel: Same as upper panel, but for the annual means of 1989 and 1994, for which no SORCE data is available.

References: Haberreiter M., et al.: 2016, A new observational solar irradiance composite, to be submitted to JGR.

Schöll M., et al.: 2016, Making of a solar spectral irradiance dataset I: Observations, uncertainties, and methods, SWSC, 6, A14.

Solar Spectral Irradiance Reconstructions Based on Different Solar Proxies

Margit Haberreiter in collaboration with University of Bradford and OAR/INAF

The solar spectra irradiance (SSI) varies on time-scales of minutes to decades and beyond. Semi-empirical models of SSI reconstruction are crucial for the understanding of these irradiance changes. Within the FP7 SOLID project, we performed a sensitivity analysis in order to further improve the reconstruction models.

In the following, we describe the reconstruction of Spectral Solar Irradiance (SSI) using images obtained with the Precision Solar Photometric Telescope (PSPT), and magnetograms and continuum images obtained with the Michelson Doppler Imager (MDI) onboard the SOHO spacecraft.

The area coverages of solar activity features in the PSPT images are determined with the analysis tools developed at the Osservatorio Astronomico di Roma (OAR), while the MDI analysis was carried out with an adopted version of the Automated Solar Activity Prediction (ASAP) tool, as described by Ashamari et al. (2015). The solar spectrum for the different solar activity features was calculated with the latest version of the PMOD/WRC Code for Solar Irradiance (COSI).

Figure 1 shows the reconstruction as obtained with the MDI segmentation along with the COSI synthetic (green), the PSPT image segmentation along with the COSI spectra (black) for 200–250 nm (top panel) and 250–300 nm (bottom panel). As an additional comparison, the SATIRE-S reconstruction (blue; Yeo et al., 2014), and SOLID observational composite (red; Haberreiter et al., 2016a) are also shown.

The plots show that for the 200–250 nm wavelength range, the PSPT/COSI reconstruction and the SOLID observational composite agree well. However, the ASAP/COSI reconstruction slightly underestimates the observed variability.

Both the PSPT/COSI and ASAP/COSI reconstructions show a higher variability than the SOLID composite and SATIRE-S reconstruction for the 250–300 nm wavelength range. A detailed comparison is currently being conducted and a publication is in preparation (Haberreiter et al., 2016b).

Acknowledgement: This work has received funding from the EC's 7th Framework Programme (FP7 2012) under grant agreement no 313188 (SOLID).

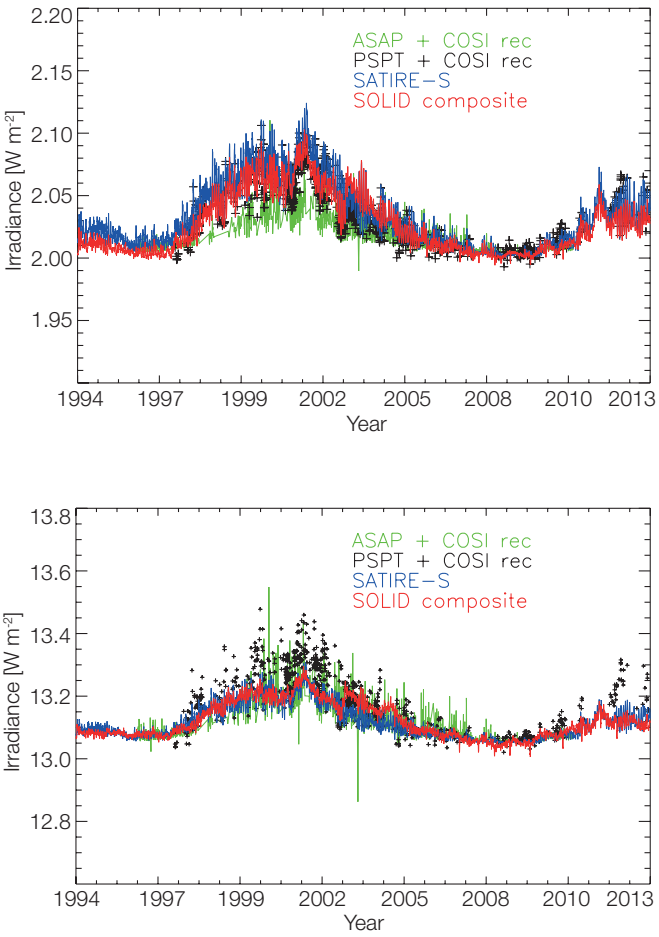

Figure 1. Shown are the SSI reconstructions using the ASAP filling factors with the COSI spectra (green), the PSPT filling factors with COSI spectra (black), the SATIRE-S reconstruction (blue), and the SOLID observational composite (red) for the wavelength ranges: Upper panel) 200–250 nm, and lower panel) 250–300 nm. The spectra have been normalised to match the 2008 solar minimum.

References:

Ashamari O., Qahwaji R., Ipson S., Schöll M., Nibouche O., Haberreiter M.: 2015, Journal of Space Weather and Space Climate, 5, A15, 15 pp., doi: 10.1051/swsc/2015013.

Haberreiter M., Schöll M., Dudok de Wit T., Kretzschmar M., Misios S., Tourpali T., Schmutz W.: 2016a, A new observational solar irradiance composite, to be submitted to JGR.

Haberreiter M. et al.: 2016b, in preparation.

Yeo, K.L., Krivova, N.A., Solanki, S.K., Glassmeier, K. H.: 2014, Reconstruction of total and spectral solar irradiance from 1974 to 2013 based on KPVT, SoHO/MDI, and SDO/HMI observations, Astron. Astrophys., 570, A85, doi: 10.1051/0004-6361/201423628.

NLTE Calculations of the Solar Spectrum Using Cross-Influence of Solar Atmospheric Structures

Cassandra Bolduc and Werner Schmutz in collaboration with Alexander Shapiro, MPS, Göttingen, Germany

We present an alternative to full 3-D magneto-hydrodynamic (MHD) and radiative transfer simulations to calculate the solar spectrum in non-local thermodynamic equilibrium (NLTE). Our method, which involves 1-D calculations of different atmospheric structures and cross-influence at every depth point, aims to represent the spatial and temporal variation effects in a simplified manner.

The solar spectrum is calculated with numerical models by solving the radiative transfer equation simultaneously with the statistical equilibrium equation in NLTE. Such a model, the Code for Solar Irradiance (COSI)/NLTE Spectrum SYnthesis code (NESSY), was developed at PMOD/WRC (Haberreiter et al., 2008; Shapiro et al., 2010). The calculations are performed in 1-D using predefined atmospheric structures. Although 1-D calculations are widely used and yield good results, it has been proved that such simple geometry fails to represent the physical properties of the atmosphere, which is inhomogeneous.

Calculations using snapshots of 3-D MHD simulations show that using the average properties of the atmosphere is unsuitable to adequately reproduce the spectrum (Uitenbroek and Criscuoli, 2011). Since NLTE calculations in 3-D are currently too computationally expensive to be performed for the entire Sun, we developed a method aimed at accounting for 3-D and time-dependent effects in a simplified manner.

The method we developed uses calculations in 1-D for any number of atmospheric structures representing different components of the quiet Sun. These components are allowed to influence each other at each depth point following:

$$I_k^j(z) = \overset{\circ}{I}_k^j(1 - e^{-\tau_k(h)}) + e^{-\tau_k(h)} \sum_i a_i \overset{\circ}{I}_i^j$$

where the intensities I on the right-hand side of the equation are calculated using the temperature and density of the local components i, and τ_k is the characteristic local optical thickness of the component k. Their combined radiation field is then used to calculate new population numbers. Consequently, the statistical populations take into account the cross-influence between atmospheric structures, although the information of their exact location and distribution is lost.

This last year was dedicated to implementing the calculation of the solar spectrum for a set of three distinct atmospheric structures in an independent manner with a single run of COSI. Outputs were compared to independent runs performed with the aforementioned structures in order to ascertain whether the results converged to a consistent solution. The sub-routine managing the cross-influence was also developed.

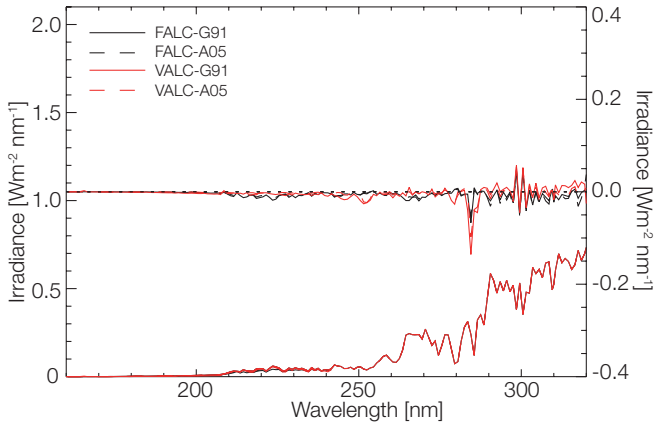

Figure 1. Calculated spectra using the Fontenla et al. (2009) atmosphere model C [FAL-C] and the Vernazza et al. (1981) model C [VAL-C] with two different sets of abundances (Asplund et al. (2005) [A05] and Grevesse et al. (1991) [G91]). The absolute difference between the synthetic spectra and an observed spectrum by SORCE/SOLSTICE is also shown. The minimisation of this quantity allowed the opacity enhancement factor in this wavelength range to be manually optimised.

At the same time, new correction factors for the artificial increase of the continuum opacity in the ultraviolet (160–320 nm) were obtained for two sets of solar atomic abundances (Grevesse and Anders, 1991; Asplund et al., 2004) and two atmospheric profiles, both corresponding to an average quiet Sun (Fontenla et al., 1999; Vernazza et al., 1981). The resulting spectra and their absolute differences to an observed spectrum are illustrated in Figure 1.

References:

Asplund M. et al.: 2004, Line formation in solar granulation. IV. [O I], O I and OH lines and the photospheric O abundance, Astron. Astrophys., 417, 751.

Fontenla J.M. et al.: 2009, Semiempirical models of the solar atmosphere. III. Set of non- LTE models for far-ultraviolet/extreme-ultraviolet irradiance Computation, Astrophys. J., 707, 482.

Grevesse N., Anders, E.: 1991, Solar element abundances, in "Solar interior and atmosphere", pp. 1227–1234.

Haberreiter M. et al.: 2008, NLTE model calculations for the solar atmosphere with an iterative treatment of opacity distribution functions, Astron. Astrophys., 492, 833.

Shapiro A. et al.: 2010, NLTE Solar irradiance modeling with the COSI code, Astron. Astrophys., 517, A48.

Uitenbroek H., Criscuoli S.: 2011, Why one-dimensional models fail in the diagnosis of average Spectra from inhomogeneous stellar atmospheres, Astrophys. J., 736, 69.

Vernazza J.E. et al.: 1981, Structure of the solar chromosphere. III - Models of the EUV brightness components of the quiet-sun, Astrophys. J. Supp., 45, 635.

Understanding the Implication of Small-Scale Heating Events in the Solar Upper Atmosphere.

Nuno Guerreiro, Margit Haberreiter, and Werner Schmutz in collaboration with the University of Oslo

The implications of small-scale heating events (SSHEs) for coronal heating, acceleration of spicules or the pervading redshifts in the lower transition region are poorly understood. We use 3-D Magneto-Hydrodynamic (MHD) simulations to understand the role of SSHEs in the above-mentioned problems. We applied a method to identify, follow over time, and study the SSHEs properties in models with different resolutions, and we report on the outcomes of applying this methodology.

The method that was developed and applied to study the SSHEs (Guerreiro et al., 2015), identifies them in the different snapshots at different stages of their lifetimes. This subsequently links the SSHEs at different stages of their life in the different snapshots while they are above the background.

One of the main outcomes of applying this method has been to show that the SSHEs can have enough energy to balance the energy losses from the corona. It was also demonstrated that the height, volume and energy distributions of the SSHEs resemble a power law when using one of the models. This is consistent with a scenario where the magnetic field in the upper layer of the solar atmosphere is in a self-organised critical state, where the power laws are a direct consequence of the physics of such a state.

We also found that for the low resolution model, the SSHEs have a height between 450 and 500 km. This result is relevant to estimate the thermal energy of SSHEs. The possibility to isolate different SSHEs has allowed their properties to be understood in much greater detail.

Figure 1 shows the properties of an SSHE and its impact on the plasma in its vicinity. This SSHE occurred in the chromosphere and has a lifetime of 160 s. The top left panel displays the maximum energy dissipation per unit mass ($\eta J^2 \rho^{-1}$) in the cell of maximum dissipation of this event over its lifetime. The middle left panel shows the profile of the energy dissipation (ηJ^2) in the same location as for the Joule heating per unit mass. The profiles of Joule heating per unit mass and the Joule heating are relatively similar except at $t = 80$ s, where the maximum energy dissipation does not correspond to the maximum of energy dissipated per unit of mass. This results from the SSHE moving upwards.

The bottom left panel represents the density (ρ) of the material in the location of maximum energy dissipation (asterisks) and the density in the 26 cells around the maximum dissipation cell of the SSHE, which is given by the solid lines with the different colours. That panel shows that the SSHE contributes to the decrease in density in the region of SSHE occurrence. The top right panel displays the total energy being dissipated at each instant (E_t) of the SSHE lifetime. Integrating, it is found that the total energy dissipated by the SSHE is about 6.2×10^{23} erg.

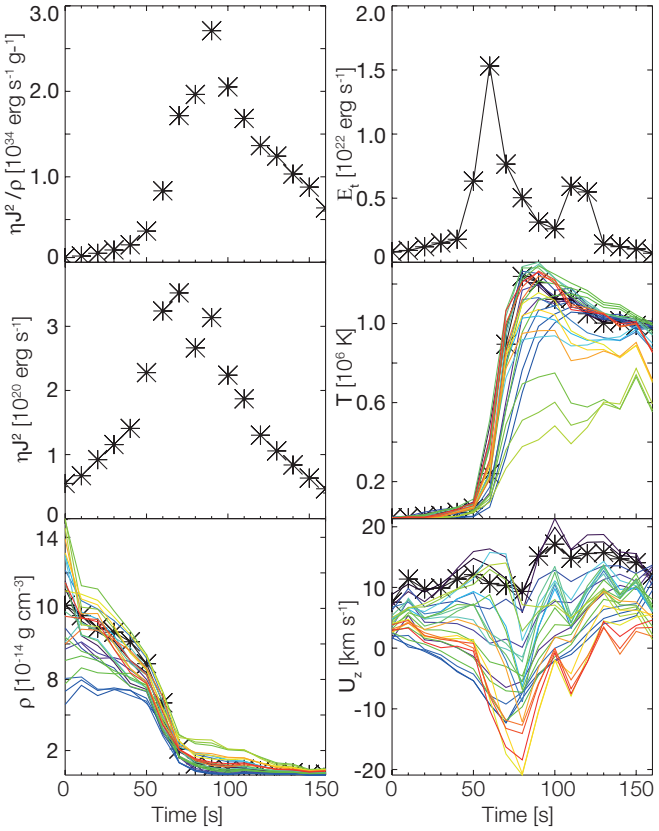

Figure 1. An SSHE that occurs in the chromosphere with a lifetime of 160 s is illustrated. The top left and middle left panels show the Joule heating per unit mass ($\eta J^2 \rho^{-1}$) and the (ηJ^2) in the cell corresponding to the maximum energy dissipation at each instant. The bottom left panel corresponds to the density in the cells, in the vicinity of the local maximum, including the local maximum cell represented by the black line with the asterisks. The top right panel displays the energy of the SSHE at each instant over its lifetime. The middle and bottom right panels show the temperature (T) and vertical component of the velocity (U_z), respectively, in the vicinity of the local maximum of the SSHE at each instant of its lifetime.

The middle right panel displays the temperature (T) in the vicinity of the SSHEs showing that the material is initially at low temperature and the SSHE contributes to increase the temperature of the material in that region to coronal values. The lower right panel shows the vertical component of the velocity (U_z) in the vicinity of the SSHE, where the colour coding is the same for the density and the temperature, and the specific colours correspond to the same cells as for the other variables. In this panel, we see that the SSHE increases the absolute velocity of the plasma, and the material in the vicinity of the plasma is propelled upwards and downwards.

References: Guerreiro, N., Haberreiter, M., Hansteen, V., Schmutz, W.: (2015), Small-scale heating events in the solar atmosphere - I: Identification, Selection and implications for coronal heating, ApJ., 813, 61.

Real-Time Reconstruction of UV Irradiance Based on Ground Radio Observations

Rinat Tagirov, Werner Schmutz in collaboration with Alexander Shapiro, MPS, Göttingen, Germany

The UV irradiance variability in the 175–360 nm range is of great importance to climate studies since it affects the chemical equilibrium of oxygen and ozone which in turn governs the heating rates in the terrestrial atmosphere. A method is being developed to reconstruct the UV irradiance variability in real-time using ground radio observations in the 1–50 cm range.

A large number of space missions have been devoted to the observation of Solar irradiance in the UV range. However, this task has proven to be quite difficult due to instrument degradation effects and the high cost of solar space missions. Therefore, a method for reconstruction of the UV variability using ground observations is called for. In this project, we are trying to develop a method that would use ground radio observations of the solar irradiance to obtain the variability in the UV range in real-time.

The solar irradiance $S(\lambda, t)$ at the wavelength λ and time t can be calculated by adding the contributions of all active features (e.g. spots, faculae, etc.) to the irradiance of the quiet Sun background $I_Q(\lambda)$:

$$S(\lambda, t) = I_Q(\lambda) + \alpha_F(t) C_F(\lambda) + \alpha_S(t) C_S(\lambda) \quad (1)$$

where $C_K(\lambda) = I_K(\lambda) - I_Q(\lambda)$ is the contrast of the active feature with respect to the quiet Sun, $I_K(\lambda)$ is the irradiance of the active feature as if it occupied the entire solar disc. The dependence of the irradiance on time enters in this model via the so-called filling factors $\alpha_K(t)$ which represent the fraction of the area on the solar disc occupied by a certain active feature. The contrasts are derived using either radiative transfer models or some empirical method. In this work, the NLTE Spectrum SYnthesis code NESSY (Tagirov et al., 2016; submitted) is used to determine $C_K(\lambda)$.

Using Eq. (1), the following can be written:

$$I_Q(\lambda_{1,RAD}) + \alpha_F(t) C_F(\lambda_{1,RAD}) + \alpha_S(t) C_S(\lambda_{1,RAD}) = S_{OBS}(\lambda_{1,RAD}, t) \quad (2)$$

$$I_Q(\lambda_{2,RAD}) + \alpha_F(t) C_F(\lambda_{2,RAD}) + \alpha_S(t) C_S(\lambda_{2,RAD}) = S_{OBS}(\lambda_{2,RAD}, t) \quad (3)$$

where $S_{OBS}(\lambda_{1,RAD}, t)$ and $S_{OBS}(\lambda_{2,RAD}, t)$ are the observed irradiances at two radio wavelengths, and $C_K(\lambda_{1,RAD})$ and $C_K(\lambda_{2,RAD})$ are the spot and facular contrasts calculated with NESSY, respectively. From Eqs. (2) and (3) we can find $\alpha_K(t)$ and then apply Eq. (1) again to reconstruct the variability in UV:

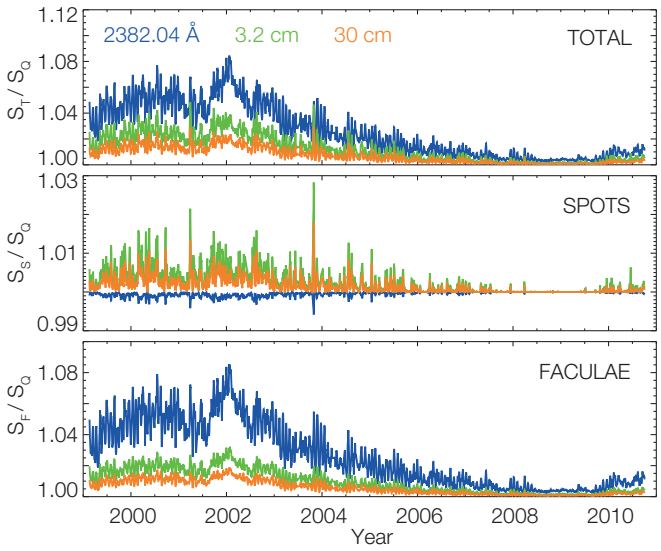

Figure 1. The ratio of the irradiance at 2382.04 Å, 3.2 cm and 30 cm to the quiet Sun irradiance as modeled with NESSY for the three cases: Total variability (spots + faculae), spot variability, and facular variability. All three wavelengths are formed at the same height. T = total, Q = quiet, F = faculae, and S = spots.

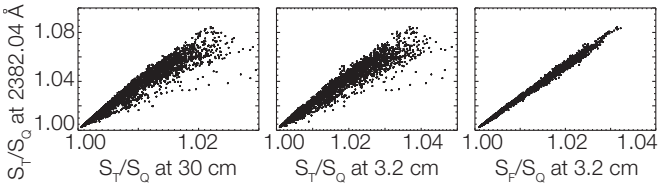

Figure 2. The scatter plot of the irradiance variability corresponding to Figure 1. Each dot corresponds to a certain time along the x-axis of Fig. 1. The left and middle panels show the decrease in correlation between the radio and UV variability because the irradiance at 3.2 and 30 cm is influenced by the spots, whereas the irradiance at 2382.04 Å is dominated by faculae. The right panel relates the facular contribution of the radio variability to the total variability at 2382.04 Å and shows a much better correlation.

$$S_{REC}(\lambda_{UV}, t) = I_Q(\lambda_{UV}) + \alpha_F(t) C_F(\lambda_{UV}) + \alpha_S(t) C_S(\lambda_{UV}) \quad (4)$$

In Equations (2), (3) and (4), the filling factors $\alpha_K(t)$, correspond to the formation height of the wavelengths $\lambda_{1,RAD}$, $\lambda_{2,RAD}$, and λ_{UV} at which the irradiance is observed or reconstructed. Hence, the proposed method works best if the formation heights of the these wavelengths are close to each other. The ultimate purpose of this project is to recommend a set of radio wavelengths suitable for the reconstruction of the UV irradiance in the 175–360 nm range.

References: Tagirov R., Shapiro A.I., Schmutz W.: 2016, NESSY: NLTE spectral synthesis code for solar and stellar atmospheres, Astron. Astrophys., submitted.

Publications

Refereed and Book Publications

Refereed Publications

Amiridis V., Marinou E., Tsekeri A., Wandinger U., Schwarz A., Giannakaki E., Mamouri R., Kokkalis P., Binietoglou I., Solomos S., Herekakis T., Kazadzis S., Gerasopoulos E., Proestakis E., Kottas M., Balis D., Papayannis A., Kontoes C., Kourtidis K., Papagiannopoulos N., Mona L., Pappalardo G., Le Rille O., Ansmann A.: 2015, LIVAS: a 3-D multi-wavelength aerosol/cloud database based on CALIPSO and EARLINET, Atmos. Chem. Phys., 15, 7127–7153, doi: 10.5194/acp-15-7127-2015.

Ashamari O., Qahwaji R., Ipson S., Schöll M., Nibouche O., Haberreiter M.: 2015, Identification of photospheric activity features from SOHO/MDI data using the ASAP tool, J. Space Weather Space Clim., 5, A15, 15 pp., doi: 10.1051/swsc/2015013.

Bolduc C., Bourqui M.S., Charbonneau P.: 2015, A comparison of stratospheric photochemical response to different reconstructions of solar ultraviolet radiative variability, J. Atm. Sol. Ter. Phys., 132, 22–32, doi: 10.1016/j.jastp.2015.06.008.

Brönnimann S., Fischer A., Rozanov E., Poli P., Compo G., Sardeshmukh P.: 2015, Southward shift of the northern tropical belt from 1945 to 1980, Nat. Geosci., 8, 969–974, doi: 10.1038/ngeo2568.

Bühler Y., Marty M., Egli L., Veitinger J., Jonas T., Thee P., Ginzler C.: 2015, Snow depth mapping in high-alpine catchments using digital photogrammetry, Cryosphere, 9, 229–243, doi: 10.5194/tc-9-229-2015.

Flaounas E., Kotroni V., Lagouvardos K., Kazadzis S., Gkikas A. and Hatzianastassiou N.: 2015, Cyclone contribution to dust transport over the Mediterranean region. Atmos. Sci. Lett., 16, 473–478. doi: 10.1002/asl.584.

Gröbner J., Reda I., Wacker S., Nyeki S., Behrens K., Gorman J.: 2015, Reply to comment by R. Philipona on "A new absolute reference for atmospheric longwave irradiance measurements with traceability to SI units", J. Geophys. Res. Atmos., 120, 6885–6886, doi: 10.1002/2015JD023345.

Guerreiro N., Haberreiter M., Hansteen V., Schmutz W.: 2015, Small-scale heating events in the solar atmosphere. I. Identification, selection, and implications for coronal heating, Astrophys. J., 813, 61, 11 pp, doi: 10.1088/0004-637X/813/1/61.

Hansteen V., Guerreiro N., De Pontieu B., Carlsson M.: 2015, Numerical simulations of coronal heating through footpoint braiding, ApJ, 811,106, doi: 10.1088/0004-637X/811/2/106/

Hood L., Misios S., Mitchell D., Rozanov E., Gray L., Tourpali K., Matthes K., Schmidt H., Chiodo G., Thieblemont R., Krivolutsky A.: 2015, Solar signals in CMIP-5 simulations: The ozone response, QJRMS, 141, 2670–2689, doi: 10.1002/qj.2553.

Kosmopoulos P. G., Kazadzis S., Lagouvardos K., Kotroni V., Bais A.: 2015, Solar energy prediction and verification using operational model forecasts and ground-based solar measurements, Energy, 93, 1918–1930, http://dx.doi.org/10.1016/j.energy.2015.10.054.

Krucker S., Saint-Hilaire P., Hudson H.S., Haberreiter M., Martinez-Oliveros J.C., Fivian M.D., Hurford G., Kleint L., Battaglia M., Kuhar M., Arnold N.G.: 2015, Co-spatial white light and hard X-ray flare footpoints seen above the solar limb, Astrophys. J., 802, 19, 10 pp., 10.1088/0004-637X/802/1/19.

Mironova I., Aplin K., Arnold F., Bazilevskaya G., Harrison R., Krivolutsky A., Nicoll K., Rozanov E., Turunen E., Usoskin I.: 2015, Energetic particle influence on the Earth's atmosphere, Space Science Reviews, 194, 1–96, doi: 10.1007/s11214-015-0185-4.

Mitchell D., Misios S., Gray L., Tourpali K., Matthes K., Hood L., Schmidt H., Chiodo G., Thieblemont R., Rozanov E., Krivolutsky A.: 2015, Solar signals in CMIP-5 simulations: The stratospheric pathway, Quarterly Journal of the Royal Meteorological Society, doi: 10.1002/qj.2530.

Muthers S., Arfeuille F., Raible C., Rozanov E.: 2015, The impact of volcanic aerosols on stratospheric ozone and the Northern Hemisphere polar vortex: Separating radiative from chemical effects under different climate conditions, Atmos. Chem. Phys., 15, 11461–14476, 10.5194/acp-15-11461-2015.

Nyeki S., Wehrli C., Gröbner J., Kouremeti N., Wacker S., Labuschagne C., Mbatha N., Brunke E.-G.: 2015, The GAW-PFR aerosol optical depth network: The 2008–2013 time series at Cape Point Station, South Africa, J. Geophys. Res. Atmos., 120, 5070–5084, doi: 10.1002/2014JD022954.

Raptis P. I., Kazadzis S., Eleftheratos K., Kosmopoulos P., Amiridis V., Helmis C., Zerefos C.: 2015, Total ozone column measurements using an ultraviolet multi-filter radiometer, Intern. J. Remote Sens., 36, 17, 4469–4482, doi: 10.1080/01431161.2015.1083631.

Revell L., Tummon F., Stenke A., Sukhodolov T., Coulon A., Rozanov E., Garny H., Grewe V., Peter T.: 2015, Drivers of the tropospheric ozone budget throughout the 21st century under the medium-high climate scenario RCP 6.0, Atmos. Chem. Phys. Discuss., 15, 481–519, doi: 10.5194/acpd-15-481-2015.

Schmidtke G., Avakyan S. V., Berdermann J., Bothmer V., Cessateur G., Ciraolo L., Didkovsky L., Dudok de Wit T., Eparvier F. G., Gottwald A., Haberreiter M., Hammer R., Jacobi C., Jakowski N., Kretzschmar M., Lilensten J., Pfeifer M., Radicella S.M., Schäfer R., Schmidt W., Solomon S.C., Thuillier G., Tobiska, W. K., Wieman S., Woods T.N.: 2015, Where does the Thermospheric Ionospheric GEospheric Research (TIGER) Program go?, Adv. Space Res., 56, 1547–1577.

Shapiro A.I., Solanki S.K., Krivova N.A., Tagirov R.V., Schmutz W.: 2015, The role of the Fraunhofer lines in solar brightness variability, Astron. Astrophys., 581, A116, 9 pp, doi: 10.1051/0004-6361/201526483.

Sheng J.-X., Weisenstein D., Luo B.-P., Rozanov E., Arfeuille F., Peter T.: 2015, A perturbed parameter model ensemble to investigate 1991 Mt Pinatubo's initial sulfur mass emission, Atmos. Chem. Phys., 15, 11501–11512, doi:10.5194/acp-15-11501-2015.

Sheng J.-X., Weisenstein D., Luo B.-P., Rozanov E., Stenke A., Anet J., Bingemer H., Peter T.: 2015, Global atmospheric sulfur budget under volcanically quiescent conditions: Aerosol-chemistry-climate model predictions and validation, J. Geophys. Res. Atmos., 120, 256–276, doi: 10.1002/2014JD021985.

Skinner S.L., Zhekov S.A., Güdel M., Schmutz W.: 2015, A Chandra observation of the eclipsing Wolf-Rayet binary CQ Cep, Astrophys. J., 799, 124, 12pp, doi: 10.1088/0004-637X/799/2/124.

Taylor M., Kazadzis S., Amiridis V., Kahn R.A.: 2015, Global aerosol mixtures and their multiyear and seasonal characteristics, Atmos. Environ., 116, 112–129, doi: 10.1016/j.atmosenv.2015.06.029.

Thuillier G., Harder J.W., Shapiro A., Woods T.N., Perrin J.M., Snow M., Sukhodolov T., Schmutz W.: 2015, The infrared solar spectrum measured by the SOLSPEC spectrometer on-board the International Space Station, Sol. Phys. 290, 1581–1600, doi: 10.1007/s11207-015-0704-1.

Tomasi C., Kokhanovsky A.A., Lupi A., Ritter C., Smirnov A., O'Neill N.T., Stone R.S., Holben B.N., Nyeki S., Wehrli C., Stohl A., Mazzola M., Lanconelli C., Vitale V., Stebel K., Aaltonen V., de Leeuw G., Rodriguez E., Herber A.B., Radionov V.F., Zielinski T., Petelski T., Sakerin S.M., Kabanov D.M., Xue Y., Mei L., Istomina L., Wagener R., McArthur B., Sobolewski P.S., Kivi R., Courcoux Y., Larouche P., Broccardo S., Piketh S. J.: 2015, Aerosol remote sensing in polar regions, Earth Sci. Rev., 140, 108-157, doi: 10.1016/j.earscirev.2014.11.001.

Wacker S., Gröbner J., Zysset C., Diener L., Tzoumanakis P., Kazantzidis A., Vuilleumier L., Stöckli R., Nyeki S., Kämpfer N.: 2015, Cloud observations in Switzerland using hemispherical sky cameras, J. Geophys. Res. Atmos., 120, 695–707, doi: 10.1002/2014JD022643.

Yeo K.L., Ball W.T., Krivova N.A., Solanki S.K., Unruh Y.C., Morrill J.: 2015, UV solar irradiance in observations and the NRLSSI and SATIRE-S models, J. Geophys. Res. Space, 120, 8, 6055–6070, doi: 10.1002/2015JA021277.

Book Chapters

Rozanov E., Sukhodolov T., Tourpali K: 2015, Chapter 3.8, Uncertainty in the modelling of the solar influence on climate, In: Earth's Climate Response to a Changing Sun, eds. T. Dudok de Wit et al., EDP Sciences, Les Ulis, France, ISBN 978-2-7598-1733-7, pp. 195–201.

Schmutz W.: 2015, Chapter 3.2, Weather and climate. In: Our Space Environment: Opportunities, Stakes, and Dangers, eds. C. Nicollier, V. Gass, EPFL Press, Lausanne, Switzerland, ISBN 978-2-940222-88-9, pp. 80–97.

Schmutz W., Haberreiter M.: 2015, Infobox 2.1, Orbital forcing of glacial - interglacial cycles. In: Earth's Climate Response to a Changing Sun, eds. T. Dudok de Wit et. al., EDP Sciences, Les Ulis, France, ISBN 978-2-7598-1733-7, pp. 103–109.

Other Publications

Aebi C., J. Gröbner, N. Kämpfer, L. Vuilleumier: 2015, Cloud radiative effect in dependence on cloud type. In EGU General Assembly Conf. Abstracts, 17, 6067.

Ball W.T., Rozanov E.V., Shapiro A.V.: 2015, Can we use the ozone response in a CCM to say which solar spectral irradiance is most likely correct? In EGU General Assembly Conf. Abstracts, 11274.

Ball W., Yeo K.-L., Krivova N., Solanki S., Unruh Y., Morrill J.: 2015, Evaluation of solar irradiance models for climate studies. In EGU General Assembly Conf. Abstracts, 11817.

Bolduc C., Schmutz W.K., Shapiro A.I.: 2015, NLTE Calculation of the SOlar spectrum with CRoss-influence of solar Atmospheric structures (SOCRAT). In 2015 Sun-Climate Symposium, 9-13 November, Savannah, Georgia, USA.

Bourqui M., Bolduc C., Charbonneau P., Charrière M., Hill D., Lopez A., Loubet E., Roy P., Winter B.: 2015, A bottom-up, scientist-based initiative for the communication of climate sciences with the general public. In EGU General Assembly Conf. Abstracts, 17, EGU2015-4686-1.

Cessateur G., Schmutz W., Shapiro A.: 2015, The solar irradiance: observations and modelling. In EGU General Assembly Conf. Abstracts 17, 10343.

Egli L., Gröbner J., Hülsen G., Bachmann L., Blumthaler M., Dubard J., Khazova M., Kift R., Hoogendijk K., Serrano A., Smedley A., Vilaplana J.-M.: 2015, Quality assessment of solar UV irradiance measured with array spectroradiometers. In Atmos. Meas. Tech. Discuss., 8, 13609–13644, 2015 doi:10.5194/amtd-8-13609-2015.

Guerreiro N., Haberreiter M., Hansteen V., Schmutz W.: 2015, Identification and characterisation of small-scale heating events in the solar atmosphere from 3D MHD simulations. In EGU General Assembly Conference Abstracts, 11100.

Haberreiter M.: 2015, Current Understanding of Solar spectral irradiance variations and their influence on climate. In Asia Oceanic Geosciences Society, 12th Annual Meeting, Abstract, ST06-08-26-A017.

Haberreiter M., Delouille V., Del Zanna G., Ermolli I., Kretzschmar M., Mampeay B., Dominique M., Schmutz W.: 2014, Reconstruction of the solar EUV irradiance as observed with PROBA2/LYRA. In EGU General Assembly Conf. Abstracts 16, 14449.

Haberreiter M., Dudok de Wit T., Kretzschmar M., Del Zanna G., Ermolli I.: 2015, The making of a new solar spectral irradiance composite - overview of the results from the SOLID Project. In AGU Fall Meeting, Abstract SH32A-04.

Halain J.-P., Rochus P., Renotte E., Hermans A., Jacques L., Auchère F., Berghmans D., Harra L., Schühle U., Schmutz W., Zhukov A. Cuadrado R.A., Delmotte F., Dumesnil C., Gyo M., Kennedy T., Smith P., Tandy J., Mercier R., Verbeeck F.: 2015, The Extreme UV Imager telescope on-board the Solar Orbiter mission – Overview of phase C and D. In SPIE Conference Series 9604, 96040G, doi: 10.1117/12.2185634.

Kosmopoulos P.G., Taylor M., Kazadzis S.: 2015, The SOLEA Project: Nowcasting solar energy spectra and UV products. In 15th European Meteorological Society (EMS) Annual Meeting & 12th European Conference on Applications of Meteorology (ECAM), Sofia, Bulgaria, 7-11 September 2015.

Kosmopoulos P.G., Taylor M., Kazadzis S., Keramitsoglou I., Kiranoudis C.T.: 2015, A brighter future. In International Innovation Journal, A Renewable Future, 178, pp 102–104.

Mamajek E.E., Prsa A., Torres G., Harmanec P., Asplund M., Bennett P.D., Capitaine N., Christensen-Dalsgaard J., Depagne E., Folkner W.M., Haberreiter M., Hekker S., Hilton J.L., Kostov V., Kurtz D.W., Laskar J., Mason B.D., Milone E. F., Montgomery M.M., Richards M.T., Schou J., Stewart S.G.: 2015, IAU 2015 Resolution B2 on Recommended Zero Points for the Absolute and Apparent Bolometric Magnitude Scales, https://www.iau.org/static/resolutions/IAU2015_English.pdf.

Mamajek E.E., Prsa A., Torres G., Harmanec P., Asplund M., Bennett P.D., Capitaine N., Christensen-Dalsgaard J., Depagne E., Folkner W.M., Haberreiter M., Hekker S., Hilton J.L., Kostov V., Kurtz D.W., Laskar J., Mason B.D., Milone E.F., Montgomery M.M., Richards M.T., Schou J., Stewart S.G.: 2015, IAU 2015 Resolution B3 on Recommended Nominal Conversion Constants for Selected Solar and Planetary Properties, https://www.iau.org/static/resolutions/IAU2015_English.pdf.

Raptis P.I., Kazadzis S., Eleftheratos K., Kosmopoulos P.G., Amiridis V.: 2015, OMI Total Ozone Column Product validated against UVMFR retrievals. In ATMOS 2015, Herakleion, Greece, 8-12 June 2015.

Schöll M., Cessateur G., Schmutz W., Gröbner J., Haberreiter M., Kretzschmar M.: 2015, Solar Spectral Irradiance Observations from the PICARD/PREMOS Radiometer. In AGU, SH32A-06.

Taylor M., Kosmopoulos P.G., Kazadzis S., Keramitsoglou I., Kiranoudis C.T.: 2015, A machine learning approach to derive surface solar irradiance spectra directly from satellite. In 15th European Meteorological Society (EMS) Annual Meeting & 12th European Conference on Applications of Meteorology (ECAM), Sofia, Bulgaria, 7-11 September 2015.

Administration

Personnel Department

Barbara Bücheler

The International Pyrheliometer Comparison IPC-XII 2015 was the central highlight of last years activities at the PMOD/WRC. Preparatory meetings were held as early as 2014, and continued with increasing anticipation until the start on 26 September 2015 when an ice-breaker meeting was held in the Hotel Seehof. The 5-yearly IPC then began in earnest. The goal of the 130 scientists from 40 different countries was to calibrate and compare their solar radiation instruments with the World Standard Group of the World Radiation Centre. The IPC participants were supported by 45 highly motivated PMOD/WRC members of staff.

The IPC ended on 16 October after successful measurements had been collected on numerous sunny days. An open-day on 14 October was held during the IPC in the framework of the "Forschung Live" national public awareness campaign, organised by the Swiss Academy of Sciences. The general public, local and regional decision-makers, and the press were invited to observe and participate in IPC measurements.

Despite a full-time schedule we looked forward to the METAS visit on 21 May and the organisation of the final EMRP-NEW07 meeting from 28–29 May. Shortly thereafter, from 17–19 June, the PMOD/WRC was audited by MeteoSwiss. We are happy that after a stringent auditing process, the PMOD/WRC passed all criteria. Besides welcoming numerous visitor groups throughout the year, we finished 2015 with the successful ESA/IDEAS project meeting from 8–9 December.

In retrospect, we experienced an exciting and eventful year with many positive and forward-looking changes to our staff line-up. At the start of the year, Dr. Cassandra Bolduc, a young motivated scientist, strengthened the solar physics group along with Dr. Micha Schöll (from June–October 2015) who had previously been at the PMOD/WRC as a PhD student. Dr. Markus Suter then joined us for the duration of the IPC. His experience proved invaluable and we thank him for his efforts. The climate group were also successful by being granted several SNF projects which allowed Drs. Eugene Rozanov and Tatjana Egorova to continue their research at Davos as members of the ETH Zürich.

The planning of the organisational restructuring in the Technical Dept. gave an impetus in 2015. Pierre-Luc who joined us as an Instrument Engineer at the start of 2015 is responsible for optimisation in the field of electronics. Etienne de Coulon returned to the PMOD/WRC in May 2015 as a civilian conscript and thereafter completed various tasks as an Electronic Engineer until August. Philipp Kuhn strengthened the team as a Systems Engineer for the Chinese space project, while Johnathan Kennedy joined as a Mechanical Engineer. Last but not least, Christoph Waupotisch's two-month stay as an Electronic Apprentice flew by.

Barbara Bücheler took over from Sandra Kissling as Head of the Administration and Human Resources in January 2015. Stefan Hartmann was enthusiastic about his apprenticeship while Alexandra Sretovic joined us in August to continue the 2nd year of her training as an Administration clerk. From April to October we were joined by Seraina Egartner who helped us during the IPC. We are pleased that Angela Lehner was able to join us in the Administration section directly after Seraina.

We are also pleased that our civil service conscripts supported us throughout 2015. We thank the following for their great help: Simon Pfister, Remo Waser, Sven Schütz, Etienne de Coulon, André Gauderon, Patrik Caspar und Ron De Capar.

Thanks to the tireless commitment and will to cross boundaries, we were again able to move forward into the future with confidence. Thank you to all those who have supported and accompanied us on our mission.

Scientific Personnel

Prof. Werner Schmutz	Director, physicist
Dr. William Ball	Postdoc climate group, physicist
Dr. Luo Beiping	Scientist climate group, physicist (since 01.10.2015)
Dr. Cassandra Bolduc	Postdoc solar physics group, physicist (since 01.01.2015)
Thomas Carlund	Scientist WORCC section, meteorologist (since 01.04.2015)
Dr. Luca Egli	Scientist WCC-UV section, physicist
Dr. Tatiana Egorova	Climate scientist, climate group, climate scientist (until 30.09.2015)
Dr. Wolfgang Finsterle	Head WRC-section solar radiometry, physicist
Dr. Julian Gröbner	Head WRC-sections IR radiometry, WORCC, and WCC-UV, physicist
Dr. Nuno Guereirro	Postdoc solar physics group, physicist
Dr. Margit Haberreiter	Head solar physics group, physicist
Dr. Gregor Hülsen	Scientist WCC-UV section, physicist
Dr. Stylianos Kazadzis	Scientist WORCC section, physicist
Dr. Natalia Kouremeti	Scientist WORCC section, physicist
Dr. Stephan Nyeki	Scientist IR radiometry section, physicist
Dr. Eugene Rozanov	Scientist climate group, physicist (until 30.09.2015)
Dr. Micha Schöll	Postdoc solar physics group (01.06.2015 – 31.10.2015)
Dr. Markus Suter	IPC scientist (15.09.2015 – 31.10.2015)
Dr. Benjamin Walter	Postdoc solar physics group, physicist
Wilnelia Adams	PhD student, SNF project, 2nd year
Christine Aebi	PhD student, SNF project, 2nd year
Timofei Sukhodolov	PhD student, ETHZ, 3rd year
Rinat Tagirov	PhD student, ETHZ, 4th year

Technical Personnel

Manfred Gyo	Head technical department, electronic engineer
Valeria Büchel	Mechanical engineer (15.08.2012 – 31.07.2015)
Etienne de Coulon	Electronic engineer (29.06.2015 – 17.07.2015, 03.08.2015 – 14.08.2015)
Fabian Dürig	Mechanic engineer (until 31.01.2015)
Jonathon Kennedy	Mechanic engineer (since 01.09.2015)
Silvio Koller	Project and system engineer, quality system manager
Philipp Kuhn	System engineer (since 15.09.2015)
Patrik Langer	Mechanical engineer
Pierre-Luc Lévesque	Instrument engineer (since 01.01.2015)
Andri Morandi	Electronics apprentice, 3rd and 4th year
Daniel Pfiffner	Project manager and electronic engineer space experiments, deputy head tech. dept.
Pascal Schlatter	Mechanic, head workshop, security officer
Marco Senft	System administrator
Marcel Spescha	Technician (until 28.02.2015)
Diego Wasser	Electronic technician
Christoph Waupotisch	Trainee electronic (11.08.2015 – 30.09.2015)

Technical Personnel within the Science Department

Nathan Mingard	Physics laboratory technician
Ricco Soder	Electronic engineer, deputy Quality System manager
Christian Thomann	Technician

Administration

Barbara Bücheler	Head administration/Human Resources (since 13.01.2015)
Sandra Kissling	Head administration/Human Resources (until 31.01.2015)
Kathrin Anhorn	Administration apprentice, 2nd year
Seraina Egartner	Administration, book-keeping (01.04.2015 - 31.10.2015)
Stefan Hartmann	Trainee Administration (29.06.2015 – 24.07.2015)
Geneviève Isnard	Administration backup (13.07.2015 – 31.08.2015)
Irene Keller	Administration, import/export
Angela Lehner	Administration, book-keeping (since 29.09.2015)
Alexandra Sretovic	Administration apprentice, 2nd year
Christian Stiffler	Accountant
Eliane Tobler	Administration book-keeping (unitl 31.01.2015)

Caretaker

Maria Sofia Ferreira Pinto	General caretaker, cleaning
Eufémia Soares Ferreira	General caretaker, cleaning (back-up)

Civilian Service Conscripts

Simon Pfister	01.09.2014 – 31.01.2015
Remo Waser	29.09.2014 – 26.01.2015
Sven Schütz	02.02.2015 – 18.05.2015
Etienne de Coulon	25.05.2015 – 05.07.2015
André Gauderon	13.04.2015 – 15.05.2015, 14.09.2015 – 09.10.2015
Patrik Caspar	14.09.2015 – 12.02.2016
Ron De Caspar	12.10.2015 – 18.01.2016

Meeting/Event Organisation

METAS	Visit, 21 May 2015
EMRP-NEW07	Final meeting, 28–29 May 2015
Audit	Federal Office of Meteorology and Climatology MeteoSwiss, 17–19 June 2015
IPC-XII	International Pyrheliometer Comparison, 28 September–16 October 2015
Forschung Live	"Open Day" during IPC-XII, 7 October 2015
Supervisory Committee	Meeting, 22–23 October 2015
ESA/IDEAS	Meeting, 8–9 December 2015

Public Seminars

19.02.2015 Lucia Kleint, FHNW, Switzerland, "The Interface Region Imaging Spectrograph (IRIS)".

31.03.2015 Philip Brückmann, Brückmann Elektronik, Switzerland, "Heating and cooling systems at PMOD/WRC".

09.04.2015 Luca Ruegg, Davos High School, Switzerland, "A protective mechanism against CME-caused effects on satellites".

29.04.2015 Dr. Pavle Arsenovic, ETH, Zürich, Switzerland, "The influence of middle-range energy electrons on chemistry and climate".

Lecture Courses, Participation in Commissions

Werner Schmutz	Lecture course in Astronomy, HS 2015, ETH-ZH Examination expert in Astronomy, BSc ETH-ZH President of the International Radiation Commission (IRC, IAMAS) Member of the Comité Consultatif de Photométrie et Radiométrie (CCPR, OICM) Swiss delegate to the Science Programme Committee, ESA Member of the Space Weather Working Team Steering Board of ESA Swiss representative in the Committee on Space Research (COSPAR) Member of the Federal Commission for Space Affairs (CFAS) Swiss Management Committee delegate to the COST action ES01005 (ECF) President of the National Committee on Space Research, SCNAT Member of the Commission for Astronomy, SCNAT Member of the GAW-CH Working Group (MeteoSwiss)
Wolfgang Finsterle	Member of CIMO ET Instrument Intercomparisons Member of CIMO TT Radiation References Member of EURAMET TC-PR Chairman of ISO/TC180 SC1 (Solar Energy, Climate - Measurement and Data) Member of "Ad-hoc group" for the approval of IPC-XII procedures and results Technical Expert for ISO17025 accreditation of Silpakorn University, Thailand Member of the PROBA-3 Science Working Team
Julian Gröbner	Lecture course in Solar Ultraviolet Radiation WS 2015, ETH-ZH GAW-CH Working Group (Meteoswiss) Chair of the NEWRAD Scientific committee Chairman of Infrared working Group of Baseline Surface Radiation Network (BSRN) Member IAMAS International Radiation Commission Member of the CIMO Task Group on Radiation - Vice Chairman Swiss delegate to the Management Group of COST ES1207 A EUropean BREWer NETwork - EUBREWNET and Working Group Leader of WG1 "Instrument characterisation and calibration" Member of the EURAMET Task Group on Environment
Margit Haberreiter	Elected President of the EGU Division on Solar-Terrestrial Sciences Member of the SPICE Science Steering Committee Co-Investigator of EUI and SPICE onboard Solar Orbiter Swiss Substitute Member of the Inter-programme Coordination Team on Space Weather (ICTSW) Member of the IAU Organising Committee of Commission E3 "Solar Impact throughout the Heliosphere" Member of the IAU Working Group "Impact of Magnetic Activity on Solar and Stellar Environment" Member of the Inter-Division A-G WG "Nominal Units for Stellar & Planetary Astronomy" Topical Editor Annales Geophysicae Member of the Swiss SCOSPTEP Committee
Eugene Rozanov	Member of SCOSTEP VarSITI ROSMIC WG1
Stelios Kazadzis	GAW-CH Working Group (Meteo Swiss) Scientific Advisory Group Aerosol (WMO/GAW)

Awards

Figure 1. Prof. Dr. Mauro Mesorotti (left), head of the organising committee of the European Space Weather Week 2015, presents the International Kristian Birkeland medal for Space Weather and Space Climate to Werner Schmutz (right).

Werner Schmutz was awarded the International Kristian Birkeland Medal for Space Weather and Space Climate during the 12th European Space Weather Week in Ostend, Belgium, 23–27 November 2015.

The International Kristian Birkeland Medal for Space Weather and Space Climate relates to outstanding scientific or technological results. The laudation is published on the ESWW12 website (www.stce.be/esww12/medals.php). The first two paragraphs read:

> *Dr. Werner Schmutz is a widely accepted authority in the area of Space Weather and Space Climate (SWSC) studies. As director of the Physikalisch-Meteorologisches Observatorium Davos and World Radiation Center (PMOD/WRC), he is conducting PMOD/WRC to be more and more deeply involved in SWSC research. His contribution to the theoretical and technological aspects of the influence of solar irradiance on Earth's atmosphere played a decisive role in the fast progress of SWCS development during the recent decade.*
>
> *The active role of Werner Schmutz regarding the development and exploitation of several space experiments measuring the Total Solar Irradiance (TSI) and Solar Spectral Irradiance (SSI) has been critical for broadening observational data sets. Such resulting databases are necessary for addressing SWSC issues regarding the solar irradiance from short term to long term variability.*

Bilanz 2015 (inklusive Drittmittel) mit Vorjahresvergleich

Aktiven	31.12.2015 CHF	31.12.2014 CHF
Flüssige Mittel	1'222'976.71	1'508'609.56
Forderungen	199'478.13	66'278.95
Aktive Rechnungsabgrenzungen	10'930.62	900.00
Total Aktiven	1'433'385.46	1'575'788.51
Passiven		
Verbindlichkeiten	215'316.65	190'046.00
Kontokorrent Stiftung	58'173.95	115'958.35
Passive Rechnungsabgrenzung	195'523.13	282'428.44
Rückstellungen	945'320.19	945'320.19
Eigenkapital	19'051.54	42'035.53
Total Passiven	1'433'385.46	1'575'788.51

Erfolgsrechnung 2015 (inklusive Drittmittel) mit Vorjahresvergleich

Ertrag	CHF	CHF
Beitrag Bund Betrieb WRC	1'366'976.00	1'366'936.00
Beitrag Bund (BBL), Umbau PMOD/WRC	0.00	300'000.00
Beitrag Kanton Graubünden	452'088.00	452'088.00
Beitrag Gemeinde Davos	589'555.00	589'555.00
Beitrag Gemeinde Davos, Mieterlass	160'000.00	160'000.00
Overhead SNF	124'866.78	111'412.61
Instrumentenverkäufe	344'849.70	126'075.00
Reparaturen und Kalibrationen	184'194.16	184'567.50
Ertrag Dienstleistungen	19'826.85	14'075.00
Übriger Ertrag	12'907.85	279'374.49
Finanzertrag	51.05	685.36
Kursdifferenzen	0.00	550.21
Ausserordentlicher Ertrag	3'258.95	1'775.35
Drittmittel	2'520'065.20	2'055'227.20
Total Ertrag	5'778'639.54	5'642'321.72

Aufwand		
Personalaufwand	4'255'398.65	4'178'914.75
Investitionen Observatorium	118'850.34	165'838.35
Investitionen Drittmittel	270'519.05	125'466.74
Unterhalt	33'658.55	41'280.89
Verbrauchsmaterial Observatorium	71'046.65	39'447.25
Verbrauchsmaterial Drittmittel	217'627.78	207'097.53
Verbrauch Commercial	153'452.73	56'363.12
Reisen, Kurse	157'363.70	198'248.26
Raumaufwand/Energieaufwand	211'628.80	206'885.57
Versicherungen, Verwaltungsaufwand	127'311.43	141'712.18
Finanzaufwand	3'008.81	2'057.23
Übriger Betriebsaufwand	50'640.80	54'456.05
BBL, Umbau PMOD/WRC	0.00	300'000.00
Ausserordentlicher Aufwand	39'154.48	2'575.08
Nicht gedeckter Aufwand EU-Projekte	91'961.76	80'198.00
Total Aufwand	5'801'623.53	5'800'541.00
Jahresergebnis vor Auflösung Rückstellungen	-22'983.99	–158'219.28
Auflösung Rückstellungen zur Defizitdeckung	0.00	155'693.55
Jahresergebnis	-22'983.99	–2'525.73
	5'778'639.54	5'642'321.72

Abbreviations

AERONET	Aerosol Robotic Network, GSFC, USA
AIT	Assembly, Integration and Test
AOCCM	Atmosphere-Ocean-Chemistry-Climate Model
AOD	Aerosol Optical Depth
BIPM	Bureau International des Poids et Mesures, Paris, France
BSRN	Baseline Surface Radiation Network of the WCRP
CCM	Chemistry-Climate Model
CCPR	Comité Consultatif de Photométrie et Radiométrie, BIPM
CIE	Commission Internationale de l'Eclairage
CIMO	Commission for Instruments and Methods of Observation of WMO, Geneva, Switzerland
CIPM	Comité International des Poids et Mesures
CLARA	Compact Light-weight Absolute Radiometer
CMC	Calibration and Measurement Capabilities
CNES	Centre National d'Etudes Spatiales, Paris, France
CNRS	Centre National de la Recherche Scientifique, Service d'Aéronomie Paris, France
COCOSIS	Combination of COSI Spectra
COSI	Code for Solar Irradiance, solar atmosphere radiation transport code developed at PMOD/WRC
COSIR	Code for Solar Irradiance Reconstruction
COSPAR	Commission of Space Application and Research of ICSU, Paris, France
COST	European Cooperation in Science and Technology
CSAR	Cyrogenic Solar Absolute Radiometer
CTM	Chemical Transport Model
DARA	Digital Absolute Radiometer
DLR	Deutsche Luft und Raumfahrt, Germany
EIT	Extreme Ultraviolet Imaging Telescope onboard SOHO
EM	Engineering Model
EMRP	European Metrology Research Programme
ESA	European Space Agency
ESF	European Science Foundation
ETHZ	Eidgenössische Technische Hochschule Zurich
EUI	Extreme Ultraviolet Imager, experiment on Solar Orbiter
EUV	Extreme Ultraviolet
FM	Flight Model
FP7	Seventh Framework Programme of the European Commission
FS	Flight Spare
FUPSOL	Future and Past Solar Influence on the Climate
GAW	Global Atmosphere Watch, a WMO Research Programme
GAWTEC	GAW Training and Education Centre
GCM	General Circulation Model
GHG	Greenhouse Gases
GSFC	Goddard Space Flight Center, Greenbelt, MD, USA
HRI	High Resolution Imagers
IACETH	Institute for Climate Research of the ETHZ, Switzerland
IAMAS	International Association of Meteorology and Atmospheric Sciences of IUGG
IAU	International Astronomical Union of ICSU, Paris, France
ICSU	International Council of Scientific Unions, Paris, France
IPC	International Pyrheliometer Comparisons
IR	Infrared
IRC	International Radiation Commission, Commission of IAMAS
IRIS	Infrared Integrating Sphere Radiometer
IRS	International Radiation Symposium of the Radiation Commission of IAMAS
IRRCAM	Infrared Cloud Camera
ISO/IEC	International Oranisation for Standardisation/International Electrotechnical Commission
ISS	International Space Station
LASP	Laboratory for Atmospheric and Space Physics, Boulder, USA
LATMOS	Laboratoire Atmosphères, Milieux, Observations Spatiales, French research institution
LVPS	Low Voltage Power Supply
LYRA	Lyman-alpha Radiometer, experiment on PROBA-2, built by PMOD/WRC
MDI	Michelson Doppler Interferometer, experiment on SOHO
METAS	Federal Office of Metrology
MIPAS	Michelson Interferometer for Passive Atmospheric Sounding
MITRA	Monitor to Determine the Integrated Transmittance
MPS	Max Planck Institute for Solar System Research
MRA	Mutual Recognition Arrangement
MRR	Manufacturing Readiness Review

NASA	National Aeronautics and Space Administration, Washington DC, USA
NEWRAD	New Developments and Applications in Optical Radiometry
NILU	Norwegian Institute for Air Research, Norway
NIR	Near Infrared
NIST	National Institute of Standards and Technology, Gaithersburg, MD, USA
NOAA	National Oceanographic and Atmospheric Administration, Washington DC, USA
NORSAT-1	Norwegian Satellite-1
NPL	National Physical Laboratory, Teddington, UK
NRL	Naval Research Laboratory, Washington DC, USA
NREL	National Renewable Energy Laboratory, Golden, CO, USA
PFR	Precision Filter Radiometer
PI	Principle Investigator, leader of an experiment/instrument/project
PICARD	French space experiment to measure the solar diameter, launched 2010
PMOD	Physikalisch-Meteorologisches Observatorium Davos, Switzerland
PMO6	PMO6 Type Radiometer
PREMOS	Precision Monitoring of Solar Variability, PMOD/WRC experiment on PICARD
PROBA-2	ESA Technology Demonstration Space Mission, launched 2 December 2009
PRODEX	PROgramme de Développement d'Expériences scientifiques, ESA
PSR	Precision Spectroradiometer
PTB	Physikalisch-Technische Bundesanstalt, Braunschweig and Berlin, Germany
QASUME	Quality Assurance of Spectral Ultraviolet Measurements in Europe
QM	Qualification Model
QMS	Quality Management System
RA	Regional Association of WMO
SATIRE-S	Spectral and Total Irradiance Reconstructions for the Satellite era
SCNAT	Swiss Academy of Sciences
SLF	Schnee und Lawinenforschungsinstitut, Davos, Switzerland
SFI	Schweiz. Forschungsinstitut für Hochgebirgsklima und Medizin, Davos, Switzerland
SI	International System of Units
SIM	Spectral Irradiance Monitor
SIAF	Schweiz. Institut für Allergie- und Asthma-Forschung, Davos, Switzerland
SNSF	Swiss National Science Foundation
SOCOL	Combined GCM and CTM Computer Model, developed at PMOD/WRC
SOHO	Solar and Heliospheric Observatory, Space Mission of ESA/NASA
SOLAR	Experiment Platform on the ISS
SOLID	Solar Irradiance Data Exploitation
SOLMOD	Solar Modelling code
SORCE	Solar Radiation and Climate Experiment, NASA Space Mission
SOTERIA	Solar-Terrestrial Investigations and Archives
SOVAC	Solar Variability and Climate Change
SOVIM	Solar Variability and Irradiance Monitoring, PMOD/WRC experiment on the International Space Station Alpha, 2008
SPICE	Spectral Imaging of the Coronal Environment, experiment on Solar Orbiter, to be launched 2017
SSI	Solar Spectral Irradiance
STM	Structural Thermal Model
SUSIM	Solar Ultraviolet Spectral Irradiance Monitor on Board UARS
SZA	Solar Zenith Angle
TIM	Total Irradiance Monitor
TRF	TSI Radiometer Facility
TSI	Total Solar Irradiance
UARS	Upper Atmosphere Research Satellite, NASA
UV	Ultraviolet
UVA	UV Radiation in the 315–400 nm range
UVB	UV Radiation in the 280–315 nm range
VIRGO	Variability of Solar Irradiance and Gravity Oscillations, PMOD/WRC experiment on SOHO
WCRP	World Climate Research Program
WDCA	World Data Centre for Aerosols
WIGOS	WMO Integrated Global Observing System
WIS	WMO Information System
WISG	World Infrared Standard Group of Pyrgeometers, maintained by WRC-IRS
WMO	World Meteorological Organisation, a United Nations Specialised Agency, Geneva, Switzerland
WRC	World Radiation Centre, Davos, Switzerland
WRC-IRS	Infrared Radiometry Section of the WRC
WRC-SRS	Solar Radiometry Section of the WRC
WRC-WORCC	World Optical Depth Research and Calibration Centre of the WRC
WRC-WCC-UV	World Calibration Centre for Ultraviolet of the WRC
WRR	World Radiometric Reference
WSG	World Standard Group, realising the WRR, maintained by WRC

Annual Report 2015

Editors: Werner Schmutz and Stephan Nyeki
Layout by Stephan Nyeki

Publication by PMOD/WRC, Davos, Switzerland
Edition: 600, printed 2016

Front cover: In addition to the World Standard Group of pyrheliometers, the sun-tracking platform was densely filled with cavity radiometers during IPC-XII. Most of the blue PMO6-type radiometers in this picture have in the meantime been sold to customers.

Back Cover: View of the Cryogenic Solar Absolute Radiometer (CSAR), which is mounted next to the WSG on the sun-tracking platform.

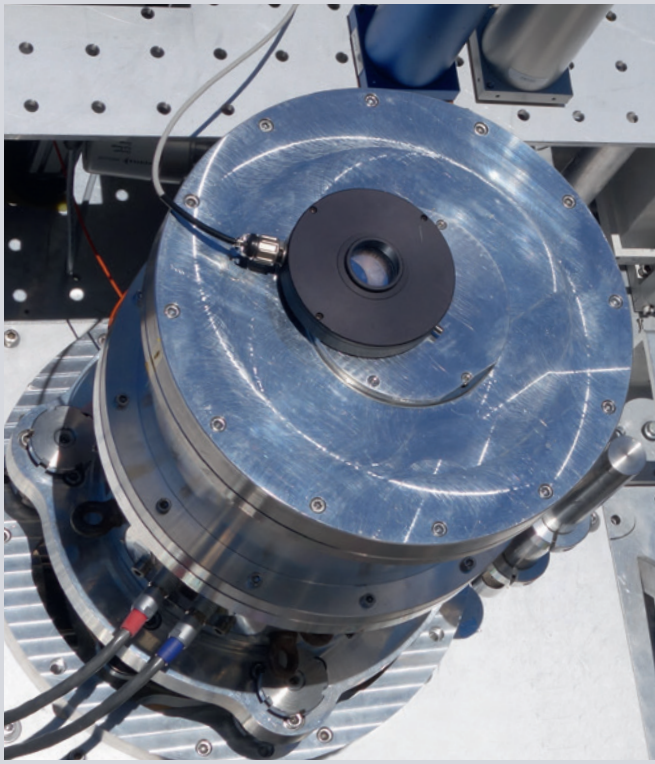

Dorfstrasse 33, 7260 Davos Dorf, Switzerland
Phone +41 58 467 51 11, Fax +41 58 467 51 00
www.pmodwrc.ch